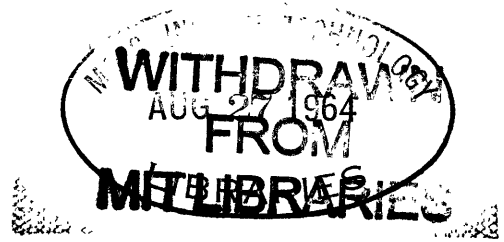


THE ROLE OF VISCOSITY
IN STRATIFIED ROTATING FLUIDS

by

JAMES REED HOLTON

B.A., Harvard University
(1960)

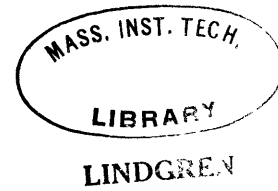


SUBMITTED IN PARTIAL FULFILLMENT OF THE REQUIREMENTS FOR
THE DEGREE OF DOCTOR OF PHILOSOPHY

at the

MASSACHUSETTS INSTITUTE OF TECHNOLOGY

September 1964



Signature of Author.
Department of Meteorology, August 24, 1964

Certified by.
Thesis Supervisor

Accepted by.
Chairman, Departmental Committee on Graduate
Students



Room 14-0551
77 Massachusetts Avenue
Cambridge, MA 02139
Ph: 617.253.5668 Fax: 617.253.1690
Email: docs@mit.edu
<http://libraries.mit.edu/docs>

DISCLAIMER OF QUALITY

Due to the condition of the original material, there are unavoidable flaws in this reproduction. We have made every effort possible to provide you with the best copy available. If you are dissatisfied with this product and find it unusable, please contact Document Services as soon as possible.

Thank you.

**Poor copy quality. Grayscale scanning
needed for text legibility.**

THE ROLE OF VISCOSITY IN STRATIFIED ROTATING FLUIDS

by

James R. Holton

Submitted to the Department of Meteorology on August 24, 1964
in Partial Fulfillment of the Requirements for the
Degree of Doctor of Philosophy

ABSTRACT

The effect of viscosity on quasi-geostrophic motions in stratified fluid systems is investigated both for simple laboratory models and circularly symmetric ocean currents.

It is shown that the motion consists of both a barotropic and a baroclinic mode. For the barotropic mode viscosity enters the system primarily through convergence in the Ekman boundary layer. The convergence in this boundary layer causes the barotropic disturbance to decay with a spin-down time proportional to $t = \sqrt{\frac{H^2}{\nu \Omega_0}}$, where H is the depth of the fluid, ν is the kinematic viscosity coefficient and Ω_0 is the basic rotation rate. The baroclinic mode is unaffected by the Ekman friction effect and its characteristic decay time is the much greater internal diffusion time scale, $t = \frac{H^2}{\nu}$.

The first part of this paper discusses the transient spin-up resulting when a rotating cylinder containing a stably stratified fluid system has its rotation rate impulsively changed at $t = 0$. The spin-up time and the quasi-steady velocity in the baroclinic mode are shown to be functions of the internal rotational Froude number. Experiments with salt solutions, both continuously stratified and two-layer, are shown to be in good agreement with the theory. Experiments with two-layer immiscible fluid systems are discussed and it is shown that Ekman layers forming at the interface between the layers control the upper layer spin-up in such cases.

In the second part of the paper simple ocean current models are discussed. It is shown that in currents generated by time varying wind stresses the barotropic amplitude is limited by Ekman friction, so that the baroclinic mode dominates for long period forcing.

The decay of a baroclinic eddy subject to internal viscous diffusion is studied and it is shown that if heat diffusion is neglected in certain asymptotic cases the eddy will diffuse horizontally but retain its initial vertical structure.

Finally, the β effect is included and certain special solutions are obtained which indicate that both β and friction enhance the baroclinic mode for long period forcing.

Thesis Supervisor: Jule G. Charney
Title: Professor of Meteorology

TABLE OF CONTENTS

| | Page | |
|--------------|---|-----|
| Chapter 1 | Introduction and Summary | 8 |
| Chapter 2 | Transient Flow in a Homogeneous Incompressible Fluid | 17 |
| Chapter 3 | The Spin-up of a Continuously Stratified Fluid | 22 |
| Chapter 4 | The Spin-up of a Two-Layer System | 42 |
| Chapter 5 | Spin-up Experiments | 59 |
| Chapter 6 | The Effect of Ekman Friction on Wind Generated Ocean Currents | 67 |
| Chapter 7 | The Evolution of a Baroclinic Vortex | 81 |
| Chapter 8 | The Influence of a Variable Coriolis Force | 88 |
| Appendix A | Baroclinic Instability | 99 |
| Appendix B | The Side Wall Boundary Layers | 102 |
| Bibliography | | 109 |

LIST OF FIGURES

| | | Page |
|------------|---|------|
| Figure 2.1 | The decay of a geostrophic current in a homogeneous fluid with bottom friction. | 20 |
| Figure 2.2 | The decay of a geostrophic current in a homogeneous fluid with lateral viscosity. | 21 |
| Figure 3.1 | The cylindrical coordinate system. | 22 |
| Figure 3.2 | Spin-up time vs. the internal rotational Froude number for the continuously stratified model. | 25 |
| Figure 3.3 | Velocity profile in the quasi-steady state for the continuous model. | 30 |
| Figure 3.4 | Quasi-steady velocity at $Z = 0$ vs. the internal rotational Froude number. | 37 |
| Figure 3.5 | The density field for $\epsilon = 1$ and $\tau = \sqrt{g_0}$ in the continuous model. | 39 |
| Figure 4.1 | The two-layer model. | 42 |
| Figure 4.2 | Spin-up of an immiscible two-layer fluid for small ϵ . | 51 |
| Figure 4.3 | Quasi-steady top layer velocity vs. the internal rotational Froude number. | 57 |
| Figure 4.4 | Spin-up time vs. the internal rotational Froude number in the two-layer model. | 58 |
| Figure 5.1 | Schematic cross section of the experimental apparatus. | 60 |
| Figure 5.2 | Baroclinic instability effects on the spin-up velocity profile. | 65 |
| Figure 6.1 | The ratio of the baroclinic to barotropic amplitudes vs. the wind stress period. | 72 |
| Figure 6.2 | Observed temperature and temperature gradient profiles for the North Atlantic (solid lines) and a simple analytic approximation (dotted lines). | 75 |

Figures cont.

Page

| | | |
|------------|--|----|
| Figure 8.3 | Vertical structure of the baroclinic mode for the constant and variable static stability models, $L = 10^8 \text{ cm}$. | 79 |
| Figure 8.1 | Rossby-wave frequencies for the two-layer model vs. the horizontal scale of motion. | 80 |
| Figure 8.2 | Amplitudes of coefficients in the two-layer model vs. forcing frequency, for $L = 10^7 \text{ cm}$. | 93 |
| Figure 8.3 | Amplitudes of coefficients in the two-layer model vs. forcing frequency, for $L = 10^8 \text{ cm}$. | 94 |
| Figure 8.4 | Amplitudes of coefficients in the continuously stratified model vs. forcing frequency. | 98 |

ACKNOWLEDGEMENTS

I wish to express my thanks to Professor Jule G. Charney for suggesting the topic of this research and acting as my thesis advisor. I am also indebted to him for introducing me to the fascinating realm of rotational fluid dynamics.

I would like to thank Professor Raymond Hide, director of the hydrodynamics of rotating fluids laboratory at M. I. T., for generously providing the facilities for the experiments described here. I am also grateful to Professor H. P. Greenspan for several valuable discussions.

This research was supported in part by my wife Margaret under contract of marriage.

Chapter 1

Introduction and Summary

"It is more important to have beauty in one's equations than to have them fit experiment"

— P.A.M. Dirac

The unique character of the viscous boundary layer established in a rotating fluid system when a geostrophically balanced current flows above a rigid boundary has been recognized for many years. The Swedish Oceanographer Ekman (1905) derived the mathematical form of the velocity profile in such a layer, now known as the Ekman spiral. However, the Ekman boundary layer effects have not generally been included in analytic studies of atmospheric and oceanic motions. Charney and Eliassen (1949) showed that the entire effect of friction in the Ekman layer could be represented by a condition on the vertical velocity at the top of this layer. The present work makes use of this fact in an effort to evaluate the role of Ekman layers in determining the response of the oceans to wind stresses.

A complete theory of the general circulation of the atmosphere must take account of the interaction of the ocean with the atmosphere at the sea surface. The wind stresses acting on the ocean generate currents, and these currents may change the heating distribution over the oceans, causing nonlinear feedback to the atmospheric driving system. It is obvious that if we hope to study this complex interaction process successfully we must first understand the response of the oceans to variable wind stresses. This problem has been treated analytically by Rossby (1938), Charney (1955) and Veronis and Stommel (1956). In these studies it was concluded that the ocean responds barotropically, provided that the forcing frequency is less than the order

of one year. That is, the currents generated reach all the way to the bottom. Veronis and Stommel, by including the latitudinal variation of the Coriolis parameter, were able to show that for very long periods the response is baroclinic, and the motion is confined primarily to the layer above the thermocline. They also found a strong dependence on the spatial scale, such that for horizontal scales less than 100 km, the baroclinic mode predominates even for periods as short as several days, whereas cyclonic scale motions (~1,000 km) produce a barotropic response for periods as great as several months. An important question is then: why don't atmospheric storms produce strong barotropic components in the observed ocean currents?

In none of the previous studies of this problem has bottom friction been specifically included in the analytic formulation. Thus, one purpose of this paper is to examine the role of bottom friction in maintaining the baroclinicity of the oceans.

In chapter 2 we briefly review Rossby's ideas on the diffusion of currents in a homogeneous fluid. The equations of motion are non-dimensionalized, and it is shown that Rossby's fourth order diffusion equation is actually the asymptotic equation appropriate for a two-layer model in which the bottom layer is infinitely deep and motionless. In most ordinary laboratory and ocean models, however, Ekman bottom friction dominates and Rossby's solution is inappropriate.

Chapter 3 is devoted to a discussion of the transient motion which results when a cylindrical vessel containing a stratified fluid in steady state rotation has its rotation rate impulsively changed. This so called spin-up problem was studied for a homogeneous fluid by Greenspan and Howard

(1963). Their problem is closely related to the generation of ocean currents by wind stresses, because in both cases the interior fluid is forced by the vertical flux of mass out of an Ekman boundary layer. Furthermore, the mathematical solutions for the spin-up problem have the distinct advantage of being verifiable by simple laboratory experiments. The theory indicates that in a stratified fluid the Ekman layer convergence spins the fluid up to a quasi-steady state which is not solid body rotation. It is, rather, a geostrophically balanced flow in which horizontal density gradients create a vertical shear in the angular velocity. This quasi-steady velocity is equal to the angular velocity of the cylinder at the top of the Ekman boundary layer, but decreases exponentially away from the boundary. The exponential decrease is proportional to the inverse square root of the parameter ϵ , where ϵ may be called the internal rotational Froude number:

$$\epsilon = \frac{\Omega_0^2 L^2}{g \frac{\Delta \rho}{\rho} H}$$

Here ϵ is the basic rotation rate of the cylinder, L and H are the radius and depth respectively, g is the gravitational acceleration and $\frac{\Delta \rho}{\rho}$ is the fractional density difference between the fluid at the bottom and top of the cylinder. ϵ may be regarded as a measure of the ratio of the rotational force to the static stability force. Similarly, the spin-up time, which is less than that for a homogeneous fluid, is a function of ϵ such that as ϵ decreases the spin-up time also decreases.

Chapter 4 extends the spin-up problem discussion to two-layer laboratory systems. It is shown that two fundamentally different two-layer models are possible. The first, composed of immiscible fluids, has a zero order

density discontinuity at the interface. In this case Ekman layer viscosity is a first order effect at the interface and the top layer spins-up to solid body rotation in a small multiple of the spin-up time for a homogeneous fluid. An instance of the second type of two-layer model is a fresh water top layer and salt water bottom layer. Here the density discontinuity is destroyed by diffusion and a boundary layer develops in which the density changes continuously from its value in the top layer to its value in the bottom layer. It turns out that Ekman friction at the interface is a second order effect in this case and the spin-up process is closely analogous to that for the continuously stratified model. The bottom layer, forced by the rigid bottom boundary, spins-up to solid body rotation. But the top layer, which has a free surface, is not forced directly by friction but responds only to the pressure field induced by curvature of the interface. Thus, in the quasi-steady state there is shear between the top and bottom layers. Only on the much longer diffusion time scale will the top layer approach solid body rotation at the new rotation rate.

In Chapter 5 a simple experimental procedure for confirming the spin-up theory of the previous two chapters is described. Results of experiments for both two-layer and continuously stratified fluids are displayed. Discussion of the problems presented by possible baroclinic instability and mixing at the vertical boundaries is relegated to the appendices.

The remaining chapters are devoted to applying the results of the spin-up theory to simplified models of the real oceans. In the sixth chapter it is shown that if a wind stress acts on the ocean for a finite time both baroclinic and barotropic currents are generated, but the barotropic mode decays on the spin-up time scale, leaving a quasi-steady baroclinic current

whose amplitude is dependent on the frequency and scale of the forcing.

In the seventh chapter the evolution of such a baroclinic vortex is studied. The theoretical development must be carried to the next higher order to include viscosity effects in the interior. The resulting solution indicates that in the absence of heat diffusion the current decays slowly through horizontal spreading due to both the meridional circulation and horizontal eddy diffusion, with very little change in its vertical structure.

Finally, in the eighth chapter the role of latitudinal variation of the Coriolis parameter (the so called β -effect) is discussed. Solutions are obtained for simple harmonic traveling disturbances. It is shown that β increases the baroclinicity of the response for low frequency driving forces, and that bottom friction enhances this effect.

Chapter 2

Transient Flow In A Homogeneous Incompressible Fluid

C.G. Rossby (1937) was the first worker to study in some detail the frictional decay of geostrophically balanced currents. In the first of his papers on the adjustment of large scale flow to the Coriolian pressure field he heuristically obtained an equation which he believed to govern the diffusion of momentum for a zonally uniform current in a homogeneous, incompressible fluid on an infinite rotating plane.

In the present chapter, as an introduction to the methods of analysis which will later be applied to stratified fluids, we reexamine the problem treated by Rossby with the addition of frictional effects at the bottom boundary. It is advantageous to express the governing equations in nondimensional form to clearly exhibit the conditions under which Rossby's solution is valid.

The equations of horizontal momentum for a fluid on an infinite rotating plane may be written

$$\frac{\partial u^*}{\partial t^*} + u^* \frac{\partial u^*}{\partial x^*} + v^* \frac{\partial u^*}{\partial y^*} + w^* \frac{\partial u^*}{\partial z^*} - f v^* = -\frac{1}{\rho^*} \frac{\partial p^*}{\partial x^*} + \nu_z \frac{\partial^2 u^*}{\partial z^{*2}} + \nu_H \nabla^{*2} u^* \quad (2.1)$$

$$\frac{\partial v^*}{\partial t^*} + u^* \frac{\partial v^*}{\partial x^*} + v^* \frac{\partial v^*}{\partial y^*} + w^* \frac{\partial v^*}{\partial z^*} + f u^* = -\frac{1}{\rho^*} \frac{\partial p^*}{\partial y^*} + \nu_z \frac{\partial^2 v^*}{\partial z^{*2}} + \nu_H \nabla^{*2} v^* \quad (2.2)$$

where f is the Coriolis parameter, u^* and v^* are the velocity components in the x^* and y^* directions respectively, p^* is the pressure, ρ^* is the constant density, ν_z and ν_H are viscosity coefficients for vertical and horizontal stresses respectively, and ∇^{*2} is the horizontal Laplacian $\frac{\partial^2}{\partial x^{*2}} + \frac{\partial^2}{\partial y^{*2}}$. If we were modelling the oceans ν_z and ν_H would be eddy stress coefficients and generally unequal. But for laboratory models with laminar flow $\nu = \nu_z = \nu_H$ where ν is the molecular kinematic viscosity coefficient. For the scales of

motion in which we are interested vertical accelerations are negligible compared to the gravitational acceleration, thus the hydrostatic approximation is valid:

$$\frac{\partial p^*}{\partial z^*} = -\rho^* g \quad (2.3)$$

To close the system we need the continuity equation:

$$\frac{\partial w^*}{\partial z^*} = -\frac{\partial u^*}{\partial x^*} - \frac{\partial v^*}{\partial y^*} \quad (2.4)$$

In the above equations, as in the rest of this work, dimensional variables are starred. All other variables are nondimensional.

We assume that the motion is independent of x and let the initial current be $u_{t=0} = u(y)$. Introducing the scales U , L and H which represent typical horizontal velocity, horizontal scale, and vertical scale respectively, we define nondimensional variables which are of order unity provided that the motions are hydrostatic and in approximate geostrophic balance:

$$\begin{aligned} u^* &= uU, & v^* &= vULRo, & w^* &= wULRo \frac{H}{L}, \\ x^* &= xL, & y^* &= yL, & z^* &= zH, \\ p^* &= p_0^* (1 + Ro \epsilon h) \quad \text{where } p_0^* = \rho^* g H \end{aligned}$$

H represents the mean free surface height of the fluid and h is a nondimensional measure of the deviation from that mean. The nondimensional parameters ϵ and Ro are defined:

$$\epsilon = \frac{f^2 L^2}{gH} \quad Ro = \frac{U}{fL}$$

Ro is the Rossby number which is small for geostrophic motions v^* and w^* are scaled with Ro because they represent the small divergent component of the motion. Using the additional parameters $\delta^2 = \frac{U^2}{L^2} \frac{y_H}{y_z}$ and $\bar{r}_H = \frac{y_H}{UL}$ the nondimensional equations may be written as:

$$R_0 \left(\frac{\partial u}{\partial t} + R_0 v \frac{\partial u}{\partial y} + R_0 w \frac{\partial u}{\partial z} \right) - R_0 v = R_0 R_H \frac{\partial^2 u}{\partial y^2} + \frac{R_0 R_H}{S^2} \frac{\partial^2 u}{\partial z^2} \quad (2.5)$$

$$R_0^2 \left(\frac{\partial v}{\partial t} + R_0 v \frac{\partial v}{\partial y} + R_0 w \frac{\partial v}{\partial z} \right) + u = -\frac{\partial h}{\partial y} + R_0^2 R_H \frac{\partial^2 v}{\partial y^2} + \frac{R_0^2 R_H}{S^2} \frac{\partial^2 v}{\partial z^2} \quad (2.6)$$

$$\frac{\partial w}{\partial z} = -\frac{\partial v}{\partial y} \quad (2.7)$$

From (2.6) we obtain

$$u = -\frac{\partial h}{\partial y} + o(R_0)^2 \quad (2.8)$$

Therefore u is independent of z to $O(R_0^2)$ provided that $R_H \lesssim 1$ which is the case for all systems of interest to us. Now, at the bottom boundary u must be zero and a boundary layer must develop. Charney and Eliassen (1949) showed that the frictional dissipation in this Ekman boundary layer may be included in the equations for the interior as a condition on the vertical velocity at $z = 0$. Dimensionally this condition may be expressed as

$$w_0^* = \sqrt{\frac{\nu_z}{a^2}} \frac{\partial u^*}{\partial y^*} \quad \text{thus,} \quad w_0 = \sqrt{\frac{\nu_z}{2D}} \frac{1}{R_0 H} \frac{\partial u}{\partial y} \quad (2.9)$$

If equation (2.5) is differentiated by $\frac{\partial}{\partial y}$ and the non-linear term which is $O(R_0)$ is neglected then we obtain the vorticity equation:

$$\frac{\partial}{\partial t} \left(\frac{\partial u}{\partial y} \right) - \frac{\partial v}{\partial y} - R_H \frac{\partial^3 u}{\partial y^3} = 0 \quad (2.10)$$

Substituting from the continuity equation and integrating in z we get

$$\frac{\partial}{\partial t} \left(\frac{\partial u}{\partial y} \right) + w_h - w_0 - R_H \frac{\partial^3 u}{\partial y^3} = 0 \quad (2.11)$$

where w_h is the vertical velocity at the free surface $w_h^* = \frac{dh^*}{dt^*}$. Thus,

$w_h = \epsilon \frac{dh}{dt}$. Now $\frac{dh}{dt} = \frac{\partial h}{\partial t} + R_0 v \frac{\partial h}{\partial y}$. Then to $O(R_0)$ the velocity at the top may be written $w_h = \epsilon \frac{\partial h}{\partial t}$. Differentiating the vorticity equation

by $\frac{\partial}{\partial y}$ and substituting from (2.9) for w , we obtain

$$\frac{\partial}{\partial t} \left(\frac{\partial^2 u}{\partial y^2} - \epsilon u \right) + E \frac{\partial^2 u}{\partial y^2} - R_H \frac{\partial^4 u}{\partial y^4} = 0 \quad (2.12)$$

where $E = \sqrt{\frac{\nu}{2f}} \frac{1}{R_0 H}$ measures the strength of Ekman friction. The three parameters ϵ , E and R_H control the nature of the time evolution of the

field. The following cases are of interest. If the fluid is very deep, so that $E \ll 1$ and $R_H/E \gg 1$, then horizontal diffusion dominates. The time scale is set by the value of R_H which may be very small but must still balance the $\frac{\partial}{\partial t}$ terms for any time dependent motion to exist. The diffusion is of two possible classes depending on the magnitude of ϵ .

1) For low rotation rates, $\epsilon \ll 1$ there will be an approximate balance between the first and last terms in equation (2.12). This is just the form of an ordinary diffusion equation and the half width of the current $u(y)$ increases as \sqrt{t} .

2) For high rotation rates, $\epsilon \gg 1$ the balance is between the second and fourth terms. The resulting equation is a fourth order diffusion-type equation in which the current half width increases as $t^{1/4}$. Therefore rotation is stabilizing against horizontal diffusion. This latter case is the equation which Rossby studied. He neglected the time derivative in both momentum equations, retaining only the time rate of change of the free surface height. His solution is valid then only in the case $\epsilon \gg 1$. For typical currents in a homogeneous ocean if the horizontal scale $L = 1,000$ km, $\epsilon = 1$, and Rossby's results are not valid. Rossby's result is however appropriate for a two layer fluid system in which the bottom layer is very deep. For in that case ϵ involves the reduced gravity $g' = g \frac{\Delta \rho}{\rho}$, where $\Delta \rho$ is the

density difference between the layers. In two layer ocean models $\Delta\rho \approx 2 \times 10^{-3}$ so that $E \approx 10^3$ (for $L \approx 10^3$ km.).

In a typical laboratory model the scales are: $L \approx 10^2$ cm, $H \approx 10$ cm, $f \approx 2 \text{ sec}^{-1}$, $U \approx 2 \text{ cm sec}^{-1}$. Therefore, $E \approx .5$ and $R_H \approx 5 \times 10^{-4}$, where we have used the molecular viscosity coefficient for water $\nu = .01 \text{ cm}^2 \text{ sec}^{-1}$. Similarly, in a homogeneous ocean model we choose scales typical of Gulf Stream eddies: $L \approx 10^7$ cm, $H \approx 10^5$ cm, $f \approx 10^{-4} \text{ sec}^{-1}$, and $U \approx 10^2 \text{ cm sec}^{-1}$. Eddy viscosity values of $\nu_H \approx 10^5 \text{ cm}^2 \text{ sec}^{-1}$ and $\nu_z \approx 10^2 \text{ cm}^2 \text{ sec}^{-1}$ are typical of those quoted in the literature (see for example Hill (1963)). Thus, $E \approx .1$ and $R_H \approx .01$. In both cases $E/R_H \gg 1$, so that bottom friction completely dominates in the decay process.

To analyze this case it is convenient to define new independent variables $S = Et$ and $\eta = \sqrt{E} y$. Then equation (2.12) may be written in the form

$$\frac{\partial}{\partial S} \left(\frac{\partial^2 u}{\partial \eta^2} - u \right) + \frac{\partial^2 u}{\partial \eta^2} = 0 \quad (2.13)$$

If we try solutions of the form

$$u(\eta, S) = \frac{1}{2\pi} \int_{-\infty}^{+\infty} f(k, S) e^{ik\eta} dk \quad (2.14)$$

we find that $f(k, S)$, the Fourier transform of u , must satisfy the equation

$$\frac{df}{dS} + \left(\frac{k^2}{k^2+1} \right) f = 0$$

Hence

$$f(k, S) = G(k, 0) e^{-\frac{k^2}{1+k^2} S} \quad (2.15)$$

where $G(k, 0)$ is the Fourier transform of the initial condition

$$G(k, 0) = \int_{-\infty}^{+\infty} u(\eta', 0) e^{-ik\eta'} d\eta'$$

For the initial condition we will assume a jet symmetric about $y=0$ with a

Gaussian distribution in y .

$$u(\eta, 0) = \frac{1}{\sqrt{2\pi} A} e^{-\frac{\eta^2}{2A^2}} \quad (2.16)$$

where A is a constant. The Fourier transform of (2.16) is,

$$G(k, 0) = e^{-\frac{k^2 A^2}{2}}$$

Hence, we obtain as an integral expression for u ,

$$u(\eta, s) = \frac{1}{\pi} \int_0^\infty e^{-\frac{k^2 A^2}{2}} e^{-\frac{k^2}{1+k^2} s} \cos k\eta \, dk \quad (2.17)$$

Equation (2.17) may be numerically integrated to obtain typical values of u for various η and s . For an initial width $A = \frac{1}{\sqrt{2}}$ the evolution of u in time for various values of η is plotted in Figure 2.1. Because $\eta = \sqrt{\epsilon} y$ increasing the value of η corresponds either to increasing the horizontal distance from the origin or increasing ϵ for a given y .

Now ϵ measures the magnitude of the free surface height perturbations. For large ϵ the change in momentum due to Ekman friction is therefore accompanied by large mass adjustments due to changes in the free surface height, and a corresponding diffusion of the geostrophic current. For small ϵ the free surface is essentially level, there is very little mass adjustment and the current simply decays exponentially with very little diffusion. The latter is essentially the spin-down problem treated by Greenspan and Howard (1953). The opposite case $R_H/\epsilon \gg 1$, which is appropriate for the motion of the top layer in a two layer model with a very deep lower layer, may be solved in a similar manner using the Fourier transform. The integral expression for the velocity is in this case

$$u(\eta, s) = \frac{1}{\pi} \int_0^\infty e^{-\frac{k^2 A^2}{2}} e^{-\frac{k^4}{1+k^2} s} \cos k\eta \, dk \quad (2.18)$$

Comparison with equation (2.17) indicates that the high wave numbers diffuse

out more rapidly in the present case. The results are plotted in Figure 2.2. Here $\eta = \sqrt{\epsilon} \gamma$ again, but $S = t \frac{gH}{\epsilon}$ so that changing the rotation rate will change the time scale. For $\eta = 4$ the weak counter current discussed by Rossby is apparent in the figure. Hence it can be seen that Rossby's results are applicable only to large scale currents confined to the surface layer in the real ocean.

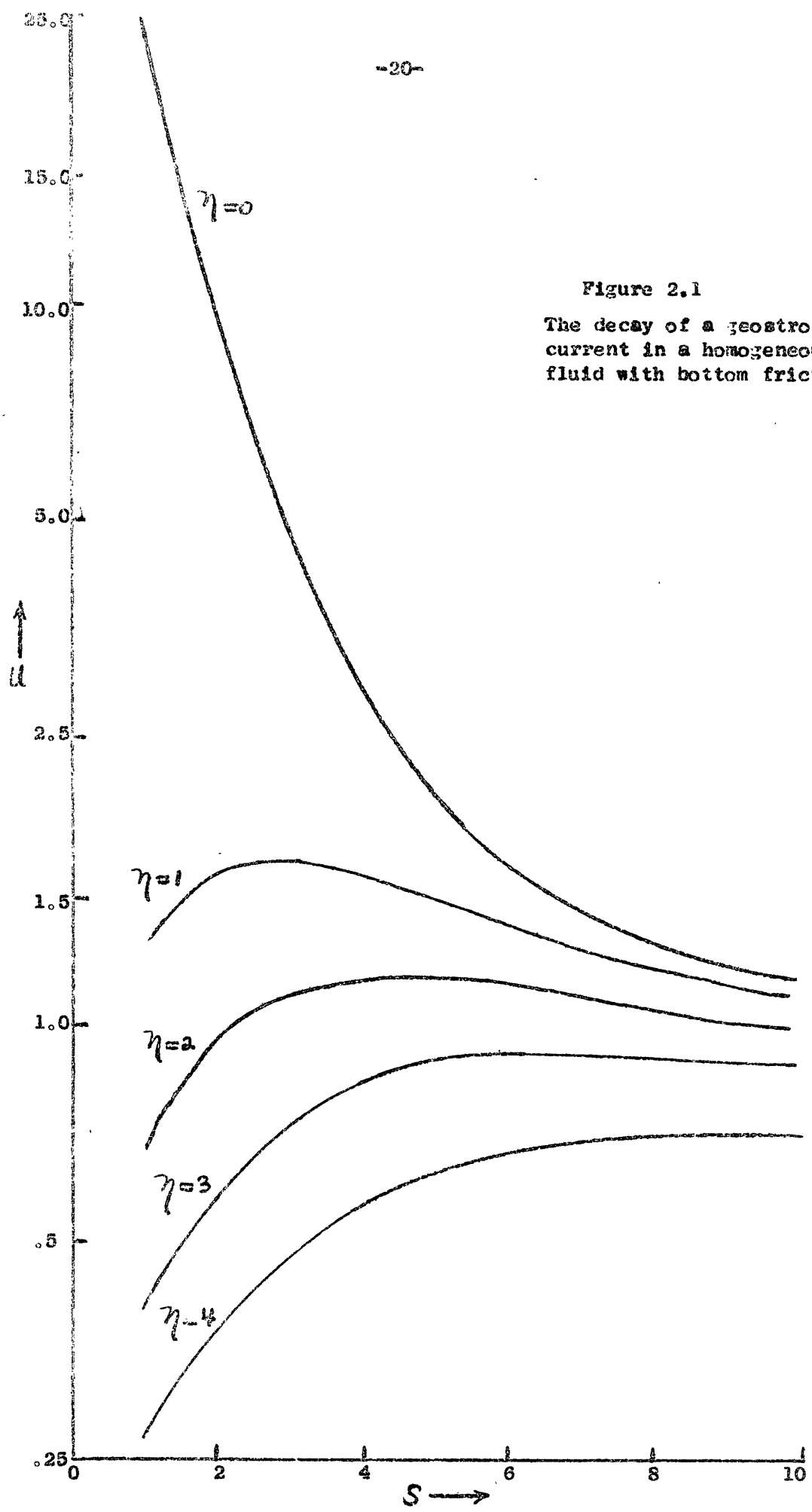


Figure 2.1
The decay of a geostrophic current in a homogeneous fluid with bottom friction.

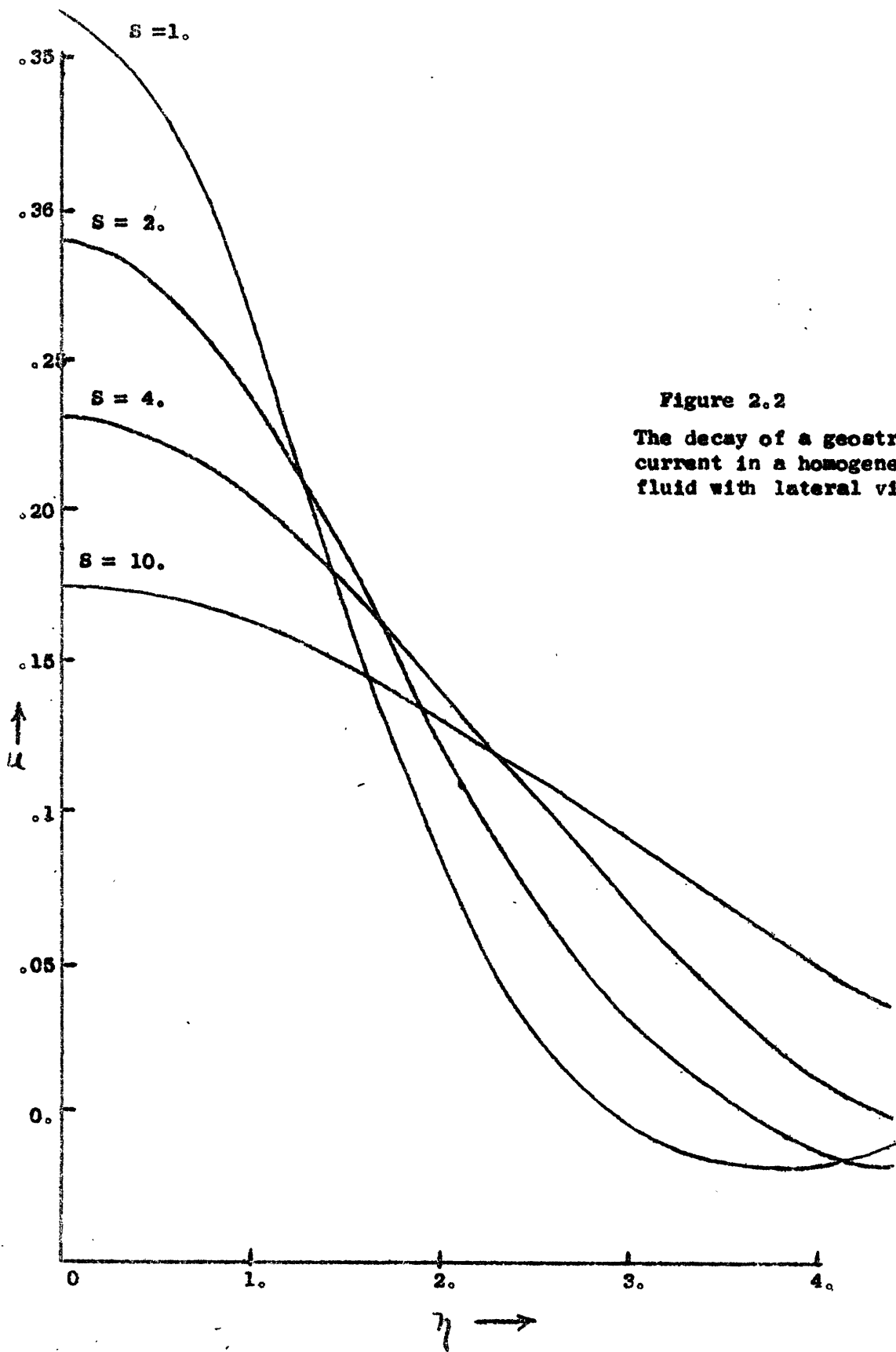


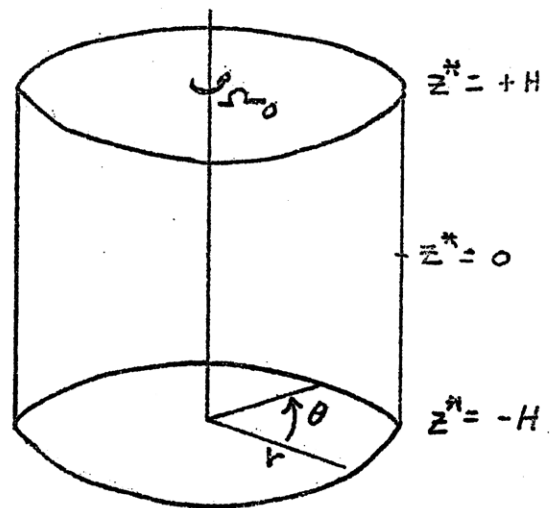
Figure 2.2
 The decay of a geostrophic current in a homogeneous fluid with lateral viscosity.

Chapter 3

The Spin-Up of a Continuously Stratified Fluid

We consider a cylindrical vessel rotating about its vertical (z) axis with angular velocity Ω_0 as illustrated in Figure 3.1. The vessel is filled with a viscous fluid confined between rigid horizontal boundaries at $z^* = \pm H$. If we assume that the radius to depth ratio of the cylinder is $\geq O(1)$, then viscous diffusion effects along the rigid vertical boundary of the vessel will play a negligible role in the spin-up of the fluid in the interior. (See Appendix B for a heuristic discussion of the side wall boundary layers).

We now solve the initial value problem in which at time $t^* < 0$ the fluid and vessel are in solid body rotation at the angular velocity $\Omega = \Omega_0$, and at $t^* = 0$ the angular velocity of the vessel is impulsively changed by a small amount ω ,



so that for $t^* > 0$, $\Omega = \Omega_0 + \omega$. We wish to determine the characteristic time for the fluid to approach solid body rotation at the new rotation rate.

Greenspan and Howard (1963) have solved this problem for a homogeneous incompressible fluid in elegant detail. They showed that the spin-up takes place in three time scales corresponding to three distinct physical mechanisms. If a nondimensional time is defined by $\bar{t} = t^* \Omega_0$, then the characteristic time scales are as follows: (1) In time $\bar{t} \sim O(1)$ Ekman boundary layers have

developed as a result of the stresses on the rigid surfaces at $z = \pm H$. The e-folding depth of these Ekman layers is $\sqrt{\frac{\nu}{4\Omega_0}}$, where ν is the kinematic viscosity. (2) In time $t = \left(\frac{\Omega_0 H^2}{\nu}\right)^{1/2}$ the interior fluid has spun-up to the new rotation rate within order e^{-1} . (3) In time $t = \frac{\Omega_0 H^2}{\nu}$ all residual inertial oscillations have decayed through viscous diffusion.

The third time scale is the time for viscous diffusion effects to penetrate to the center of the fluid. (In a nonrotating system this is the characteristic time for response of the interior to boundary stresses). For cases of physical interest $\frac{\Omega_0 H^2}{\nu}$ is large, and since in the rotating case the interior responds in a time of order $\left(\frac{\Omega_0 H^2}{\nu}\right)^{1/2}$ we see that rotation decreases immensely the time in which the interior responds to boundary stresses. The physical reason for this behavior of rotating fluids is that boundary stresses cause a centrifugal outflow in the Ekman layer. Continuity then demands a slow radial inflow in the interior to preserve mass. Viscosity effects are negligible in the interior so that angular momentum is conserved and the radial inflow increases the vorticity in the interior by replacing low angular momentum fluid with high angular momentum fluid. In this manner the interior is brought up to the new rotation rate in a time which is approximately Ω_0^{-1} times the ratio of the depth of the vessel to the depth of the Ekman layers.

In the homogeneous incompressible case the mathematics may be simplified because it is possible to reduce the Eulerian equations of motion to two equations in the variables V and ϕ , where V is the azimuthal velocity and ϕ is a stream function for the meridional (r, z plane) motion. The radial dependence is easily separated out because V and ϕ are both

linear functions of the radius. The final equations involve only the independent variables \bar{z} and \bar{t} , and may be solved by use of the Laplace transform. For a stratified fluid it is not possible to separate out the radial dependence so simply and reduce the Eulerian equations to a tractable form. We must therefore employ the methods of dimensional scaling in hopes of obtaining a simplified mathematical formulation while retaining the important physical features of the problem.

We designate V_θ^* , V_r^* , and w^* as the azimuthal, radial and vertical velocities respectively and assume polar symmetry ($\frac{\partial}{\partial \theta} \equiv 0$). The equations of motion are then in polar coordinates:

$$\frac{\partial V_r^*}{\partial t^*} + \left(V_r^* \frac{\partial V_r^*}{\partial r^*} - \frac{V_\theta^{*2}}{r^*} + w^* \frac{\partial V_r^*}{\partial z^*} \right) - 2\Omega_0 V_\theta^* = -\frac{1}{\rho^*} \frac{\partial p^*}{\partial r^*} + \nu \left(\nabla^{*2} V_r^* + \frac{\partial^2 V_r^*}{\partial z^{*2}} \right) \quad (3.1)$$

$$\frac{\partial V_\theta^*}{\partial t^*} + \left(V_r^* \frac{\partial V_\theta^*}{\partial r^*} + \frac{V_r^* V_\theta^*}{r^*} + w^* \frac{\partial V_\theta^*}{\partial z^*} \right) + 2\Omega_0 V_r^* = \nu \left(\nabla^{*2} V_\theta^* + \frac{\partial^2 V_\theta^*}{\partial z^{*2}} \right) \quad (3.2)$$

$$\frac{\partial w^*}{\partial t^*} + \left(V_r^* \frac{\partial w^*}{\partial r^*} + w^* \frac{\partial w^*}{\partial z^*} \right) = -\frac{1}{\rho^*} \frac{\partial p^*}{\partial z^*} - g + \nu \left(\nabla^{*2} w^* + \frac{\partial^2 w^*}{\partial z^{*2}} \right) \quad (3.3)$$

The equation of continuity is,

$$\frac{\partial \rho^*}{\partial t^*} = \frac{1}{r^*} \frac{\partial}{\partial r^*} \left(r^* \rho^* V_r^* \right) - \frac{\partial \rho^* w^*}{\partial z^*} \quad (3.4)$$

We assume that the fluid is incompressible so that the equation of state may be written,

$$\rho^* = \rho_s^* (1 - \alpha T'^*)$$

where $\rho_s^*(z)$ is a standard density dependent on depth alone, T'^* is the deviation of temperature from a standard temperature $T_s^*(z)$, and α is

the coefficient of thermal expansion. Alternatively, if the stratification is produced by salinity gradients we may write in place of (2.5)

$$\rho^* = \rho_s^* (1 - \rho')$$

where ρ' is a nondimensional departure from the standard density $\rho_s^*(z)$. The final equation necessary to close the system is the first law of thermodynamics. There are no internal heat sources in the system, so diffusion of heat is the only contribution to the heating rate. Using the assumption of incompressibility the first law becomes

$$\frac{\partial T^*}{\partial t^*} + v_r^* \frac{\partial T^*}{\partial r^*} + w^* \frac{\partial T^*}{\partial z^*} = \kappa \left(\nabla^{*2} T^* + \frac{\partial^2 T^*}{\partial z^{*2}} \right) \quad (3.6)$$

where κ is the thermometric conductivity. Equations (2.1) - (2.6) are now nondimensionalized so that the fundamental physical parameters which determine the character of the motion are isolated and all dependent variables become of order unity.

We define the scale lengths L and H where L is the radius of the cylinder and H is its depth. To set the time scale we utilize Greenspan and Howard's result for the spin-up time of a homogeneous incompressible fluid. We let $\tau = \left(\frac{H^2}{2\Omega_0 \nu} \right)^{1/2}$ and anticipate that in the stratified case the transient meridional circulation forced by convergence in the Ekman layers has a time scale of order τ . This assumption is justified a posteriori by the the solution. The velocity scale is determined by the magnitude of ω (the change in angular velocity of the cylinder). Using the scales L , H , τ and ω we define the nondimensional variables

$$\begin{aligned} r &= r^*/L, & z &= z^*/H, & t &= t^*/\tau \\ v_\theta &= v_\theta^*/\omega L, & v_r &= v_r^*/\omega L, & w &= w^*/\omega H \end{aligned} \quad (3.7)$$

We utilize the following nondimensional numbers:

$$\lambda^2 = 2\Omega_0 H^2 / \nu \quad (\text{Taylor number})$$

$$\sigma = \nu / \kappa \quad (\text{Prandtl number})$$

$$\epsilon = \frac{4\Omega_0^2 L^2}{gKH} \quad (\text{Internal rotational Froude number})$$

$$Ro = \frac{U}{2\Omega_0} \quad (\text{Rossby number})$$

where $K = H\alpha \frac{dT_s^*}{dz^*} = -\frac{H}{\rho_s^*} \frac{d\rho_s^*}{dz^*}$. We also need $\delta = L/H$ and

$\mu = \frac{\rho_s^* g H}{\rho_s^*}$ (the standard temperature, density and pressure respectively) are functions of z^* alone. For quasi-geostrophic

motions it is appropriate to scale the pressure, density and temperature as follows (see Charney and Stern (1952)):

$$p^* = p_s^* (1 + \mu K \epsilon Ro p)$$

$$\rho^* = \rho_s^* (1 - K \epsilon Ro T) = \rho_s^* (1 - K \epsilon Ro p)$$

$$T^* = T_s^* + \frac{K \epsilon Ro}{\alpha} T$$

Applying the variables of (2.7) to equations (2.1) through (2.4)

we obtain the following nondimensional equations. For horizontal momentum

$$\lambda \frac{\partial v_r}{\partial t} + Ro \left(v_r \frac{\partial v_r}{\partial r} + w \frac{\partial v_r}{\partial z} - \frac{v_\theta^2}{r} \right) - v_\theta = -\frac{\partial p}{\partial r} + \lambda^2 \left(\nabla_s^2 + \frac{\partial^2}{\partial z^2} \right) v \quad (3.8)$$

$$\lambda \frac{\partial v_\theta}{\partial t} + Ro \left(v_r \frac{\partial v_\theta}{\partial r} + w \frac{\partial v_\theta}{\partial z} + \frac{v_r v_\theta}{r} \right) + v_r = \lambda^2 \left(\nabla_s^2 + \frac{\partial^2}{\partial z^2} \right) v_\theta \quad (3.9)$$

If the standard dimensional variables p_s^* and ρ_s^* are chosen to satisfy

the hydrostatic relationship,

$$\frac{dP_s^*}{dz^*} = -\rho_s^* g \quad (3.10)$$

then equation (3.3) becomes

$$\lambda \frac{\partial W}{\partial t} + R_0 \left(v_r \frac{\partial W}{\partial r} + w \frac{\partial W}{\partial z} \right) = \delta^2 \left(T - \frac{\partial P}{\partial z} \right) + \lambda^2 \left(\nabla_{\delta^2}^2 + \frac{\partial^2}{\partial z^2} \right) W \quad (3.11)$$

The continuity equation (3.4) becomes,

$$\mathcal{K} \epsilon \left[\lambda \frac{\partial T}{\partial t} + R_0 \left(v_r \frac{\partial T}{\partial r} + w \frac{\partial T}{\partial z} \right) \right] + \mathcal{K} W = -\frac{1}{r} \frac{\partial r v_r}{\partial r} - \frac{\partial W}{\partial z} \quad (3.12)$$

And the heat equation is

$$\lambda \frac{\partial T}{\partial t} + R_0 \left(v_r \frac{\partial T}{\partial r} + w \frac{\partial T}{\partial z} \right) = -\frac{W}{\epsilon} + \frac{\lambda^2}{\sigma} \left(\nabla_{\delta^2}^2 + \frac{\partial^2}{\partial z^2} \right) T \quad (3.13)$$

Equations (3.8) - (3.13) involve the six independent parameters σ , \mathcal{K} ,

ϵ , R_0 , δ and λ . To further simplify the system we must place restrictions on the values of these parameters. We limit the discussion to

fluid systems which are Boussinesq (i.e., the total density variation is small compared to the mean density). In such fluids $\mathcal{K} \ll 1$, and provided that

ϵ is not too great $\mathcal{K} \epsilon \ll 1$ also. As stated previously we assume $\delta \gg 0(1)$.

Furthermore, we require that $R_0 \equiv \frac{\omega}{2\Omega_0} \ll 1$ so that the motion is quasi-

geostrophic. We must allow ϵ to vary over a rather large range in order to study the effect of varying static stability.

The parameter λ is small for all cases of interest and since it multiplies the diffusion terms it is a natural parameter to use in a perturbation series expansion of the equations. In the lowest order expansions of the heat and momentum equations the terms involving the second derivative with respect to z will be lost. Therefore, boundary layer type solutions will in general be necessary to satisfy the boundary conditions at $z = \pm 1$. It turns out that solutions valid throughout the region $-1 \leq z \leq +1$ may be

written in the form

$$\{v_r; v_\theta; w; p\} \equiv \{v_r^I(z,t); v_\theta^I(z,t); w^I(z,t); p^I(z,t)\} \\ + \{v_r^B(\xi,t); v_\theta^B(\xi,t); w^B(\xi,t); p^B(\xi,t)\} \quad (3.14)$$

where the I superscripted variables represent the solution in the interior and B superscripted variables are boundary layer contributions which approach zero exponentially as $\xi \rightarrow -\infty$. Here ξ is the stretched coordinate

$$(1 - |z|) = -\lambda \xi \quad (3.15)$$

The boundary layer thickness is just the Ekman layer depth measure λ .

Using the above formalism we expand the variable formally as follows:

$$f(r, z, t) = f^I(r, z, t) + f^B(r, \xi, t) \\ = \sum_{n=0}^{\infty} F_n^I(r, z, t) \lambda^n + \sum_{n=0}^{\infty} F_n^B(r, \xi, t) \lambda^n \quad (3.16)$$

where $f(r, z, t)$ stands for any of the variables v_θ , v_r , w or p . All of the coefficients F_n^B must become exponentially small as $\xi \rightarrow -\infty$.

We first examine the equations valid for the interior region. The zero order expansion for the interior is from equations (3.8), (3.9), (3.11) and (3.13):

$$v_{\theta 0}^I = \frac{\partial p_0^I}{\partial r} \\ v_{r 0}^I = 0 \\ T_0^I = \frac{\partial p_0^I}{\partial z} \\ w_0^I = 0 \quad (3.17)$$

where terms of $O(R_0)$ are neglected. These zero order equations are the

diagnostic geostrophic and hydrostatic equations which exhibit the coupling between the pressure, azimuthal velocity and temperature fields.

To get time dependent prediction equations for the interior we must go to the first order in λ . Equations (3.9), (3.12), (3.13) and (3.17) give the first order system correct to $O(R_0)$ as :

$$\frac{\partial V_{0\theta}^I}{\partial t} + V_{1r}^I = 0 \quad (3.18)$$

$$\frac{\partial W_1^I}{\partial z} = -\frac{1}{r} \frac{\partial (r V_{1r}^I)}{\partial r} \quad (3.19)$$

$$\epsilon \frac{\partial T_0^I}{\partial t} = -W_1^I \quad (3.20)$$

Thus, in the interior $V_{0\theta}$ is of order unity but V_r and W are of order R_0^2 as can be seen from (3.9) and (3.13).

The interior motion may be expressed in a single conservation equation the so called potential vorticity equation. If we define a stream function $\Psi = P_0$ we have from (3.17)

$$\frac{\partial \Psi}{\partial r} = V_{0\theta}^I, \quad \frac{\partial \Psi}{\partial z} = T_0^I \quad (3.21)$$

Differentiating (3.18) with respect to $\frac{\partial}{\partial r}(r)$ and (3.20) with respect to $\frac{\partial}{\partial z}$, combining with the aid of (3.19) and expressing the result in terms of Ψ we obtain

$$\frac{\partial}{\partial t} \left(\nabla^2 \Psi + \epsilon \frac{\partial^2 \Psi}{\partial z^2} \right) = 0 \quad (3.22)$$

Equation (3.22) is a linearized form of the potential vorticity equation derived by Charney and Stern (1962).

It is obvious from the symmetry of the problem that the structure of the boundary layers in the vicinity of $z=+1$ and $z=-1$ is identical.

Thus, we need only examine the boundary layer at $z=0$. Expanding equations (3.8) - (3.13) for $\xi \leq O(1)$ we get as the first order balance in the boundary layer (after interior components have been subtracted out),

$$-V_{0\theta}^B = -\frac{\partial P_0^B}{\partial r} + \frac{\partial^2 V_{0r}^B}{\partial \xi^2} \quad (3.23)$$

$$V_{0r}^B = \frac{\partial^2 V_{0\theta}^B}{\partial \xi^2} \quad (3.24)$$

$$\frac{\partial P_0^B}{\partial \xi} = 0 \quad (3.25)$$

$$\frac{1}{r} \frac{\partial}{\partial r} (r V_{0r}^B) = -\frac{\partial W_1^B}{\partial \xi} \quad (3.26)$$

$$\frac{\partial^2 T_0^B}{\partial \xi^2} = 0 \quad (3.27)$$

From equation (3.12) $\frac{\partial W_0^B}{\partial \xi} = 0$. The boundary condition on W_0 at a rigid surface is $W_0 = W_0^I + W_0^B = 0$. Therefore $W_0^B(0) = 0$ and $W_0^B(\xi) = 0$. Furthermore from (3.27) we see that $T^B(\xi) = 0$ is the only solution which satisfies the condition $T^B \rightarrow 0$ as $\xi \rightarrow -\infty$. Therefore, there is no thermal boundary layer of thickness λ .

The boundary layer equations (3.23) - (3.26) can be solved subject to the boundary conditions that $V_{0\theta} = r$, $V_{0r} = W_1 = 0$ at $z = \pm 1$. The boundary conditions in the boundary layer stretched coordinates are then at $\xi = 0$

$$V_{0\theta}^B = r - V_{0\theta}^I \quad (3.28)$$

$$V_{0r}^B = 0 \quad (3.29)$$

$$W_1^B = -W_1^I \quad (3.30)$$

And as $\xi \rightarrow -\infty$, $V_{0\theta}^B$, V_{0r}^B , $W_1^B \rightarrow 0$. Multiplying (3.23)

by \bar{t} and adding to (3.24) we get the simple second order equation

$$\frac{\partial^2}{\partial \bar{z}^2} (V_{0\theta}^B + i V_{0r}^B) = -i (V_{0\theta}^B + i V_{0r}^B) \quad . \quad \text{The solution}$$

subject to boundary conditions (3.28) is

$$V_{0\theta}^B = (r - V_{0\theta}^I(\pm 1)) e^{i\bar{z}/\sqrt{2}} \cos \bar{z}/\sqrt{2} \quad (3.31a)$$

$$V_{0r}^B = -(r - V_{0\theta}^I(\pm 1)) e^{i\bar{z}/\sqrt{2}} \sin \bar{z}/\sqrt{2} \quad (3.31b)$$

Differentiating (3.29b) by $\frac{1}{r} \frac{\partial}{\partial r} (r \quad)$ and applying (3.26) and (3.21) we

get

$$-\frac{\partial W_1}{\partial \bar{z}} = (2 - \nabla^2 \psi(\pm 1)) e^{i\bar{z}/\sqrt{2}} \sin \bar{z}/\sqrt{2} \quad (3.32)$$

Integrating (3.30) with respect to \bar{z} from $\bar{z} = 0$ to $\bar{z} \Rightarrow -\infty$ we have finally,

$$-W_1^B(0) = W_1^I(\pm 1) = \pm \frac{1}{\sqrt{2}} (2 - \nabla^2 \psi(\pm 1)) \quad (3.33)$$

This expression gives the vertical flux from the interior into the Ekman layers at $\bar{z} = \pm 1$, and will be used to formulate the boundary conditions for equation (3.22).

We now solve for the time dependent interior flow correct to order λ for $t \approx o(1)$. We first express W_1^I at $\bar{z} = \pm 1$ in terms of the stream function by substituting the adiabatic equation (3.20) into equation (3.31). The resulting boundary condition is

$$\epsilon \frac{\partial^2 \psi}{\partial t \partial \bar{z}} = \mp \frac{1}{\sqrt{2}} (2 - \nabla^2 \psi) \quad \text{at } \bar{z} = \pm 1 \quad (3.34)$$

Now $\psi = \psi(r, \bar{z}, t)$, so it will obviously be necessary to separate out the r dependence to solve (3.22) with boundary conditions (3.34).

In Greenspan and Howard's problem this was easily done because it turned out that the dependent variables were linear functions of r . In the

present case that is not true. The separation can only be accomplished by expanding Ψ in an orthogonal series appropriate to the geometry of the cylindrical tank. We choose $\Psi=0$ at $r=1$ as the boundary condition in the horizontal. This condition implies zero horizontal divergence at $r=1$ which is physically reasonable since the horizontal divergence must change sign from the interior to the side boundary layer. Ψ may then be expanded in a zero order Fourier - Bessel series

$$\Psi = \sum_{n=1}^{\infty} \Psi(k_n, z, t) J_0(k_n r) \quad (3.35)$$

where the k_n are the n zeroes of $J_0(k)$, and the $\Psi(k_n, z, t)$ are coefficients to be determined. (In Appendix B the problem of matching this solution to the side boundary layers is discussed.) Substituting (3.35) into equation (3.22) and boundary conditions (3.34) we obtain the equation and boundary conditions determining the $\Psi(k_n, z, t)$.

$$\frac{\partial}{\partial t} \left(-k_n^2 \Psi + \epsilon \frac{\partial^2 \Psi}{\partial z^2} \right) = 0 \quad (3.36a)$$

$$\epsilon \frac{\partial^2 \Psi}{\partial t \partial z} = \mp \frac{1}{\sqrt{2}} \left(\Omega_n + k_n^2 \Psi \right) \text{ at } z = \pm 1 \quad (3.36b)$$

where the Ω_n are constants in the Fourier - Bessel expansion of z ;

$$z = \sum_{n=1}^{\infty} \Omega_n J_0(k_n r)$$

Therefore,

$$\Omega_n = z \left(\frac{2}{k_n J_1(k_n)} \right) \quad (3.37)$$

This expansion is valid in the region $0 < r < 1$ which is the region of interest in the present problem.

The time dependence is eliminated from equations (2.3) by application of a Laplace transform. We let

$$\bar{\Psi} = \int_0^{\infty} \Psi e^{-pt} dt \quad (3.38)$$

then because the initial value of Ψ is zero we get from (3.36)

$$\frac{\partial^2 \bar{\Psi}}{\partial z^2} - \frac{k^2}{\epsilon} \bar{\Psi} = 0 \quad (3.39a)$$

$$p \frac{\partial \bar{\Psi}}{\partial z} = \mp \frac{1}{\epsilon} \left(\frac{\Omega_n}{p} + k_n^2 \bar{\Psi} \right) \text{ at } z = \pm 1 \quad (3.39b)$$

The solution is

$$\bar{\Psi} = \frac{-\Omega_n \cosh \frac{k_n}{\sqrt{\epsilon}} z}{p k_n \sqrt{\epsilon} \left(p + \frac{k_n}{\sqrt{\epsilon}} \coth \frac{k_n}{\sqrt{\epsilon}} \right) \sinh \frac{k_n}{\sqrt{\epsilon}}} \quad (3.40)$$

The only singularities of $\bar{\Psi}$ are poles at $p=0$ and $p = -\frac{k_n}{\sqrt{\epsilon}} \coth \frac{k_n}{\sqrt{\epsilon}}$.

Hence we may invert (3.40) by a simple residue calculation to get,

$$\Psi = -\frac{\Omega_n \cosh \frac{k_n}{\sqrt{\epsilon}} z}{k_n^2 \cosh \frac{k_n}{\sqrt{\epsilon}}} \left[1 - e^{-\left(\frac{k_n}{\sqrt{\epsilon}} \coth \frac{k_n}{\sqrt{\epsilon}} \right) t} \right] \quad (3.41)$$

For a given horizontal wave number k_n the spin-up occurs in time $t \approx \frac{\sqrt{2\epsilon}}{k_n} \tanh \frac{k_n}{\sqrt{\epsilon}}$.

As the stratification approaches zero $\epsilon \rightarrow \infty$ and (3.41) is asymptotically

$$\Psi = -\frac{\Omega_n}{k_n^2} \left(1 - e^{-\sqrt{2} t} \right)$$

Substituting into (2.3) and taking the Laplacian we get $\nabla^2 \Psi = 2(1 - e^{-\sqrt{2} t})$

for $\epsilon \rightarrow \infty$. This is just Greenspan and Howard's result for a homogeneous incompressible fluid. Therefore, the present solution approaches the correct asymptotic limit. (The $\sqrt{2}$ factor appears because we have scaled the problem with $2\Omega_0$ rather than Ω_0). Summing the Fourier - Bessel series

for coefficients (3.41) we obtain the stream function

$$\Psi = -\sum_{n=1}^{\infty} \frac{\Omega_n}{k_n^2} \frac{\cosh \frac{k_n}{\sqrt{\epsilon}} z}{\cosh \frac{k_n}{\sqrt{\epsilon}}} \left[1 - e^{-\left(\frac{k_n}{\sqrt{\epsilon}} \coth \frac{k_n}{\sqrt{\epsilon}} \right) t} \right] J_0(k_n r) \quad (3.42)$$

the zero order temperature profile,

$$\frac{\partial \Psi}{\partial z} = T_0 = -\sum_{n=1}^{\infty} \frac{\Omega_n}{k_n \sqrt{\epsilon}} \frac{\sinh \frac{k_n}{\sqrt{\epsilon}} z}{\cosh \frac{k_n}{\sqrt{\epsilon}}} \left[1 - e^{-\left(\frac{k_n}{\sqrt{\epsilon}} \coth \frac{k_n}{\sqrt{\epsilon}} \right) t} \right] J_0(k_n r) \quad (3.43)$$

and the zero order zonal velocity

$$v_{\theta 0} = \frac{\partial \Psi}{\partial r} = \sum_{n=1}^{\infty} \frac{\Omega_n}{k_n} \frac{\cosh \frac{k_n}{\sqrt{\epsilon}} z}{\cosh \frac{k_n}{\sqrt{\epsilon}}} \left[1 - e^{-\left(\frac{k_n}{\sqrt{\epsilon}} \coth \frac{k_n}{\sqrt{\epsilon}} \right) t} \right] J_1(k_n r) \quad (3.44)$$

All of these series converge rather rapidly and may easily be evaluated numerically by summing the first several terms.

In the present stratified case it is obvious from equation (3.44) that for large τ the fluid has reached a quasi-steady state, but one which involves vertical shear of the azimuthal velocity. This shear increases with decreasing ϵ (increasing static stability). The physical reason for this dependence is that static stability suppresses the vertical circulation and thus the interior radial inflow necessary to balance the outflow in the Ekman layer is greatest just above the boundary layer and decreases towards the center of the fluid.

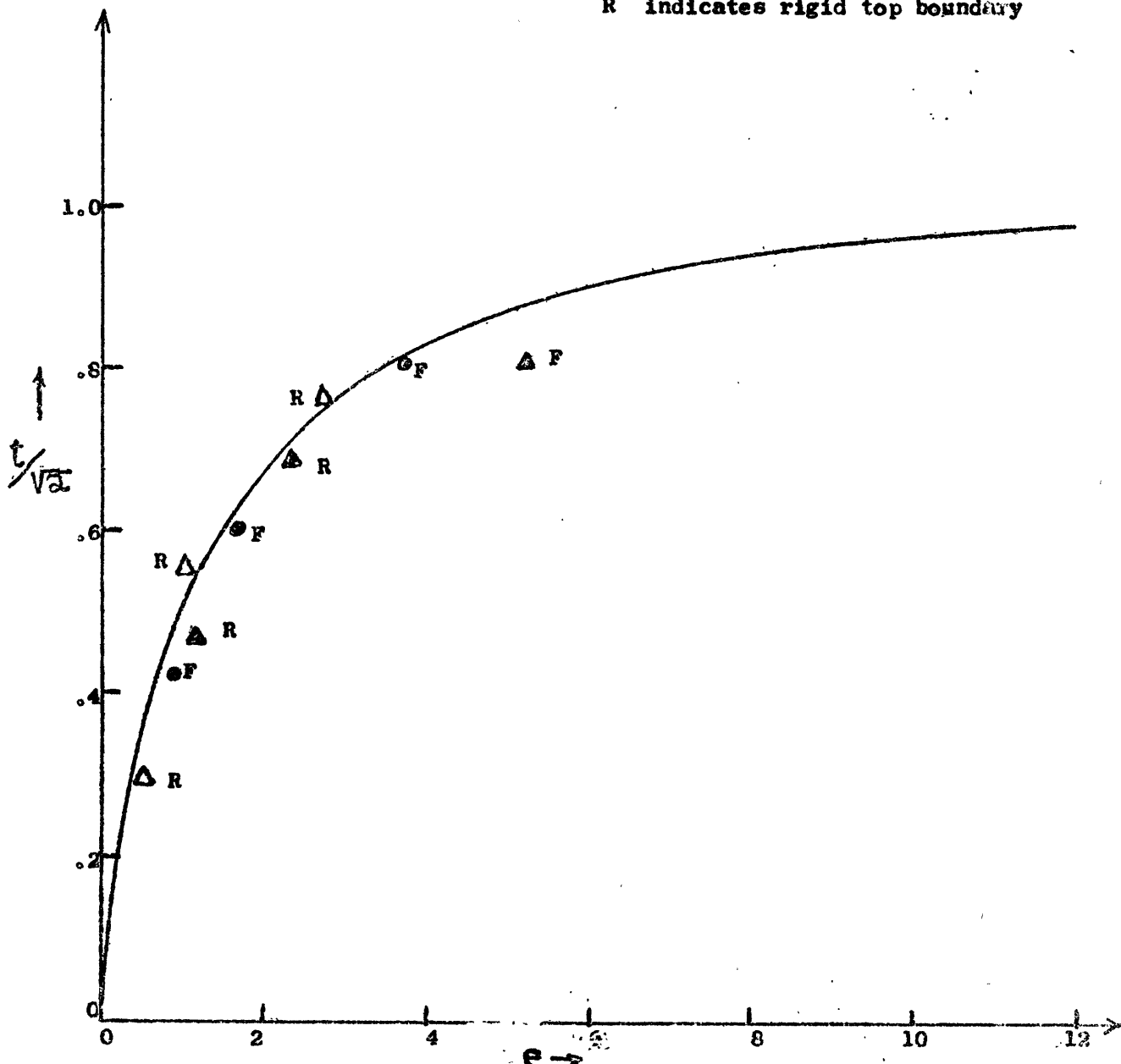
In Figure 3.2 the spin-up time obtained by summing the series in equation (3.44) for $r = .5$ and $Z = 1$ is plotted as a function of ϵ . Experimentally obtained values are also indicated in the figure. The vertical profile of zonal velocity in the quasi-steady state is illustrated in Figure 3.3 for the cases $\epsilon = 2.2$ and $\epsilon = .5$ ($r = .5$ in both cases). The abscissae V_{ω_0}/r is the nondimensional angular velocity. In Figure 3.4 the quasi-steady angular velocity at $r = .5$ and $Z = 0$ is plotted against ϵ to indicate the strong dependence of vertical shear on the static stability.

There is a small radial dependence of the spin-up time and the vertical shear. As r increases the contribution of the higher modes in the Fourier-Bessel expansion for the stream function becomes greater. In these higher modes the horizontal scale of the motion is restricted so that effectively $\epsilon = \frac{4\Omega_0^2 L^2}{g H K}$ is smaller and the baroclinicity of the flow is greater. Physically, the decrease in the horizontal scale as r becomes

$$\Delta = \left\{ \begin{array}{l} .02 - \triangle \\ .025 - \triangle \\ .03 - \bullet \end{array} \right\} \quad \begin{array}{l} \text{Experimental} \\ \text{Data Points} \end{array}$$

F indicates free surface experiment

R indicates rigid top boundary



Spin-up time vs. the Internal Rotational Frequency Number in the Continuously Stratified Model.

Figure 3.2

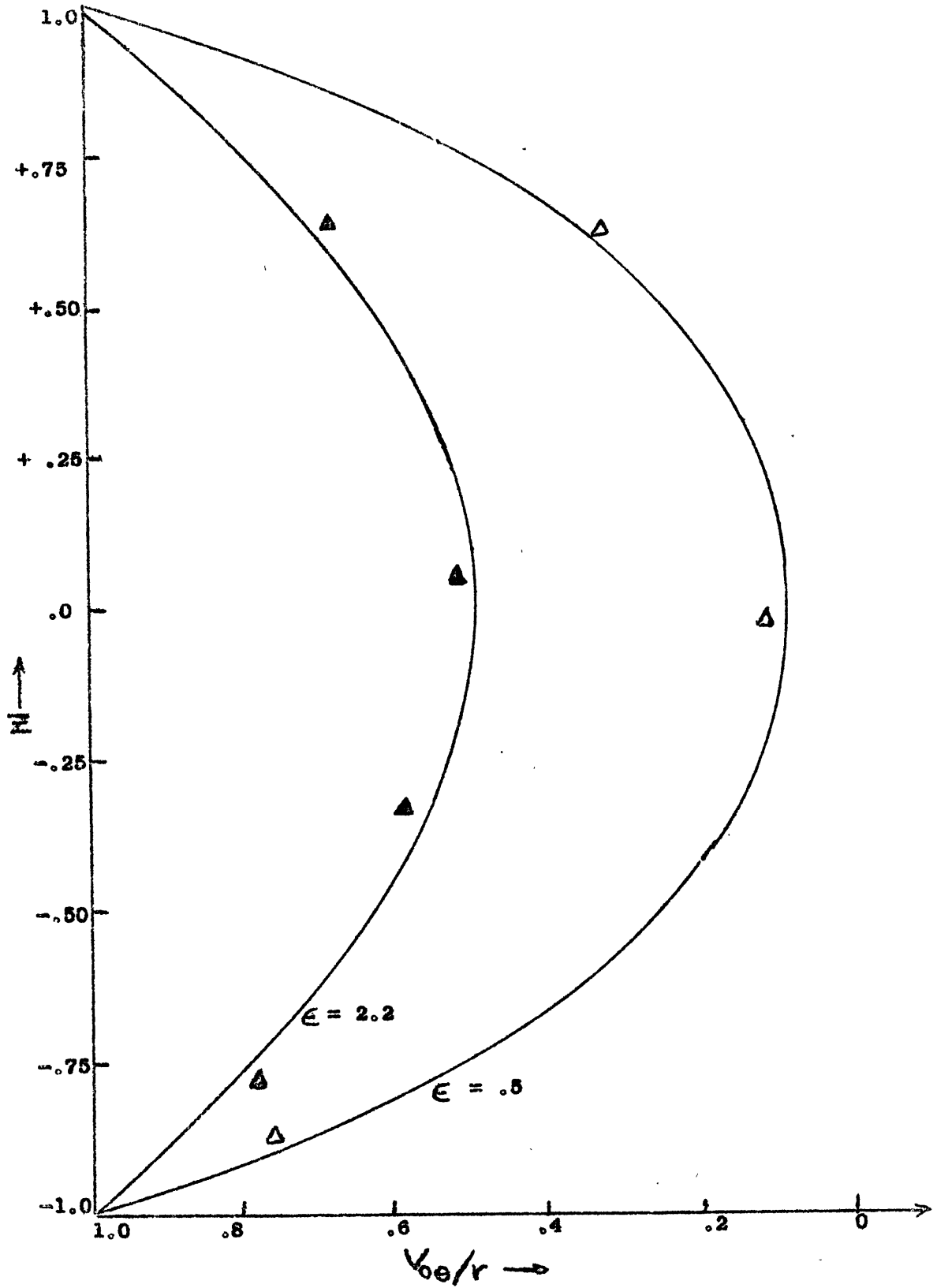


Figure 3.3

Velocity profile in the Quasi-Steady State
for the Continuous Model at $r = .5$

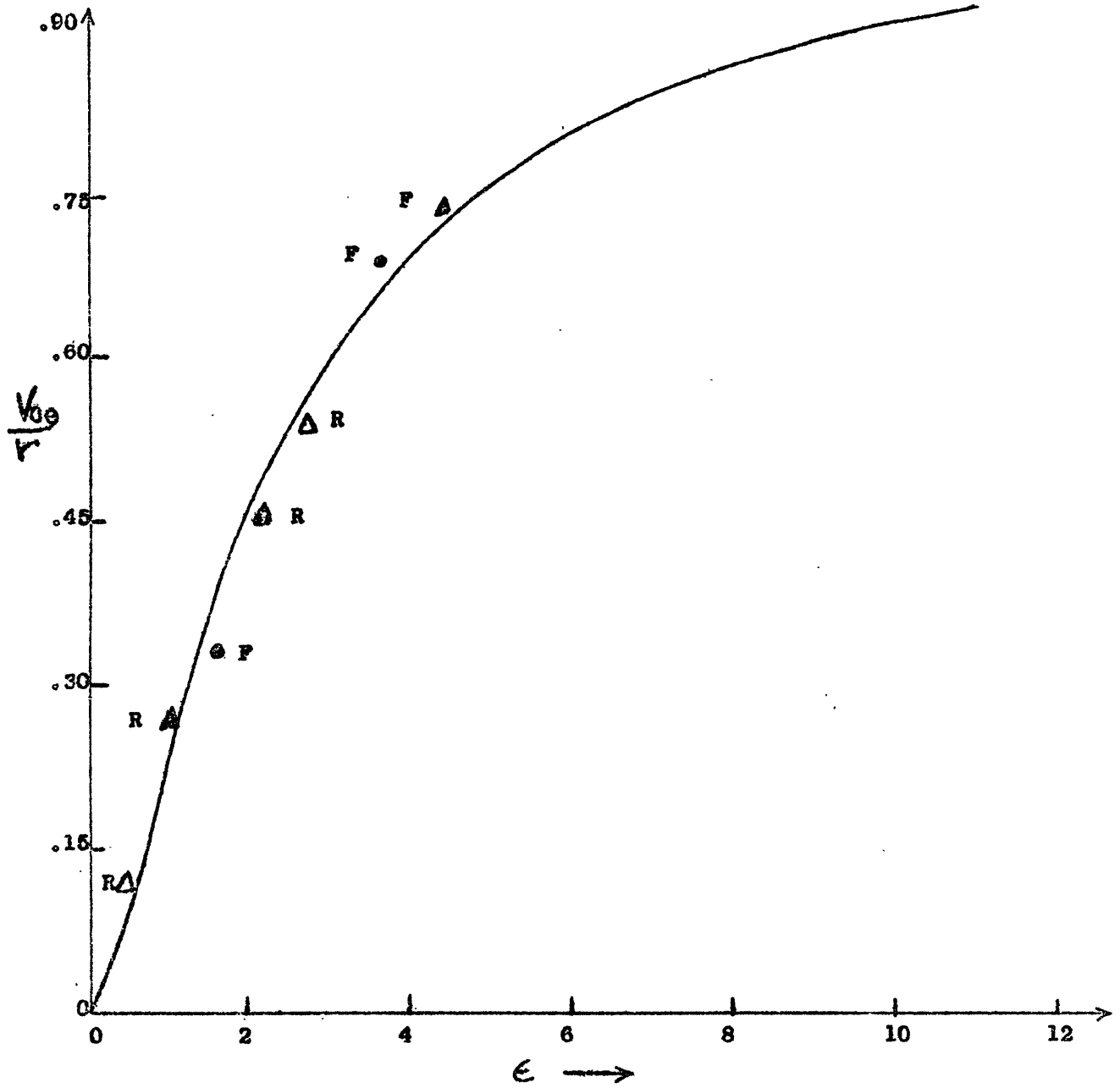


Figure 3.4

Quasi-Steady Velocity at $z = 0$ vs. the Internal Rotational Froude Number

larger is due to the constraint of zero normal velocity at the rigid vertical boundary .

In Figure 3. the interior density field is shown for the case and $t = 1/\sqrt{2}$. Note that the greatest density perturbations occur quite close to the boundary layers at $\bar{z} = \pm 1$, which indicates that strong vertical motions are suppressed away from the boundaries. Only the lower half of the cylinder is shown in the Figure, for $\frac{\partial \psi}{\partial \bar{z}}$ is symmetric about $\bar{z} = 0$.

Finally, we compare the energy relationships for the homogeneous and stratified cases respectively. Differentiating (3.18) by $\frac{1}{r} \frac{\partial}{\partial r} (r \quad)$ and substituting from (3.21), then multiplying through by ψ and integrating over the cylindrical volume we obtain with the aid of Green's theorem.

$$\frac{1}{2} \frac{d}{dt} \iint (\nabla^2 \psi)^2 r dr dz = - \int [\psi w]_{\bar{z}=-1}^{\bar{z}=+1} r dr + \iint w_1 \frac{\partial \psi}{\partial \bar{z}} r dr dz \quad (3.45)$$

The lefthand side is the time rate of change of the kinetic energy. The first term on the right is the work done by frictional stresses in the boundary layers and the second term expresses the conversion between potential and kinetic energy. An equation for the rate of change of potential energy is obtained by multiplying equation (3.20) through by $\frac{\partial \psi}{\partial \bar{z}}$ and integrating to get

$$\frac{\epsilon}{2} \frac{d}{dt} \iint \left(\frac{\partial \psi}{\partial \bar{z}} \right)^2 r dr dz = - \int w_1 \frac{\partial \psi}{\partial \bar{z}} r dr dz \quad (3.46)$$

Combining (3.45) and 3.46) we obtain the energy equation for the quasi-geostrophic system,

$$\frac{1}{2} \frac{d}{dt} \iint \left[(\nabla \psi)^2 + \epsilon \left(\frac{\partial \psi}{\partial \bar{z}} \right)^2 \right] r dr dz = - \int [\psi w_1]_{\bar{z}=-1}^{\bar{z}=+1} r dr \quad (3.47)$$

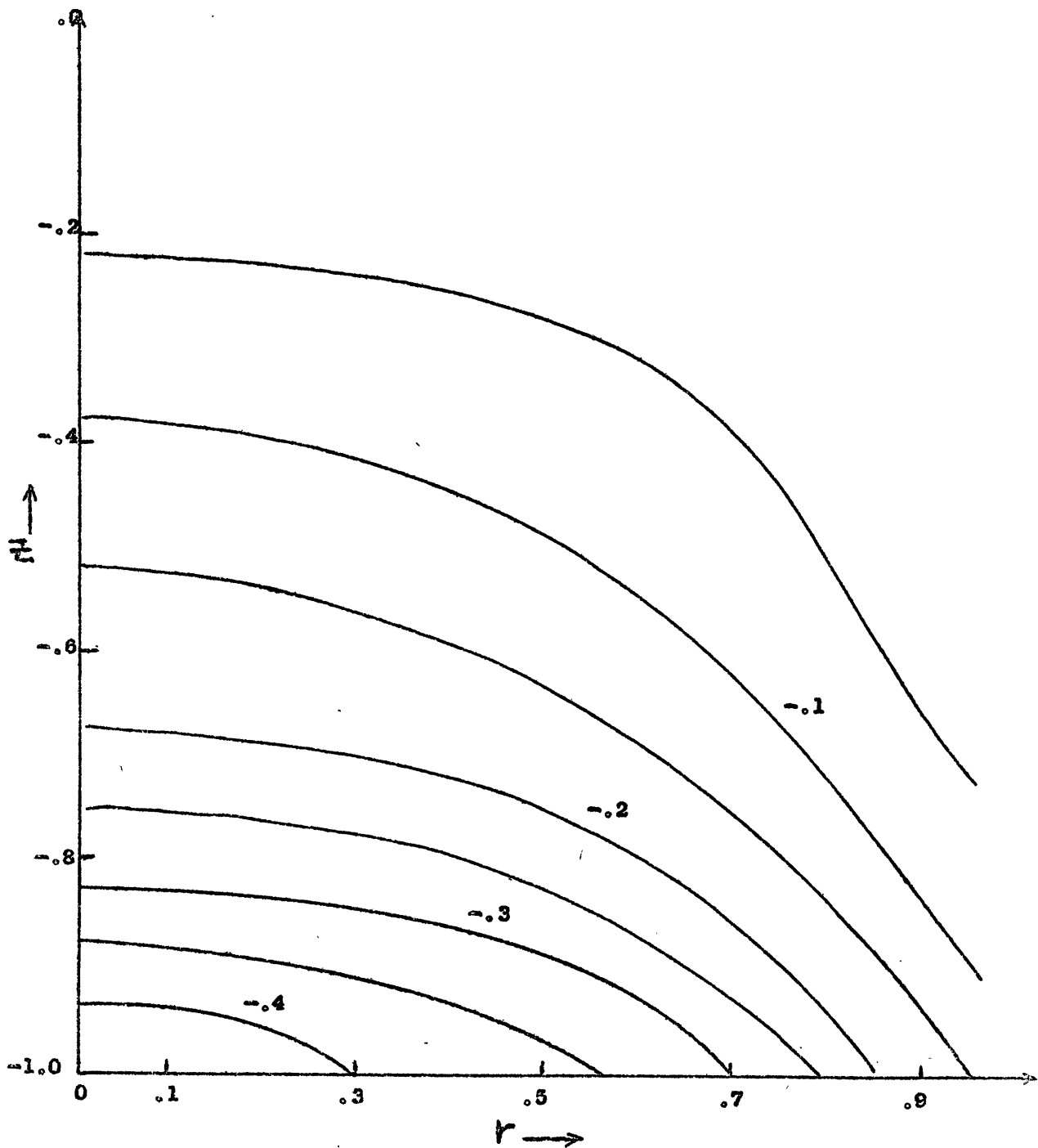


Figure 3.5
Density field for $C_1 = 1$ and $t = \frac{1}{\sqrt{2}}$ in the continuous model.

This equation shows that the volume integrated rate of change of the kinetic plus potential energy equals the work done by boundary stresses in the Ekman layers. Using Green's theorem we may express the sum of potential plus kinetic energy as

$$P + K = \pi \iint \epsilon \left(\frac{\partial \psi}{\partial z} \right)^2 r dr dz + \pi \iint (-\psi \nabla^2 \psi) r dr dz$$

Substituting from the series solutions (3.24) and (3.42) we obtain for $t \gg 1$

$$K = \sum_{n=1}^{\infty} \frac{8\pi}{k_n^4} \frac{\left(\frac{\sqrt{\epsilon}}{k_n} \sinh \frac{k_n}{\sqrt{\epsilon}} \cosh \frac{k_n}{\sqrt{\epsilon}} + 1 \right)}{\cosh^2 \frac{k_n}{\sqrt{\epsilon}}} \quad (3.48)$$

$$P = \sum_{n=1}^{\infty} \frac{8\pi}{k_n^4} \frac{\left(\frac{\sqrt{\epsilon}}{k_n} \sinh \frac{k_n}{\sqrt{\epsilon}} \cosh \frac{k_n}{\sqrt{\epsilon}} - 1 \right)}{\cosh^2 \frac{k_n}{\sqrt{\epsilon}}} \quad (3.49)$$

According to (3.48) and (3.49) $K > P$ for all values of the stability. But for highly stratified fluids where $\epsilon \rightarrow 0$, $P \rightarrow K$. In the other asymptotic limit $\epsilon \rightarrow \infty$, $P \rightarrow 0$ and the kinetic energy becomes

$$K \rightarrow 16\pi \sum_{n=1}^{\infty} \frac{1}{k_n^4} = \frac{\pi}{2}$$

which is just the volume integrated kinetic energy for the homogeneous case.

To justify this summation we note that the steady state solution for the homogeneous spin-up problem is in the present notation

$$\psi = r^2/2$$

The total kinetic energy is therefore,

$$\pi \int_0^{+1} \int_{-1}^{+1} (\nabla \psi)^2 r dr dz = \frac{\pi}{2} = \pi \iint (-\psi \nabla^2 \psi) r dr dz$$

Expanding the vorticity $\nabla^2 \psi = 2$ in a Fourier-Bessel series for the region

$$0 < r < 1 \text{ we obtain } \nabla^2 \psi = \sum_{n=1}^{\infty} \frac{4 J_0(k_n r)}{k_n J_1(k_n)}$$

(see equation (3.37)).

Therefore,

$$\pi \iint (-\psi \nabla^2 \psi) r dr dz = \sum_{n=1}^{\infty} \frac{16}{k_n^4 [J_1(k_n)]^2} \iint [J_0(k_n r)]^2 r dr dz$$

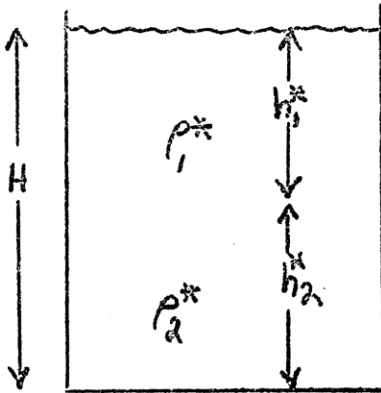
$$= 16 \pi \sum_{n=1}^{\infty} \frac{1}{k_n^4}$$

Finally, we may write the total energy as

$$P + K = \sum_{n=1}^{\infty} 16 \pi \left(\frac{\sqrt{\epsilon}}{k_n^5} \right) \tanh \frac{k_n}{\sqrt{\epsilon}} \quad (3.50)$$

Equation (3.50) indicates that increasing the static stability decreases the total energy in the quasi-steady spun-up regime. For small ϵ the energy $P+K$ decreases as the square root of ϵ .

Chapter 4

The Spin-Up of a Two-Layer System

The physical set-up is the same as in the previous chapter. But in the present case the fluid consists of two homogeneous and immiscible layers of density ρ_1^* and ρ_2^* respectively (see Figure 4.1), where subscript 1 denotes the top layer

and subscript 2 denotes the bottom layer. The system is statically stable so that $\rho_1^* < \rho_2^*$. The equations of motion are again scaled using the barotropic spin-up time $\tau = \left(\frac{H^2}{2\Omega_0 \nu}\right)^{1/2}$. We then define nondimensional variables in analogy with the previous scaling as follows;

$$r = r^*/L, \quad z = z^*/H, \quad t = t^*/\tau$$

$$V_{1,2\theta} = V_{1,2\theta}^*/\omega L, \quad V_{1,2r} = V_{1,2r}^*/\omega L, \quad W_{1,2} = W_{1,2}^*/\omega H$$

We utilize the nondimensional parameters $\lambda^{-2} = \frac{2\Omega_0 H^2}{\nu}$, $\epsilon_1 = \frac{4\Omega_0^2 L^2}{g' H_1}$, $\epsilon_2 = \frac{4\Omega_0^2 L^2}{g' H_2}$, $\epsilon = \frac{4\Omega_0^2 L^2}{g H}$, $\delta = L/H$ where $g' = g \frac{\rho_2^* - \rho_1^*}{\rho_1^*}$ is the reduced gravity. In addition we define $\mu = \frac{\rho_1 \nu_1}{\rho_2 \nu_2}$ and $\gamma^2 = \nu_1/\nu_2$, where ν_1 and ν_2 are the viscosities of the upper and lower layer respectively.

From equation (3.11) we see that since W_1 and W_2 are of $O(R_0)$, the pressure is hydrostatic to $O(R_0 \lambda)$. Integrating the hydrostatic relationship through each layer we find that

$$\begin{aligned} p_1^* &= \rho_1^* g (h_1^* - z^*) \\ p_2^* &= \rho_1^* g h_1^* + \rho_2^* g (h_2^* - z) \end{aligned} \quad (4.1)$$

These expressions may then be substituted into the horizontal momentum equations to eliminate pressure. If we scale the heights as

$$\begin{aligned} h_1^* &= H_1 (1 + \epsilon_1 R_0 h_1) \\ h_2^* &= H_2 (1 + \epsilon_2 R_0 h_2) \\ h^* &= H (1 + \epsilon R_0 h) \end{aligned} \quad (4.2)$$

we may write the nondimensional momentum equations as follows: for the top layer

$$\lambda \frac{\partial v_{1r}}{\partial t} + R_0 \left(v_{1r} \frac{\partial v_{1r}}{\partial r} + w_1 \frac{\partial v_{1r}}{\partial z} - \frac{v_{1\theta}^2}{r} \right) - v_{1\theta} = -\frac{\partial h}{\partial r} + \gamma^2 \lambda^2 \left(\nabla_{\delta}^2 + \frac{\partial^2}{\partial z^2} \right) v_{1r} \quad (4.3)$$

$$\lambda \frac{\partial v_{1\theta}}{\partial t} + R_0 \left(v_{1r} \frac{\partial v_{1\theta}}{\partial r} + w_1 \frac{\partial v_{1\theta}}{\partial z} + \frac{v_{1r} v_{1\theta}}{r} \right) + v_{1r} = \gamma^2 \lambda^2 \left(\nabla_{\delta}^2 + \frac{\partial^2}{\partial z^2} \right) v_{1\theta} \quad (4.4)$$

with the continuity equation

$$\frac{1}{r} \frac{\partial r v_{1r}}{\partial r} + \frac{\partial w_1}{\partial z} = 0 \quad (4.5)$$

and for the bottom layer

$$\begin{aligned} \lambda \frac{\partial v_{2r}}{\partial t} + R_0 \left(v_{2r} \frac{\partial v_{2r}}{\partial r} + w_2 \frac{\partial v_{2r}}{\partial z} - \frac{v_{2\theta}^2}{r} \right) - v_{2\theta} &= -\frac{\partial (h-h_1)}{\partial r} \\ &+ \lambda^2 \left(\nabla_{\delta}^2 + \frac{\partial^2}{\partial z^2} \right) v_{2r} \end{aligned} \quad (4.6)$$

$$\lambda \frac{\partial v_{2\theta}}{\partial t} + R_0 \left(v_{2r} \frac{\partial v_{2\theta}}{\partial r} + w_2 \frac{\partial v_{2\theta}}{\partial z} + \frac{v_{2r} v_{2\theta}}{r} \right) + v_{2r} = \lambda^2 \left(\nabla_{\delta}^2 + \frac{\partial^2}{\partial z^2} \right) v_{2\theta} \quad (4.7)$$

with the continuity equation

$$\frac{1}{r} \frac{\partial r v_{2r}}{\partial r} + \frac{\partial w_2}{\partial z} = 0 \quad (4.8)$$

This set of equations is then to be solved subject to the appropriate boundary conditions. At $\bar{z} = 0$, the bottom boundary, we use rigid viscous

boundary conditions

$$V_{2r} = W_2 = 0 \quad \text{and} \quad V_{2\theta} = r \quad (t > 0) \quad (4.9)$$

Thus, a unit angular velocity change is imparted to the cylinder at $t=0$.

At the top free boundary we apply the no stress boundary conditions:

$$\frac{\partial V_{1r}}{\partial z} = \frac{\partial V_{1\theta}}{\partial z} = 0, \quad w_1(h) = \epsilon R_0 \frac{dh}{dt} \quad \text{at } z=h \quad (4.10)$$

At the interface, $z=h_2$, we require continuity of velocity and stress.

$$W_1 = W_2, \quad V_{1\theta} = V_{2\theta}, \quad V_{1r} = V_{2r}, \quad \rho_1 \nu_1 \frac{\partial V_{1\theta}}{\partial z} = \rho_2 \nu_2 \frac{\partial V_{2\theta}}{\partial z}, \quad \rho_1 \nu_1 \frac{\partial V_{1r}}{\partial z} = \rho_2 \nu_2 \frac{\partial V_{2r}}{\partial z} \quad (4.11)$$

Because the two fluids are immiscible there is no diffusion across the interface and the density changes discontinuously from ρ_1^* to ρ_2^* . It

is convenient to write the vertical velocities as

$$W_1(h_2) = \lambda \frac{H_1 \epsilon_1}{H} \frac{dh_1}{dt} - \epsilon \lambda \frac{dh}{dt} \quad (4.12)$$

$$W_2(h_2) = \lambda \frac{H_2 \epsilon_2}{H} \frac{dh_2}{dt}$$

We now apply boundary layer theory to solve this system in a manner analogous to the continuous case. We let $\eta \lambda = z$, $\zeta \lambda = (h_2 - z)$, and $\xi \lambda = (z - h_2)$ where η , ζ and ξ are stretched coordinates for the boundary layers at $z=0$ and $z=h_2$ in the lower layer, and $z=h_2$ in the upper layer respectively. For the lower layer we write all variables in the form

$$f_2(r, z, t) = f_2^I(r, z, t) + f_2^B(r, \zeta, t) + f_2^{B'}(r, \eta, t) \quad (4.13)$$

and for the upper layer we write

$$f_1(r, z, t) = f_1^I(r, z, t) + f_1^B(r, \xi, t) \quad (4.14)$$

Rather than following the formal expansion procedure of the previous chapter which would lead to an awkward number of subscripts, we merely write down the lowest order equations for the interior where it is understood that terms of $O(R_0)$ and $O(\lambda)$ are neglected. For the upper layer

$$V_{1\theta}^I = \frac{\partial h}{\partial r} \quad (4.15)$$

$$\frac{\partial V_{1\theta}^I}{\partial t} + V_{1r}^I = 0 \quad (4.16)$$

$$\frac{1}{r} \frac{\partial r V_{1r}^I}{\partial r} + \frac{\partial W_1^I}{\partial z} = 0 \quad (4.17)$$

and for the lower layer

$$V_{2\theta}^I = \frac{\partial (h-h_0)}{\partial r} \quad (4.18)$$

$$\frac{\partial V_{2\theta}^I}{\partial t} + V_{2r}^I = 0 \quad (4.19)$$

$$\frac{1}{r} \frac{\partial r V_{2r}^I}{\partial r} + \frac{\partial W_2^I}{\partial z} = 0 \quad (4.20)$$

where V_{1r}^I , V_{2r}^I , W_1^I and W_2^I are all $O(\lambda)$. (4.15 and (4.18) indicate that $V_{1\theta}^I$ and $V_{2\theta}^I$ are independent of z . Therefore, if we differentiate (4.16) and (4.19) with respect to $\frac{1}{r} \frac{\partial}{\partial r} (r)$ we obtain, after integrating in z :

$$\frac{H_1}{H} \frac{\partial}{\partial z} \nabla^2 h + \frac{W_1^I(h_2) - W_1^I(h)}{\lambda} = 0 \quad (4.21)$$

$$\frac{H_2}{H} \frac{\partial}{\partial z} (\nabla^2 h - \nabla^2 h_0) + \frac{W_2^I(0) - W_2^I(h_2)}{\lambda} = 0 \quad (4.22)$$

Where we have in each case utilized the equation of continuity.

The vertical velocities in the above equations are determined by the vertical flux into the various boundary layers. For the top surface the boundary conditions (4.10) are satisfied by the interior solution, so there is no boundary layer. Furthermore, in cases of interest $\epsilon \approx 0(\lambda)$ so that $W_1(h) \sim 0(R_0\lambda)$ (4.23)

and is negligible compared to the interior W_1 . The bottom boundary layer which must be present if boundary conditions (4.9) are to be satisfied is just the ordinary Ekman layer which was treated in the previous chapter. The result was that,

$$W_2^I(0) = -\frac{\lambda}{\sqrt{2}} \left(2 - \frac{1}{r} \frac{\partial r V_{2\theta}^I}{\partial r} \right) \quad (4.24)$$

It remains to analyze the boundary layers at the interface. If we write the variables $W_2, V_{2\theta}$ and V_{2r} in the form (4.13), and the variables $W_1, V_{1\theta}, V_{1r}$ in the form (4.14), then since ξ and ζ are stretched coordinates we have

$$W_2^B, V_{2\theta}^B, V_{2r}^B \rightarrow 0 \text{ as } \zeta \rightarrow -\infty \quad (4.25a)$$

$$W_1^B, V_{1\theta}^B, V_{1r}^B \rightarrow 0 \text{ as } \xi \rightarrow -\infty \quad (4.25b)$$

Utilizing boundary conditions (4.11) at $z=h_2$ we get

$$V_{2\theta}(h_2) = V_{2\theta}^B(0) + V_{2\theta}^I = V_{1\theta}^B(0) + V_{1\theta}^I = V_{1\theta}(h_2) \quad (4.25c)$$

And since $V_{1r}^I, V_{2r}^I \approx 0(\lambda)$ we have $V_{2r}^B(0) = V_{1r}^B(0)$ (4.25d)

also

$$W_2^B(0) + W_2^I(h_2) = W_1^B(0) + W_1^I(h_2) \quad (4.25e)$$

and the stress continuity condition at the interface is

$$\frac{\partial V_{2r}^B}{\partial \zeta} = -\mu \frac{\partial V_{1r}^B}{\partial \xi}, \quad \frac{\partial V_{2\theta}^B}{\partial \zeta} = -\mu \frac{\partial V_{1\theta}^B}{\partial \xi} \quad (4.25f)$$

Scaling the equations of motion for the boundary layer variables and discarding terms of $O(R_0)$ we obtain for the upper layer

$$-V_{1\theta}^B = \gamma^2 \frac{\partial^2 V_{1r}}{\partial \xi^2}, \quad V_{1r}^B = \gamma^2 \frac{\partial^2 V_{1\theta}^B}{\partial \xi^2} \quad (4.26)$$

and for the lower layer,

$$-V_{2\theta}^B = \frac{\partial^2 V_{2r}}{\partial \xi^2}, \quad V_{2r}^B = \frac{\partial^2 V_{2\theta}^B}{\partial \xi^2} \quad (4.27)$$

The solutions of (3.26) and (3.27) subject to boundary conditions (3.25)

are

$$V_{2\theta}^B = \frac{\mu}{\gamma} \left(\frac{V_{1\theta}^I - V_{2\theta}^I}{1 + \mu/\gamma} \right) e^{+z/\sqrt{2}} \cos k/\sqrt{2} \quad (4.28a)$$

$$V_{2r}^B = \frac{\mu}{\gamma} \left(\frac{V_{1\theta}^I - V_{2\theta}^I}{1 + \mu/\gamma} \right) e^{z/\sqrt{2}} \sin k/\sqrt{2} \quad (4.28b)$$

$$V_{1\theta}^B = - \left(\frac{V_{1\theta}^I - V_{2\theta}^I}{1 + \mu/\gamma} \right) e^{z/\sqrt{2}\gamma} \cos z/\sqrt{2}\gamma \quad (4.28c)$$

$$V_{1r}^B = - \left(\frac{V_{1\theta}^I - V_{2\theta}^I}{1 + \mu/\gamma} \right) e^{z/\sqrt{2}\gamma} \sin z/\sqrt{2}\gamma \quad (4.28d)$$

To obtain the vertical fluxes into the interior of the upper and lower layers we differentiate (4.28b and d) by $\frac{1}{r} \left(r \frac{\partial}{\partial r} \right)$ and substitute the results into the continuity equations (4.17) and (4.20) respectively. Integration across the boundary layer then gives

$$W_2^B(0) = \frac{\lambda \mu}{\sqrt{2}\gamma(1 + \mu/\gamma)} \left[\frac{1}{r} \frac{\partial}{\partial r} (r V_{2r}^I) - \frac{1}{r} \frac{\partial}{\partial r} (r V_{1\theta}^I) \right]$$

$$W_1^B(0) = \frac{\lambda \gamma}{\sqrt{2}(1 + \mu/\gamma)} \left[\frac{1}{r} \frac{\partial}{\partial r} (r V_{2\theta}^I) - \frac{1}{r} \frac{\partial}{\partial r} (r V_{1\theta}^I) \right]$$

Substituting from equation (4.12) and the boundary conditions (4.25) we

obtain the following boundary values for the interior vertical velocity:

$$W_1^I(h_2) = \frac{-\lambda\gamma}{\sqrt{2}(1+\mu/\gamma)} \left[\frac{1}{r} \frac{\partial}{\partial r} (rV_{20}^I) - \frac{1}{r} \frac{\partial}{\partial r} (rV_{10}^I) \right] - \frac{H_1\epsilon_1\lambda}{H} \frac{dh_1}{dt} + \lambda\epsilon \frac{dh}{dt} \quad (4.27)$$

$$W_2^I(h_2) = \frac{-\lambda\mu}{\gamma(1+\mu/\gamma)\sqrt{2}} \left[\frac{1}{r} \frac{\partial}{\partial r} (rV_{20}^I) - \frac{1}{r} \frac{\partial}{\partial r} (rV_{10}^I) \right] + \frac{H_2\epsilon_2\lambda}{H} \frac{dh_2}{dt}$$

We now define stream functions for the zonal velocity in each layer. Let

$$\Psi_1 = h \quad \text{and} \quad \Psi_2 = h - h_1, \quad \text{then}$$

$$\frac{\partial \Psi_1}{\partial r} = V_{10} \quad , \quad \frac{\partial \Psi_2}{\partial r} = V_{20} \quad (4.30)$$

Equations (4.28a and b) may now be expressed in terms of the stream function. It will simplify the analysis somewhat if we note that $\epsilon \ll \epsilon_1$, ϵ_2 . Therefore, we may neglect the term of $O(\epsilon)$ in (4.29). Physically this means that the deviation of the free surface height from its mean is negligible compared to the deviation of the interface height from the mean.

Further, we note that

$$\frac{dh_1}{dt} = \frac{\partial h_1}{\partial t} + V_{1r} \frac{\partial h_1}{\partial r} \quad \text{and} \quad \frac{dh_2}{dt} = \frac{\partial h_2}{\partial t} + V_{2r} \frac{\partial h_2}{\partial r}$$

V_{1r} and V_{2r} are both $O(\lambda)$, thus the local change of height is much greater than the advection by the divergent radial flow, and the advection terms may be neglected. Hence from equations (4.29) and (4.30)

$$W_1^I(h_2) = -\frac{\lambda\gamma(\nabla^2 \Psi_2 - \nabla^2 \Psi_1)}{\sqrt{2}(1+\mu/\gamma)} - \frac{H_1\epsilon_1\lambda}{H} \frac{\partial(\Psi_1 - \Psi_2)}{\partial t} \quad (4.31)$$

$$W_2^I(h_2) = -\frac{\lambda\mu(\nabla^2 \Psi_2 - \nabla^2 \Psi_1)}{\sqrt{2}\gamma(1+\mu/\gamma)} + \frac{H_2\epsilon_2\lambda}{H} \frac{\partial(\Psi_2 - \Psi_1)}{\partial t}$$

Substituting from (4.31), (4.24) and (4.29) into (4.21) and (4.22) we obtain the two layer model equations for immiscible fluids.

$$\frac{\partial}{\partial t} \nabla^2 \psi_1 + \epsilon_1 \frac{\partial (\psi_2 - \psi_1)}{\partial t} - \frac{H \delta (\nabla^2 \psi_2 - \nabla^2 \psi_1)}{H_1 \sqrt{2} (1 + \mu/\delta)} = 0 \quad (4.32)$$

$$\begin{aligned} \frac{\partial}{\partial t} \nabla^2 \psi_2 - \epsilon_2 \frac{\partial (\psi_2 - \psi_1)}{\partial t} + \frac{H \mu (\nabla^2 \psi_2 - \nabla^2 \psi_1)}{H_2 \delta \sqrt{2} (1 + \mu/\delta)} \\ - \frac{H}{\sqrt{2} H_2} (2 - \nabla^2 \psi_2) = 0 \end{aligned} \quad (4.33)$$

In general this set of partial differential equations must be solved in terms of a Fourier-Bessel expansion. But in the case $\epsilon_1, \epsilon_2 \ll 1$ (where the coupling between layers is primarily frictional) an approximate solution is easily obtained by expanding the streamfunctions in perturbation series in ϵ_1 . We note that $\epsilon_2 = \epsilon_1 \frac{H_1}{H_2}$, thus if $\epsilon_1 \ll 1$ then we require only that $H_1 \approx H_2$ to insure that $\epsilon_2 \ll 1$. Formally, we expand ψ_1 and ψ_2 as

$$\psi_1 = \psi_{10} + \epsilon_1 \psi_{11} + \epsilon_1^2 \psi_{12} + \dots$$

$$\psi_2 = \psi_{20} + \epsilon_1 \psi_{21} + \epsilon_1^2 \psi_{22} + \dots$$

and equate like powers of ϵ_1 in (4.32) and (4.33). The lowest order equations are then

$$\frac{\partial}{\partial t} \nabla^2 \psi_{10} - S_1 (\nabla^2 \psi_{20} - \nabla^2 \psi_{10}) = 0 \quad (4.34)$$

$$\frac{\partial}{\partial t} \nabla^2 \psi_{20} + S_2 (\nabla^2 \psi_{20} - \nabla^2 \psi_{10}) + S_3 (\nabla^2 \psi_{20} - 2) = 0 \quad (4.35)$$

where $S_1 = \frac{H \delta}{H_1 \sqrt{2} (1 + \mu/\delta)}$, $S_2 = \frac{H \mu}{H_2 \delta \sqrt{2} (1 + \mu/\delta)}$, $S_3 = \frac{H}{H_2 \sqrt{2}}$

If we now let χ_1 and χ_2 be the Laplace transformed variables

defined by

$$\chi_1 = \int_0^{\infty} \nabla^2 \psi_{10} e^{-pt} dt, \quad \chi_2 = \int_0^{\infty} \nabla^2 \psi_{20} e^{-pt} dt$$

we obtain from (4.34) and (4.35)

$$\chi_1 = \frac{2s_1 s_3}{p(p+r_1)(p+r_2)}$$

$$\chi_2 = \frac{2s_3(p+s_1)}{p(p+r_1)(p+r_2)}$$

where $r_1, r_2 = \frac{(s_1+s_2+s_3) \pm \sqrt{(s_1+s_2+s_3)^2 - 4s_1 s_3}}{2}$

Inverting the Laplace transform we obtain

$$\nabla^2 \psi_{10} = 2 \left[1 - \frac{r_1 e^{-r_2 t} - r_2 e^{-r_1 t}}{r_1 - r_2} \right] \quad (4.36)$$

$$\nabla^2 \psi_{20} = 2 \left[1 - \frac{r_1 (1 - r_2/s_1) e^{-r_2 t} - r_2 (r_2/s_1 - 1) e^{-r_1 t}}{r_1 - r_2} \right] \quad (4.37)$$

Comparison with the complete solution to be derived below indicates that the perturbation method gives quite good results even for E_1 as large as 1. Therefore, if $E_1 \lesssim O(1)$ the interface may be treated as a plane boundary because viscous effects completely overwhelm the interface height perturbations. In Figure 4.2 the zero order solutions (4.36) and (4.37) are plotted for $H_1 = 6 \text{ cm}$, $H_2 = 8 \text{ cm}$, $\gamma = 1.57$ and $\mu = 1.26$, which are the values appropriate to the kerosene and water experiments described in Chapter 5. The points correspond to velocity measurements in two of the spin-up experiments; one for the upper layer in which $E_1 = .54$, and one for the lower layer in which $E_1 = .77$.

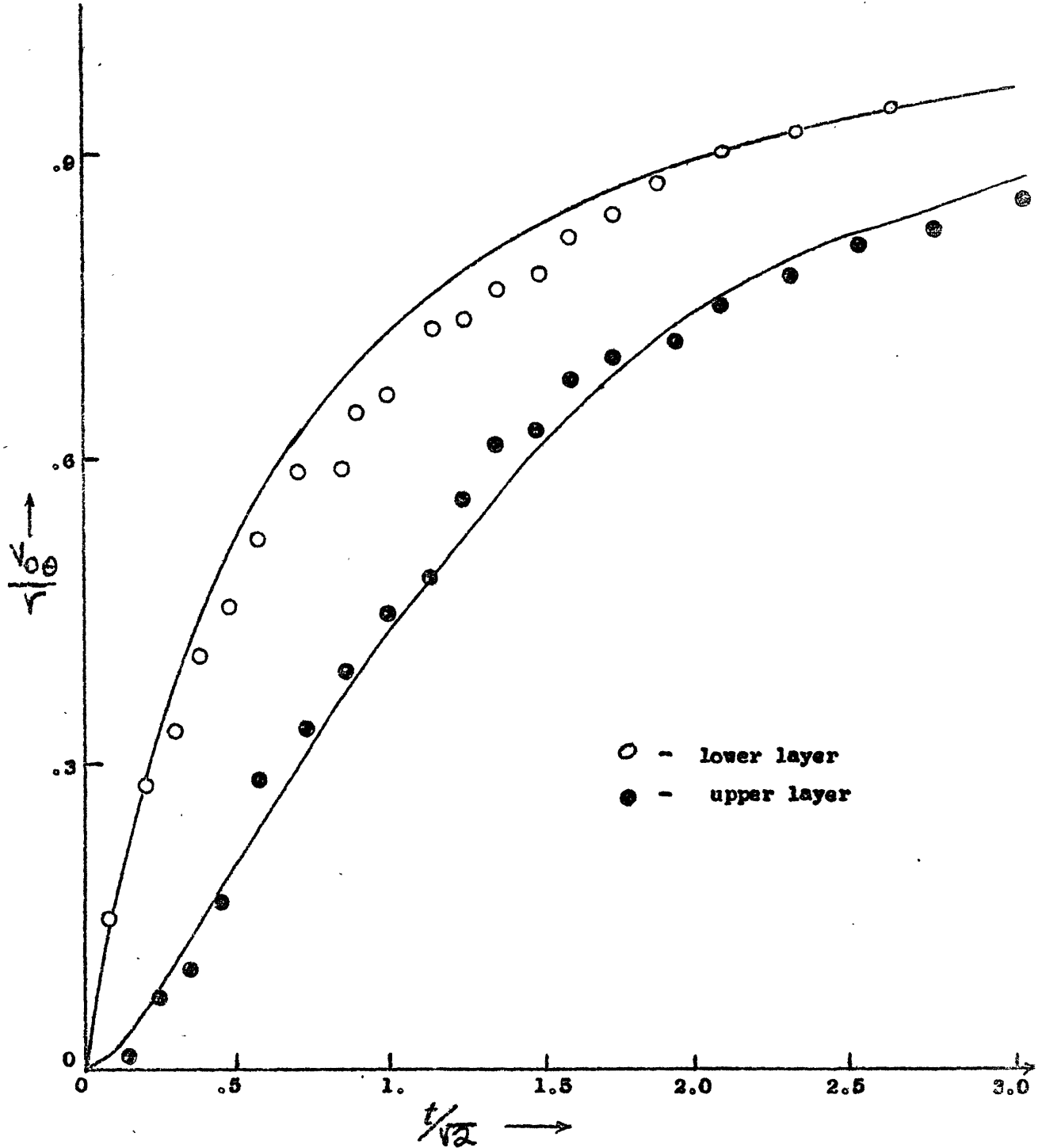


Figure 4.2

Spin-up of Immiscible Two-Layer Fluid for Small ϵ .

We now consider the more general case where ϵ_1 and ϵ_2 are large.

We define the Fourier-Bessel expansions of the stream functions as

$$\Psi_{1,2} = \sum_{n=1}^{\infty} \Psi_{1,2}(k_n, t) J_0(k_n r) \quad (4.43)$$

where $J_0(k_n)$ for all n . Substituting the expansion (4.43) into equations (4.32) and (4.33) we obtain as equations for the coefficients

$$-k_n^2 \frac{\partial \Psi_1}{\partial t} + \epsilon_1 \frac{\partial (\Psi_2 - \Psi_1)}{\partial t} + S_1 k_n^2 (\Psi_2 - \Psi_1) = 0 \quad (4.44)$$

$$-k_n^2 \frac{\partial \Psi_2}{\partial t} - \epsilon_2 \frac{\partial (\Psi_2 - \Psi_1)}{\partial t} - S_2 (\Psi_2 - \Psi_1) k_n^2 - S_3 (k_n^2 \Psi_2 + \Omega_n) \quad (4.45)$$

where $S_1 = \frac{H\sigma}{H_1 \sqrt{2} (1 + \mu_1)}$, $S_2 = \frac{H\mu}{H_2 \sigma \sqrt{2} (1 + \mu_2)}$, $S_3 = \frac{H}{H_2 \sqrt{2}}$ and Ω_n is defined in equation (3.37).

To solve the set (4.44) and (4.45) we again apply the Laplace transform and get the transformed set

$$-\bar{\Psi}_1 (p+a) + \bar{\Psi}_2 d_1 (p+b_1) = 0 \quad (4.46)$$

$$-\bar{\Psi}_2 (p+c) + \bar{\Psi}_1 d_2 (p+b_2) = \frac{S_3 \Omega_n d_1}{p \epsilon_2} \quad (4.47)$$

where

$$a = \frac{S_1 k_n^2}{k_n^2 + \epsilon_1}, \quad b_1 = \frac{S_1 k_n^2}{\epsilon_1}, \quad b_2 = \frac{S_2 k_n^2}{\epsilon_2}$$

$$c = \frac{(S_2 + S_3) k_n^2}{k_n^2 + \epsilon_2}, \quad d_1 = \frac{\epsilon_1}{k_n^2 + \epsilon_1}, \quad d_2 = \frac{\epsilon_2}{k_n^2 + \epsilon_2}$$

We define

$$B = \frac{[(b_1 + b_2) d_1 d_2 - a - c]}{(d_1 d_2 - 1)}$$

$$C = \frac{(b_1 b_2 d_1 d_2 - ac)}{(d_1 d_2 - 1)}$$

Then if $\sigma_1, \sigma_2 = \frac{-B \pm \sqrt{B^2 - 4AC}}{2}$

we have finally,

$$\bar{\Psi}_1 = \frac{S_3 \Omega_n d_1 d_2 (p + b_1)}{p E_2 (d_1 d_2 - 1) (p - \sigma_1) (p - \sigma_2)}$$

$$\bar{\Psi}_2 = \frac{S_3 \Omega_n d_2 (p + a)}{p E_2 (d_2 d_1 - 1) (p - \sigma_1) (p - \sigma_2)}$$

Inverting the Laplace Transform we obtain,

$$\begin{aligned} \Psi_1 &= \frac{S_3 \Omega_n d_1 d_2}{E_2 (d_1 d_2 - 1)} \left[\frac{b_1}{\sigma_1 \sigma_2} + \frac{(1 + \frac{b_1}{\sigma_2})}{\sigma_2 - \sigma_1} e^{\sigma_2 t} - \frac{(1 + \frac{b_1}{\sigma_1})}{\sigma_1 - \sigma_2} e^{\sigma_1 t} \right] \\ \Psi_2 &= \frac{S_3 \Omega_n d_2}{E_2 (d_1 d_2 - 1)} \left[\frac{a}{\sigma_1 \sigma_2} + \frac{(1 + \frac{a}{\sigma_2})}{\sigma_2 - \sigma_1} e^{\sigma_2 t} - \frac{(1 + \frac{a}{\sigma_1})}{\sigma_1 - \sigma_2} e^{\sigma_1 t} \right] \end{aligned} \quad (4.48)$$

The vorticity may then be obtained by substituting (4.48) into the series expansions:

$$\begin{aligned} \nabla^2 \psi_1 &= - \sum_{n=1}^{\infty} k_n^2 \Psi_1(k_n) J_0(k_n r) \\ \nabla^2 \psi_2 &= - \sum_{n=1}^{\infty} k_n^2 \Psi_2(k_n) J_0(k_n r) \end{aligned} \quad (4.49)$$

For numerical work it is easier to use velocities because the series expansions converge faster, and the experiments measure velocity. The velocities may be expressed in terms of series expansions in the first order Bessel

function

$$\begin{aligned} \frac{\partial \psi_1}{\partial r} = V_{1\theta} &= - \sum_{n=1}^{\infty} k_n \Psi_1(k_n, t) J_1(k_n r) \\ \frac{\partial \psi_2}{\partial r} = V_{2\theta} &= - \sum_{n=1}^{\infty} k_n \Psi_2(k_n, t) J_1(k_n r) \end{aligned} \quad (4.50)$$

The theoretical spin-up times listed in Table 3.1 are the result of summing numerically the first 12 terms in the series of equation (4.49) with Ψ_1 and Ψ_2 defined as in (4.48)

As ϵ_1 increases the difference in the upper and lower layer spin-up times decreases. Asymptotically for $\epsilon_1 \rightarrow \infty$ (corresponding to $\Delta\rho \rightarrow 0$) we see that $a \rightarrow b_1$, and from (4.48)

$$\Psi_1 \rightarrow \Psi_2 \rightarrow -\frac{\Omega_n}{k^2} [1 - e^{-s_3 t}]$$

Summing the Fourier-Bessel series we obtain

$$\nabla^2 \Psi_1 = \nabla^2 \Psi_2 = 2 (1 - e^{-s_3 t}) \quad \text{for } \epsilon_1 \rightarrow \infty$$

Therefore, the two-layer solution reduces to the familiar homogeneous-incompressible case when the density difference goes to zero.

It is instructive to compare the above results with the spin-up for a two layer model in which the viscous effects at the interface are neglected. In most applications of two layer models this is no doubt the correct approach because the two layer model is merely a simplification introduced to approximate a continuous stratification with no internal discontinuities. Only in a laboratory two-layer system composed of immiscible fluids is the density discontinuity at the interface a physical reality.

In the laboratory two-layer model composed of a fresh water layer over a layer of salt water there is not a discontinuous interface. Instead a diffusive boundary layer is formed in which the vertical diffusion term is of order unity in the adiabatic equation (3.13). The nondimensional depth of this boundary layer is $\lambda^{1/2}$, which is an order of magnitude larger than the depth of the Ekman boundary layer. Therefore, the conditions of continuity in velocity across the interface are satisfied in the zero order by vertical shear of the geostrophic currents in the $\lambda^{1/2}$ boundary layer. The Ekman boundary layer becomes a second order effect equivalent in magnitude to ordinary viscous diffusion. It should be noted that the diffusion coefficient of salt is extremely small so that the Prandtl number in the experiments with salt water layers is $\sigma \approx 10^2$. It might, therefore, seem that

diffusion of salt would be very small even at the interface discontinuity.

But the crucial point here is that in the experiments several hours are required to establish a complete two layer system. Hence, $\bar{t} \sim 10^4$ so that molecular diffusion will act through a depth $O(\lambda^{1/2})$.

Equations (4.32) and (4.33) simplify to

$$\frac{\partial \nabla^2 \Psi_1}{\partial t} + \epsilon_1 \frac{\partial (\Psi_2 - \Psi_1)}{\partial t} = 0 \quad (4.51)$$

$$\frac{\partial \nabla^2 \Psi_2}{\partial t} - \epsilon_1 \frac{\partial (\Psi_2 - \Psi_1)}{\partial t} - s_2 (2 - \nabla^2 \Psi_2) = 0 \quad (4.52)$$

Again applying the Fourier-Bessel series and using the Laplace transform we obtain the equations

$$\begin{aligned} -\bar{\Psi}_1 (pk_n^2 + p\epsilon_1) + \bar{\Psi}_2 (p\epsilon_1) &= 0 \\ -\bar{\Psi}_2 (pk_n^2 + p\epsilon_2 + s_2 k_n^2) + \bar{\Psi}_1 (p\epsilon_2) &= \frac{s_2 \Omega_n}{p} \end{aligned} \quad (4.53)$$

Inversion of the Laplace transform after solving for $\bar{\Psi}_1$ and $\bar{\Psi}_2$ gives

$$\Psi_1 = -\frac{\Omega_n}{k_n^2} \left(\frac{\epsilon_1}{k_n^2 + \epsilon_1} \right) (1 - e^{-\mu t}) \quad (4.54a)$$

$$\Psi_2 = -\frac{\Omega_n}{k_n^2} (1 - e^{-\mu t}) \quad (4.54b)$$

where $\mu = \frac{s_2 (k_n^2 + \epsilon_1)}{(k_n^2 + \epsilon_1 + \epsilon_2)}$

Velocities may again be obtained by substituting from (4.54a,b) into (4.38a,b).

We also see that as $\epsilon_1 \rightarrow \infty$ the solution again approaches that for the homogeneous spin-up case.

In Figures 4.3 and 4.5 the quasi-steady top layer velocity and the spin-up time respectively are plotted as function of ϵ_1 . These should be compared with Figures 3.2 and 3.4 which illustrate the same functions for the continuously stratified model. It is apparent that the two-layer system closely models the mathematically more complex continuous system. The points in Figures 4.3 and 4.4 are results of the experiments described in the next chapter.

$$\Delta \rho = \begin{cases} \blacktriangle & .02 \\ \triangle & .025 \\ \bullet & .03 \\ \circ & .04 \end{cases}$$

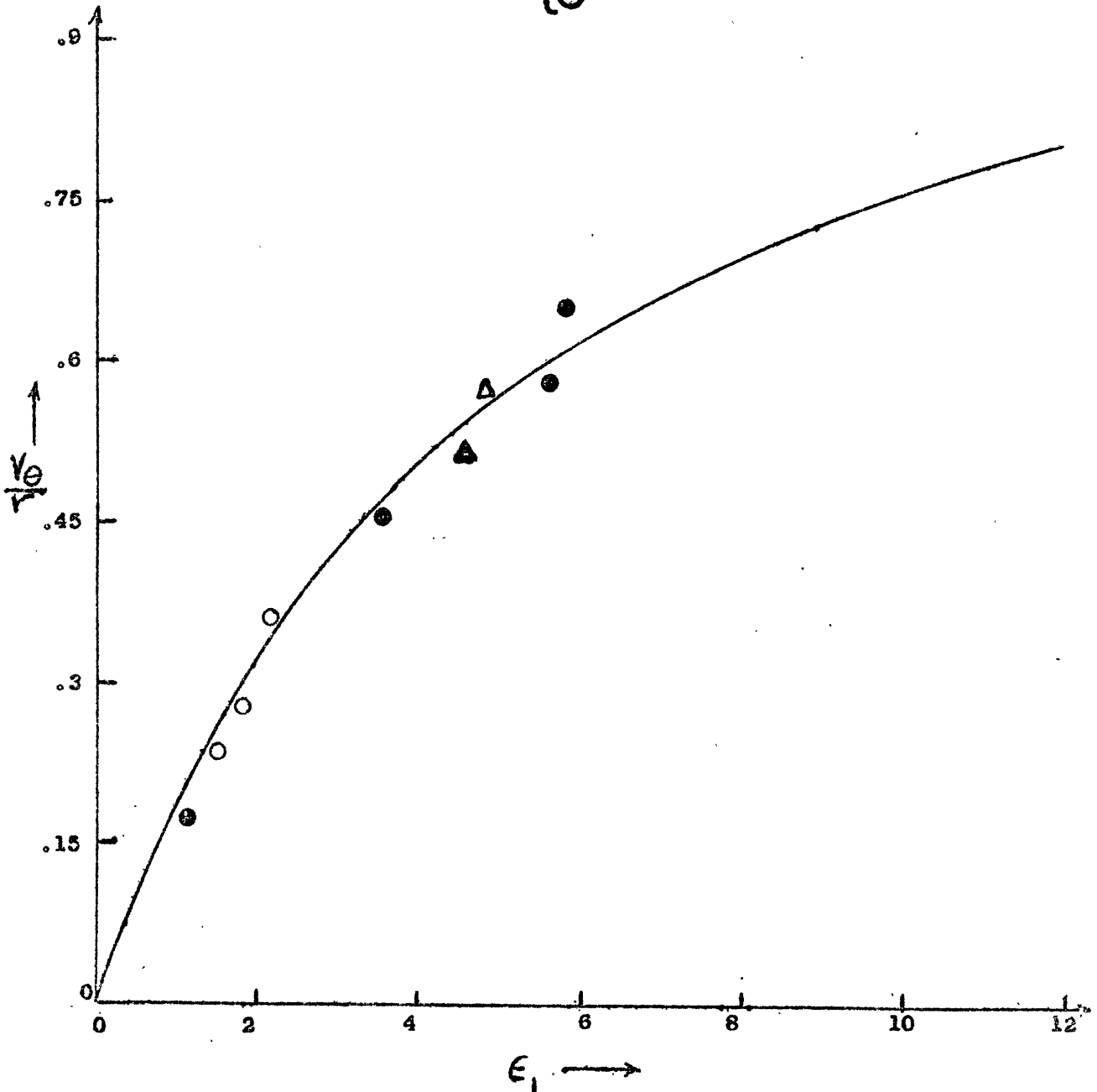


Figure 4.3
Quasi-Steady Top Layer Velocity vs. the
Internal Rotational Froude Number

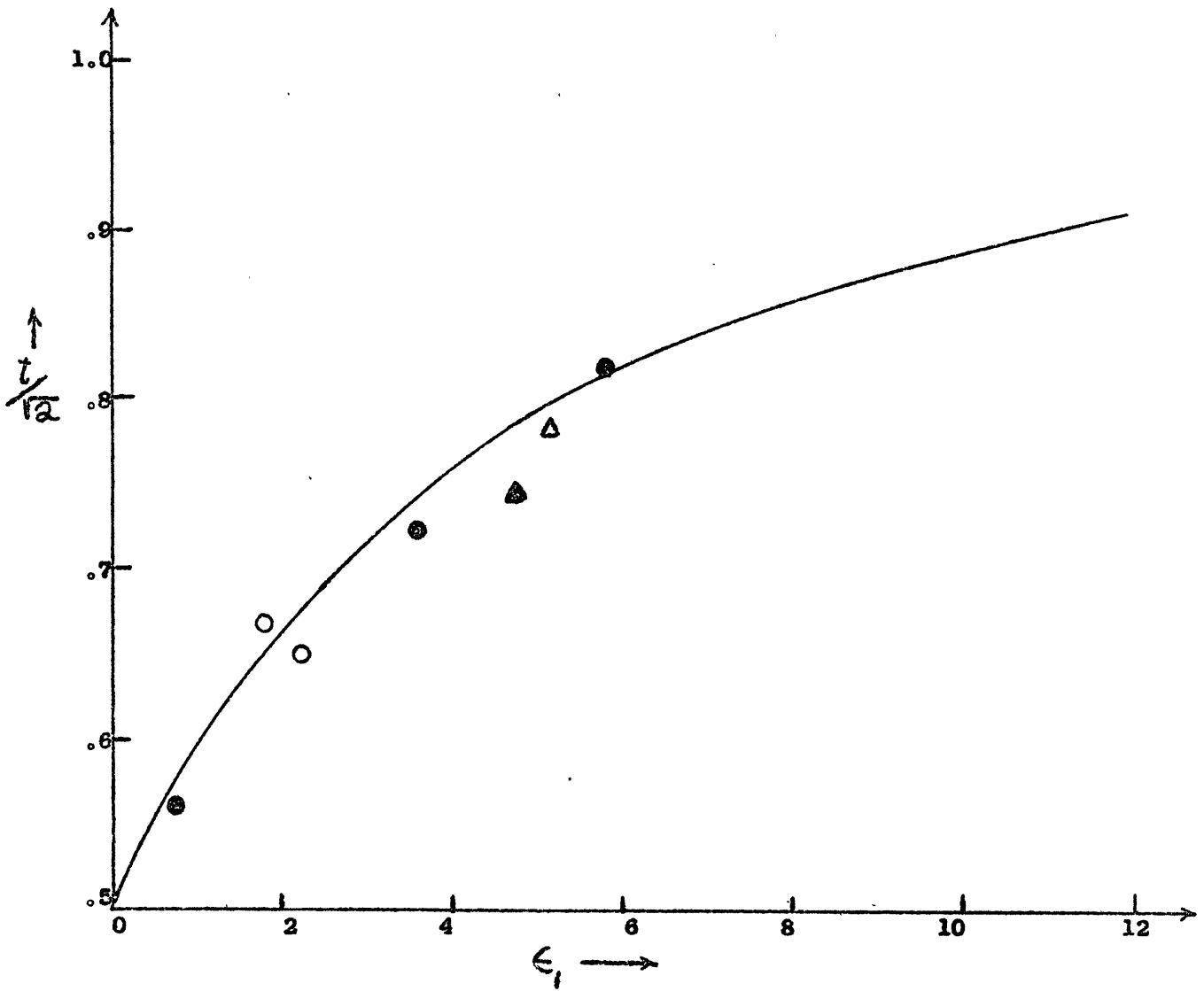


Figure 4.4

Spin-up Time vs. Internal Rotational Froude Number In The Two-Layer Model

Chapter 5

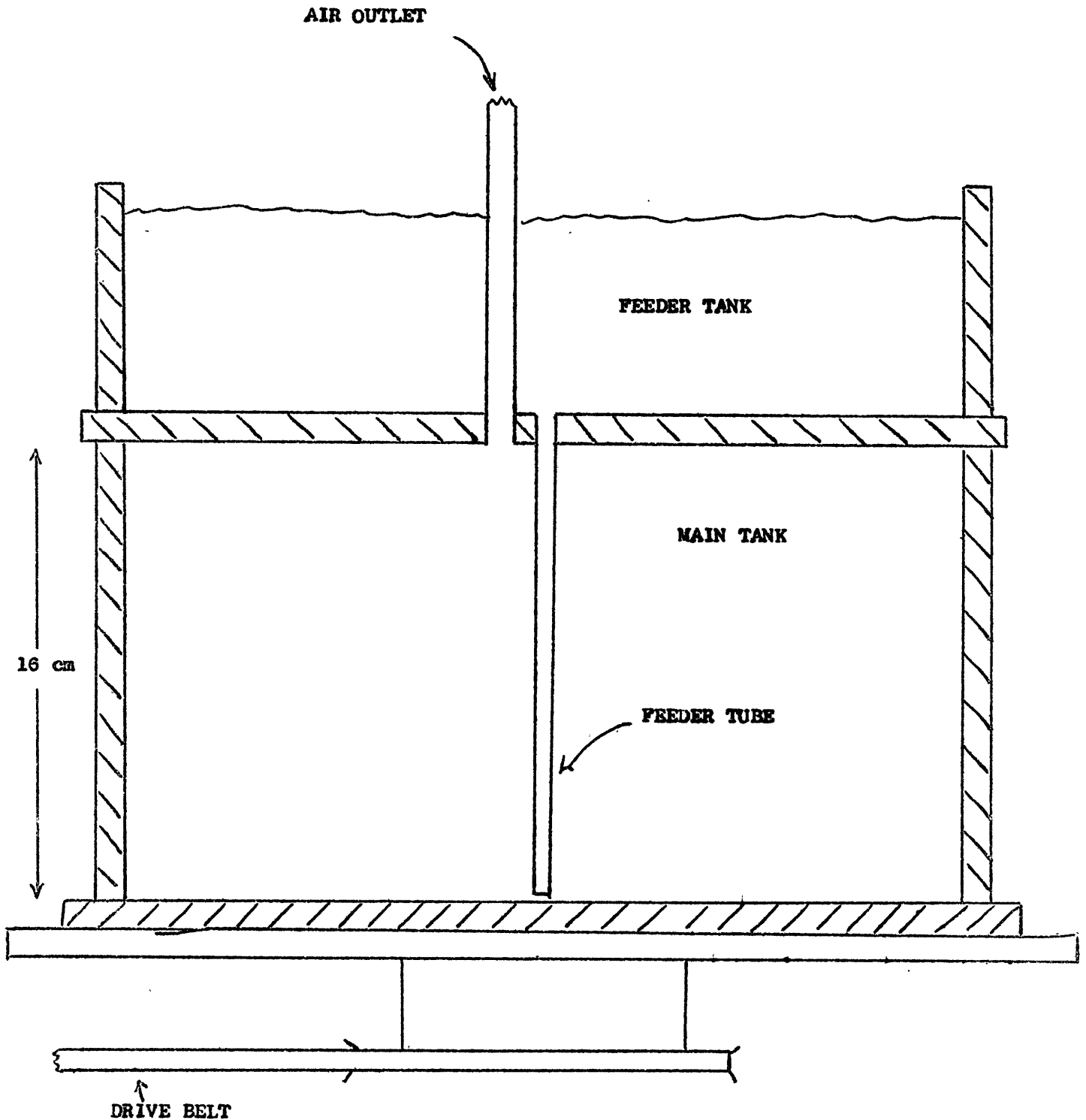
Spin-Up Experiments

The theoretical results of the two previous chapters may easily be verified in the laboratory with rather simple experiments. To test all these results three types of spin-up experiment are necessary: (1) two-layer systems composed of immiscible fluids, (2) two-layer systems consisting of a fresh water upper layer and a salt water lower layer, and (3) continuously stratified fluid systems.

The experimental apparatus is illustrated schematically in Figure 5.1. The rotating tank consists of two 29 cm. diameter plexiglass cylinders, 13 cms. and 8 cms. tall respectively. The former is mounted on a plexiglass plate and topped by another plexiglass plate. The volume thus enclosed contains the working fluid in the experiments. The latter cylinder is mounted on top of the main tank and serves as a feeder tank for the saline solutions. A narrow tube along the axis of rotation allows the dense fluid from the feeder tank to flow into the bottom boundary layer of the main tank. The apparatus is connected to a motor by a variable speed transmission. A polar diagram with 45 degree radial lines is painted on the lower plate and this may be viewed through a rotoscope device which subtracts the basic rotation of the cylinder so that relative motions are easily measured.

The two-layer system is obtained by filling the main tank to the desired level with fresh water, then allowing a dyed salt water solution to flow in slowly while the tank is rotating. If the flow is slow enough a quite sharp interface is formed with a transition layer of less than one centimeter thickness. If a continuously stratified system is desired several layers of linearly

(but see bottom of p. 64 & top of p. 66)



**SCHEMATIC CROSS SECTION OF
EXPERIMENTAL APPARATUS**

Figure 5.1

increasing density are placed in the tank and allowed to diffuse for about a day. Relative velocities in the top and bottom layers may be determined by timing the displacement of wax pellets which are weighted to attain neutral buoyancy in the top or bottom layer.

In an actual experiment the fluid is allowed to achieve solid body rotation at a given rotation rate Ω_0 . The rotation rate is then impulsively changed by a small angular velocity ω and two stop watches are used to time the float displacement between successive radial lines 45 degrees apart. Velocities can then be determined by the finite difference expression $\Delta\theta/\Delta t$, where $\Delta\theta = \pi/4$ and Δt is the measured time interval.

An accurate estimate of the probable error is difficult but several sources of error are worth mentioning. The viscosity of water changes by about 2% per degree temperature change. The temperature of the fluid could only be determined at the end of an experiment because a thermometer disturbs the flow. Thus the temperature is probably only known to $\pm 0.5^\circ\text{C}$. The rotation rate must be determined by timing a large number of rotations, and although this can be done to within about $\pm 0.1\%$, ω is a small difference between two large numbers Ω and Ω_0 and the error in ω may be $\pm 5\%$. For $R_0 \equiv \frac{\omega}{2\Omega_0} \gg 1$ nonlinear effects such as the radial advection of relative vorticity begin to modify the results. As a rough estimate we can assume that for $R_0 = 1$ the experimental results might differ from the linear theory predictions by 10%. In most of our experiments $R_0 \sim 0(1)$. This circumstance was necessitated by the difficulty of measuring relative velocities when ω was too small. As shown in appendix A, baroclinic instability may also enter as an error source. Typical experimental results, however, seem to agree with the theory to within $\pm 5\%$ as can be seen from the experimental points

in the figures of chapter 3 and 4. This is probably as good as can be expected for a linear theory.

In Table 5.1 we present the results of some experiments with immiscible two layer systems. The lower layer is water in all cases and the top layer is either kerosene with density .81 and viscosity $2.37 \text{ cm}^2 \text{ sec}^{-1}$ at 25°C , or a silicone oil with density .818 and viscosity $1.07 \text{ cm}^2 \text{ sec}^{-1}$ at 25°C . A severe experimental difficulty encountered in working with these immiscible fluid systems is the presence of large surface tension at the interface. This makes measurement of the float displacement in the bottom layer extremely difficult whenever the rotation rate is large enough to produce non-negligible curvature of the interface. In such cases the radial component of the float velocity quickly causes the float to approach the boundary at $r=1$. Therefore, the most accurate spin-up time values in the table refer in general to the float in the upper layer.

Of greater interest for geophysical problems are the experiments done with stratified salt solutions. The two-layer experiments were of course done with a free surface. The addition of a small amount of detergent to the water served to reduce surface tension effects. In cases where $E_1 > 1$ some difficulty was encountered due to baroclinic instability. In Appendix A baroclinic instability of two-layer systems is discussed. It turns out that a two-layer system in which viscosity acts only at the bottom boundary is very unstable, but Ekman layer friction damps the growth rate to such an extent that if the Rossby number is kept small enough, baroclinic waves will not grow to significant amplitude during the transient spin-up

TABLE 5.1

| Experiment | H_1 (cm) | H_2 (cm) | ω_0 (sec ⁻¹) | ω^* (sec ⁻¹) | ϵ_1 | τ (sec) | theoretical time (nondimensional) | theoretical time (nondimensional) |
|------------|------------|------------|---------------------------------|---------------------------------|--------------|--------------|--------------------------------------|--------------------------------------|
| K, U | 0 | 8 | .850 | .105 | .34 | 157 | 1.47 | 1.50 |
| K, U | 6 | 8 | 1.760 | .158 | 2.75 | 113 | 1.47 | 1.48 |
| K, S | 6 | 8 | .657 | .134 | .30 | 229 | .76 | .71 |
| K, B | 3 | 8 | 1.780 | .150 | 2.39 | 107 | .76 | .94 |
| K, U | 3 | 11 | .971 | .129 | 1.42 | 146 | 1.25 | 1.36 |
| K, B | 3 | 11 | 1.465 | .164 | 3.27 | 120 | .90 | .96 |
| SO U | 3.7 | 9.5 | 2.310 | .160 | 6.80 | 61.2 | 1.50 | 1.48 |
| SO U | 3.7 | 9.5 | .509 | .123 | .37 | 194 | 1.57 | 1.43 |
| SO B | 3.7 | 9.5 | .521 | .091 | .35 | 192 | .61 | .67 |
| SO B | 3.7 | 9.5 | 1.970 | .130 | 4.95 | 99.0 | .60 | .65 |

Nondimensional Spin-Up Time For Experiments With Immiscible Fluids

Code: U = Upper Layer, B = Bottom Layer, K = Kerosene Experiment

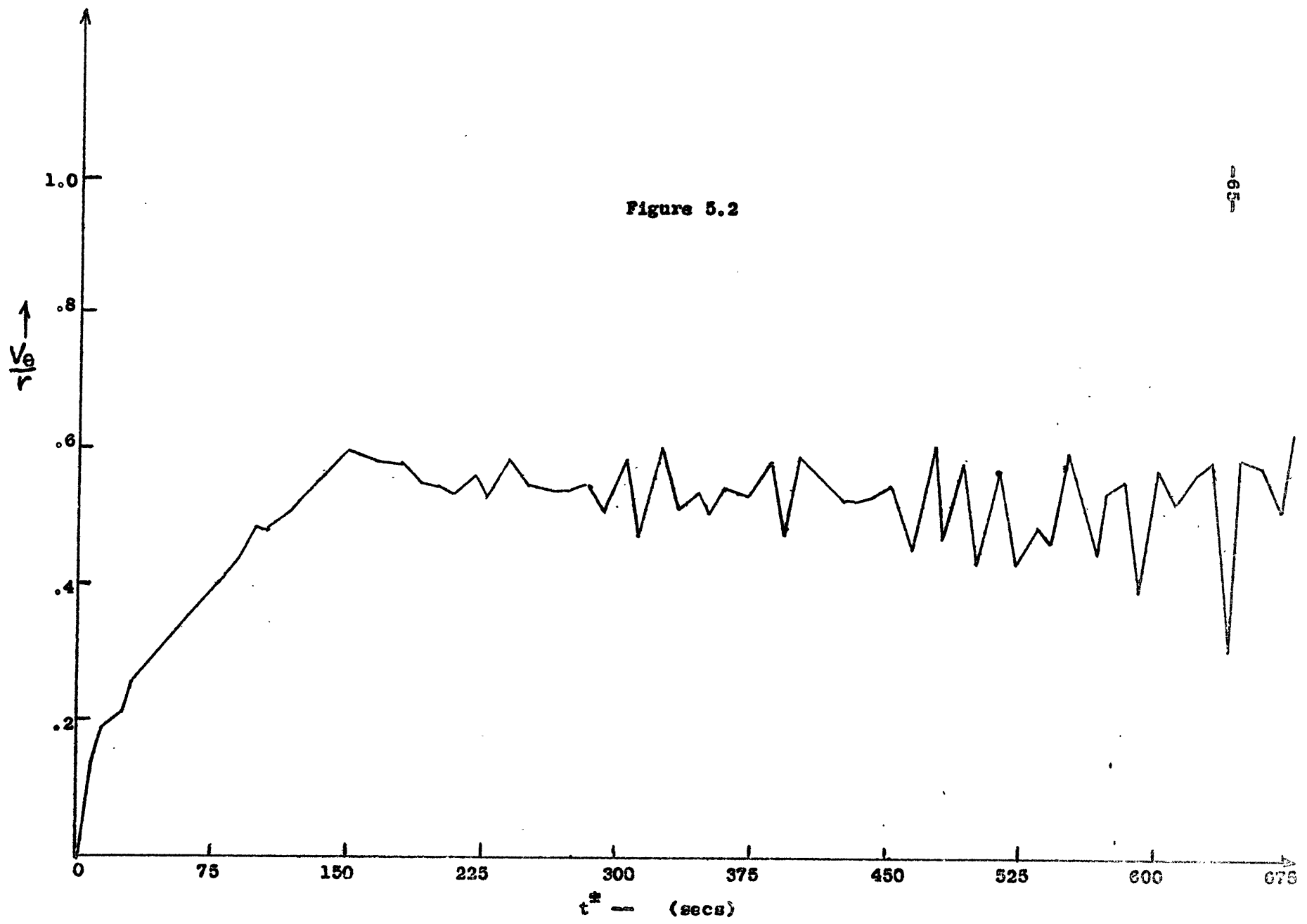
S.O. = Silicone Oil Experiment

phase of the motion. This is because R_0 reflects the magnitude of the vertical shear of the zonal velocity, and the growth rate depends on the shear.

In Figure 5.2 the experimental data for an unstable case are shown. Here $G_1 = 9.1$ and $R_0 = .3$. The theoretical quasi-steady velocity is and the theoretical spin-up time is 92 seconds. The measured spin-up time is only 73 seconds, indicating substantial nonlinear advection which causes the fluid to spin-up faster than the theoretically predicted spin-up time. In addition, the growth of unstable waves prevents the layer from reaching the quasi-steady state. Hence, we must keep the Rossby number quite small to be able to successfully test the predictions of the spin-up theory for large values of the internal rotational Froude number. In Figures 4.4 and 4.5 of chapter 4 the experimental results for spin-up time and velocity of the upper layer in the quasi-steady state are shown along with the theoretical curves. The scatter of experimental results is greater for the spin-up time measurements than for the quasi-steady state velocities. This merely reflects the fact that in the former case transient velocities must be estimated by a finite difference approximation, whereas in the latter a steady velocity can be achieved.

Continuously stratified fluids were also studied experimentally. The best experiments were done with a rigid top boundary. In this case, as the theory of chapter 2 indicates, the motion is symmetrical about the mid point between the two horizontal boundaries. Neutrally buoyant wax pellets were used to measure the velocity at several levels both above and below $Z = 0$. Some free surface experiments were also done with a continuously stratified system. In these cases the continuous stratification was obtained merely

Figure 5.2



Baroclinic Instability Effects

by mixing a two layer system. The density profile obtained in this manner was probably not closely linear, but fortunately the spin-up theory results are not very sensitive to moderate vertical variation of ϵ . The results of these experiments are included in Figures 3.2 and 3.4 and show reasonable agreement with the theory. Better controlled experiments could obviously be designed. However, the added effort does not seem worthwhile for study of the interior flow because even the simple experiments described here are adequate proof of the essential ^{qualitative} validity of the theory.

On the other hand, a detailed study of the side boundary layer structure would require much more accurate flow measurement techniques. Such a study could probably best be done in a thermally stratified system with the aid of thermocouples to measure the density field.

Chapter 6

The Effect of Ekman Friction on Wind Generated Ocean Currents

The mathematical techniques developed for the laboratory spin-up problem may be applied in a straight forward manner to determine the response of a stratified ocean to the wind stress of an idealized circular storm. If we assume $\beta \equiv 0$ we may again restrict the theory to a circularly symmetric storm. In a later chapter we discuss modifications due to the β -effect. We refer the motion to a tangent plane coordinate system, i.e. a plane coordinate system which is tangent at its origin to some point on the spherical earth. Letting this point be at latitude $\phi = 45^\circ$ we obtain for the Coriolis parameter $f = 2\Omega_0 \sin\phi \approx 10^{-4} \text{ sec}^{-1}$. Here Ω_0 is the angular velocity of the earth about its axis. The equations of motion in this coordinate system are the same as for the rotating tank except that f replaces $2\Omega_0$ in the horizontal momentum equations. Similarly f replaces $2\Omega_0$ in the time scale $\tau = \left(\frac{H^2}{f\nu}\right)^{1/2}$ and in all the nondimensional parameters.

The problem may now be scaled exactly as in chapter 3 if we define $\omega = \frac{u}{L}$ where u is a typical horizontal current velocity. The nondimensional governing equations are then (3.8) - (3.13) and the parameters R_0 and λ are again small. To fix ideas it is desirable at this point to assign realistic values to the various scaling quantities. For example:

$$\begin{aligned}
 H &= 5 \times 10^5 \text{ cm} \\
 u &= 2 \text{ cm sec}^{-1} \\
 f &= 10^{-4} \text{ sec}^{-1} \\
 \nu_z &= 10^2 \text{ cm}^2 \text{ sec}^{-1} \\
 L &= 10^8 \text{ cm}
 \end{aligned}
 \tag{6.1}$$

The eddy viscosity coefficient is difficult to measure and probably varies a good deal with depth. However, the theory of the Ekman layer depends on the square root of ν_2 and terms containing ν_2 are negligible outside the boundary layer. The value selected here corresponds to an Ekman layer depth of 10 meters which is typical of the real oceans.

The scale L represents a typical quarter wavelength for a circular storm. According to White and Cooley (1953) the maximum kinetic energy for transient tropospheric disturbances is in wave number 8 at 45°N. This corresponds to a quarter wavelength of about 800 km. For comparison we also will consider a horizontal scale $L = 10^7$ cm, which does not correspond to any real wind systems (except possibly hurricanes), but will help elucidate the role of horizontal scale in determining the response of the ocean to surface stresses.

Using the numerical values given in (5.1) we find that $\tau = 5 \times 10^6$ sec which means that the decay time for a barotropic current is about 50 days. For the various nondimensional parameters we have

$$\lambda = \left(\frac{\nu_2}{fH^2} \right)^{1/2} \approx 10^{-2} \quad R_0 = \frac{w}{f} = \begin{cases} 10^{-3} & \text{for } L = 10^7 \text{ cm} \\ 10^{-4} & \text{for } L = 10^8 \text{ cm} \end{cases}$$

$$E = \frac{f^2 L^2}{gH^2K} = \begin{cases} 1 & \text{for } L = 10^7 \\ 100 & \text{for } L = 10^8 \end{cases}$$

For convenience in the analysis we select a wind stress whose curl is proportional to $\nabla_0^2(h, r)$ and whose magnitude is such that the induced non-dimensional geostrophic current velocity is of order unity if the wind stress acts for a time $t^* \sim O(\tau)$. Further, we let the wind stress have a time dependence defined by $F(t)$, where

$$F(t) = \begin{cases} 0 & t < 0 \\ 1 & 0 < t < S \\ 0 & t > S \end{cases}$$

We now determine the character of the response of the ocean as a function of the wind stress period S .

We expand the governing equations using a perturbation series in λ exactly as in chapter 3. Since $R_0 \ll \lambda$ the error caused by neglecting the inertial terms is much smaller in this case than it was in the laboratory model. The boundary conditions at $z=1$ and $z=0$ must again be determined by boundary layer theory. A nondimensional stress at the free surface of the form $\lambda \frac{\partial V_\theta}{\partial z} = \frac{1}{k_1} J_1(k_1 r) F(t)$, $\frac{\partial V_r}{\partial z} = 0$ satisfied the requirements mentioned above. The boundary conditions at $z=1$ for the first order Ekman layer equations (3.23) - (3.26) are then

$$\frac{\partial V_{\theta}^B}{\partial z} = \frac{J_1(k_1 r) F(t)}{k_1}, \quad \frac{\partial V_{or}^B}{\partial z} = 0 \quad \text{at } z=0 \quad (6.2)$$

The solution is the familiar Ekman spiral

$$\begin{aligned} V_{\theta}^B &= \frac{J_1(k_1 r)}{k_1} F(t) e^{z/\sqrt{2}} \sin\left(\frac{z}{\sqrt{2}} + \frac{\pi}{4}\right) \\ V_{or}^B &= \frac{J_1(k_1 r)}{k_1} F(t) e^{z/\sqrt{2}} \cos\left(\frac{z}{\sqrt{2}} + \frac{\pi}{4}\right) \end{aligned} \quad (6.3)$$

Integrating the continuity equation (3.26) across the boundary layer we obtain the vertical velocity at the bottom of the boundary layer.

$$-W^B(0) = W^I(1) = J_0(k_1 r) F(t) \quad (6.4)$$

The first order boundary layer at the bottom in the Ekman layer for a rigid boundary obtained in chapter 3. The vertical mass flux out of this layer is

$$W^I(0) = \frac{\nabla^2 \psi}{\sqrt{2}} \quad (6.5)$$

The expansion for the interior is identical to that of chapter 3 and will not be repeated here. The resulting first order system in terms

of the stream function ψ is the potential vorticity equation

$$\frac{\partial}{\partial t} \left(\nabla^2 \psi + \epsilon \frac{\partial^2 \psi}{\partial z^2} \right) = 0 \quad (6.6)$$

subject to the boundary conditions

$$\frac{\partial}{\partial t} \left(\frac{\partial \psi}{\partial z} \right) = - \frac{J_0(k,r)}{\epsilon} F(t) \quad \text{at } z=1$$

$$\frac{\partial}{\partial t} \left(\frac{\partial \psi}{\partial z} \right) + \frac{\nabla^2 \psi}{\sqrt{2} \epsilon} = 0 \quad \text{at } z=0 \quad (6.7)$$

To solve we separate their dependence by letting $\psi = \Psi(k, z, t) J_0(k, r)$

and take the Laplace transform of Ψ

$$\bar{\Psi} = \int_0^\infty \Psi e^{-pt} dt$$

We then obtain from (6.6) and (6.7)

$$\bar{\Psi} = \frac{-(1 - e^{-ps}) \left[\frac{\cosh \frac{k_1}{\sqrt{2}\epsilon} z}{k_1} + \frac{\sinh \frac{k_1}{\sqrt{2}\epsilon} z}{\sqrt{2}\epsilon p} \right]}{p \sqrt{2}\epsilon \sinh \frac{k_1}{\sqrt{2}\epsilon} \left(p + \frac{k_1}{\sqrt{2}\epsilon} \coth \frac{k_1}{\sqrt{2}\epsilon} \right)} \quad (6.8)$$

Inverting the Laplace transform we get

$$\nabla^2 \psi = \left[\frac{\sqrt{2} \cosh \frac{k_1}{\sqrt{2}\epsilon} z}{\cosh \frac{k_1}{\sqrt{2}\epsilon}} G(t) + \frac{k_1}{\sqrt{2}\epsilon} \frac{\sinh \frac{k_1}{\sqrt{2}\epsilon} z}{\cosh \frac{k_1}{\sqrt{2}\epsilon}} H(t) \right] J_0(k, r) \quad (6.9)$$

where

$$G(t) = \begin{cases} 1 - e^{-\alpha t} & \text{for } t < s \\ e^{-\alpha(t-s)} - e^{-\alpha t} & \text{for } t > s \end{cases}$$

$$H(t) = \begin{cases} t - \frac{(1 - e^{-\alpha t})}{\alpha} & \text{for } t < s \\ s - \frac{e^{-\alpha(t-s)} - e^{-\alpha t}}{\alpha} & \text{for } t > s \end{cases}$$

and $\alpha = \frac{k_1}{\sqrt{2}\epsilon} \coth \frac{k_1}{\sqrt{2}\epsilon}$ is the inverse of the spin-up time for a stratified fluid.

As noted above $\epsilon \approx 10^2$ for real wind systems. But for large ϵ (6.9) is approximately

$$\nabla^2 \psi = \left[\sqrt{2} G(t) + \frac{k_1^2}{\epsilon} z H(t) \right] J_0(k_1 r)$$

Thus, it is appropriate to call the first term on the right the barotropic mode and the second term the baroclinic mode. The function $G(t)$ reaches its maximum value at $t = s$ and for $t > s$ decays at the barotropic spin-down rate. Therefore as $t \rightarrow \infty$ only the baroclinic mode remains and for large ϵ

$$\nabla^2 \psi \rightarrow \frac{S k_1^2 z}{\epsilon} \quad \text{as } t \rightarrow \infty \quad (6.10)$$

Now $k_1 = 2.404$, hence if $\epsilon = 10^2$ this baroclinic mode (6.10) approaches order unity for $S \sim O(10)$, corresponding to a period of about one year. We further note that the barotropic mode attains its full magnitude for $S \sim O(1)$ and that it remains of order unity as S increases. Physically this occurs because for $S \gtrsim O(1)$ a balance is achieved between the energy added by the wind stress and the dissipation by spin-down in the bottom Ekman layer. The baroclinic mode is, however, not influenced by the bottom Ekman layer. It therefore continues to grow as long as the wind stress is present, and remains constant for $t > s$.

In Figure 6.1 the ratio of the vertically integrated amplitudes of the baroclinic and barotropic modes is plotted as a function of the wind stress frequency S . Shapiro and Ward (1960) analyzed the time-space spectrum of the tropospheric geostrophic meridional kinetic energy. At 45°N they found that in wave numbers 6 to 8 (for which $\epsilon \sim 10^2$) the amplitude was virtually constant for periods ranging from 2 to 400 days. Therefore, the wind stress amplitude is nearly independent of S . From Figure 6.1 we

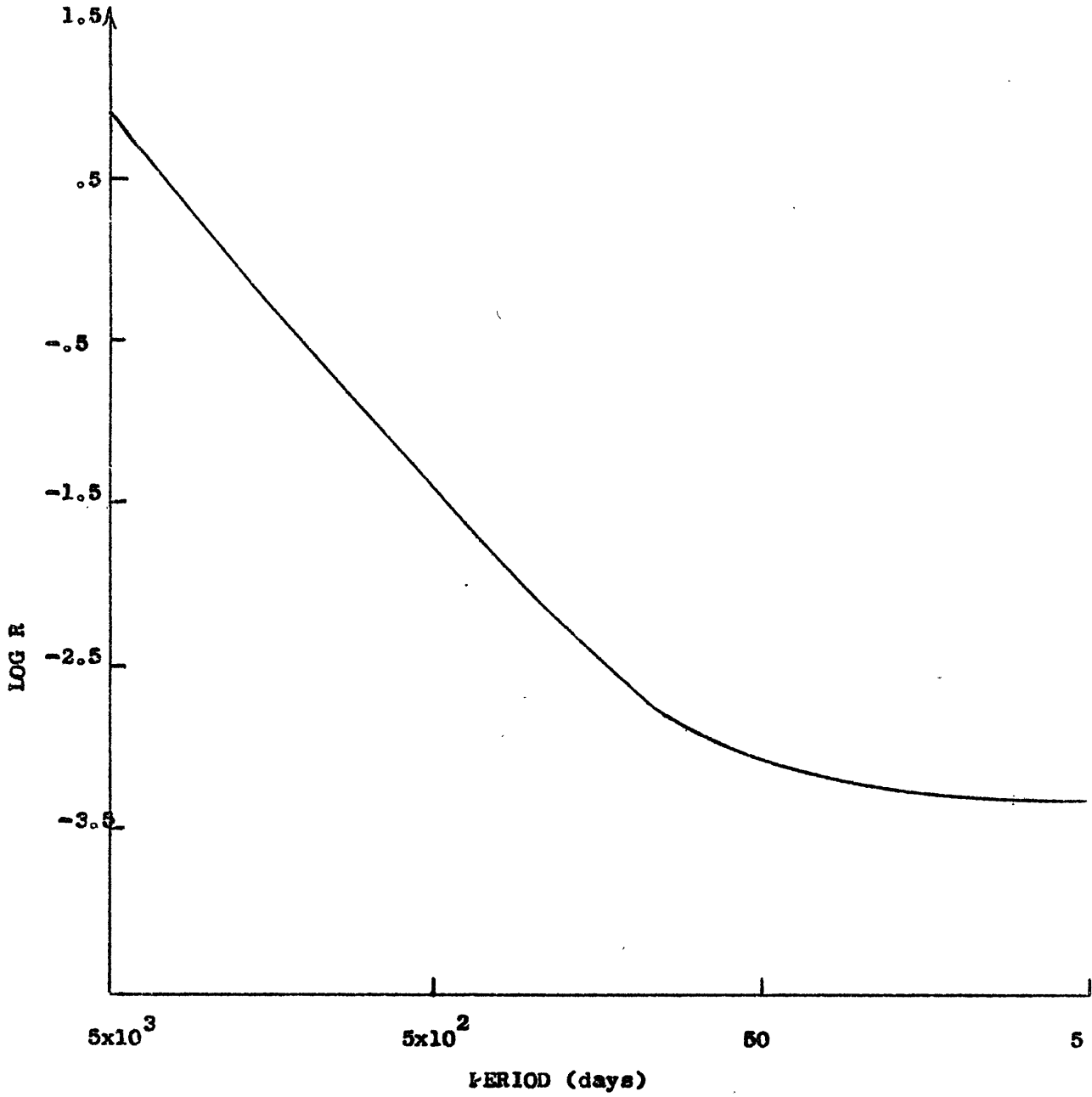


Figure 6.1

The ratio R of the Baroclinic to Barotropic Amplitudes vs. Wind Stress period

may conclude that most of the energy input for the baroclinic mode is at the long periods of several months or more. Stommel and Veronis (1956) arrived at the same conclusion using a two-layer model. However, in their case the β -effect was responsible for the baroclinic response at long periods. The present analysis suggests that it is not necessary to include β for a qualitative explanation of the baroclinicity of the oceans because Ekman layer friction provided a strong damping effect on the barotropic response. It also appears that in studies of large scale air-sea interaction the transient effects of individual synoptic systems can be neglected, for such systems excite primarily the barotropic mode and due to Ekman damping the ocean has a short "memory" for this sort of energy input.

On the other hand, climatic variations on the time scale of several months excite the baroclinic mode which decays very slowly on the internal diffusion time scale. Hence, the ocean has a long "memory" for baroclinic energy inputs and therefore feedback to the atmosphere may be significant.

The two-layer model of chapter 4 may also be used to derive an expression analogous to (3.8). In the two-layer model the wind stress acts as a body force on the top layer and Ekman friction acts as a body force on the bottom layer. Using the scaling of the present chapter the results for the two-layer model may be written

$$\begin{aligned} \nabla^2 \psi_1 &= \left[\frac{H_2 \sqrt{2} (1 + \frac{\epsilon_2}{k_2^2})}{H_1 (1 + \frac{\epsilon_1}{k_1^2})} G(t) + \frac{H}{H_1 (1 + \frac{\epsilon_1}{k_1^2})} H(t) \right] J_0(k, r) \\ \nabla^2 \psi_2 &= \left[\frac{\sqrt{2} \epsilon_1}{(1 + \frac{\epsilon_1}{k_1^2}) k_1^2} G(t) \right] J_0(k, r) \end{aligned} \quad (6.11)$$

where $G(t)$ and $H(t)$ are defined in (3.8), but the inverse spin-up time

$$\alpha \text{ is now } \alpha = \frac{(1 + \frac{\epsilon_1}{k_1^2}) H / H_2}{\sqrt{2} (1 + \frac{\epsilon_1}{k_1^2} + \frac{\epsilon_2}{k_2^2})}$$

We see that for $\epsilon_1 \gg 1$ the barotropic component has decayed and the steady state baroclinic mode remains. For $\epsilon_1 \gg 1$ this is just

$$\nabla^2 \psi_1 \approx \frac{s_1 k_1^2}{\epsilon_1} \left(\frac{H}{H_1} \right)$$

which is equal to the result for the continuous model (6.10) at $z = 1$.

This is an indication that the two-layer model represents a constant static stability continuously stratified system quite well.

In the real oceans static stability is of course not constant with depth, but varies from a maximum at about 100 ms. depth, where the temperature gradient is 4°C per 100 ms., to a value an order of magnitude smaller in very deep water. We now construct a simple function to represent the depth dependence of static stability, and examine the consequent modifications in the previous theory. Strictly speaking we should take the slight compressibility of sea water into account by using the potential density gradient rather than merely the density gradient in evaluating the static stability. However, the two differ only slightly except at great depths so that for an approximate theory we may retain the incompressibility assumption. It should be kept in mind, though, that in reality ϵ at great depths is even larger than the value computed from the density gradient.

In Figure 0.2 the mean vertical temperature profile for the North Atlantic as reported by Defant (1961) is shown together with the simple analytic representation

$$T_s^* = \frac{2.0}{(1.35 - 1.25 z)} \quad (6.12)$$

In addition the Figure shows the observed temperature gradient along with the derivative of (6.12).

$$\frac{dT_s^*}{dz} = \frac{2.5}{(1.35 - 1.25 z)^2}$$

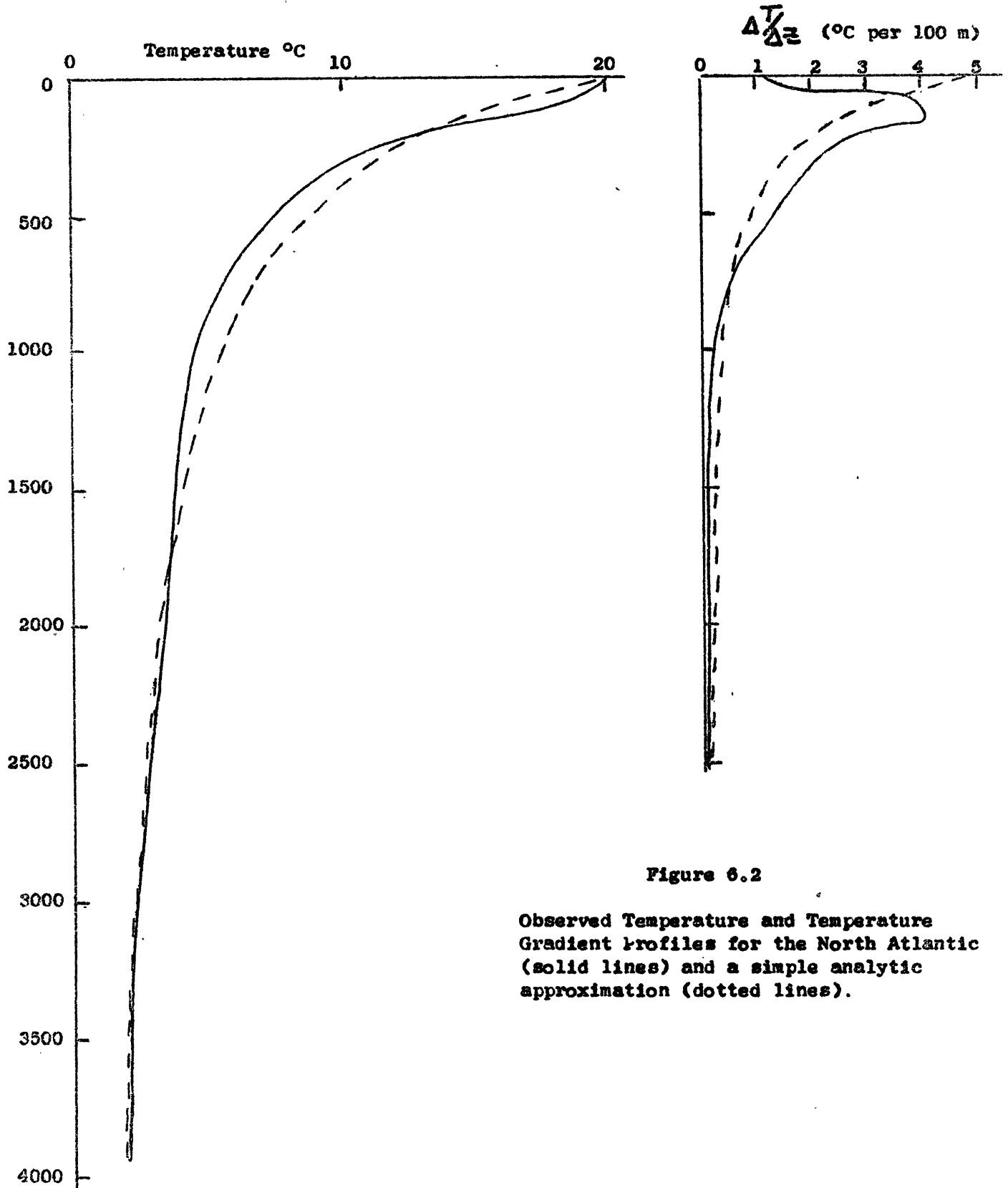


Figure 6.2

Observed Temperature and Temperature Gradient profiles for the North Atlantic (solid lines) and a simple analytic approximation (dotted lines).

Recalling the definition of ϵ we have

$$\epsilon = \frac{f^2 L^2}{g H \alpha \frac{dT_s}{dz}} = \epsilon_0 (1 + \gamma - \gamma z)^2$$

where $\epsilon_0 = f^2 L^2 / g H \alpha \frac{dT_s}{dz}$ and $\gamma = 12.5$. Therefore, for the scale of a typical wind stress, $L = 10^8$, $\epsilon_0 = 8$. This simple quadratic representation is a good qualitative approximation of the actual static stability variation except in the top 100 m, where it fails to represent the mixed isothermal layer. The mixed layer is essentially a boundary layer effect, however, and the failure to include it should not substantially effect large scale dynamic processes.

In the present case the potential vorticity equation (6.6) becomes

$$\frac{\partial}{\partial t} \left\{ \nabla^2 \psi + \epsilon_0 \frac{\partial}{\partial z} \left[(1 + \gamma - \gamma z)^2 \frac{\partial \psi}{\partial z} \right] \right\} = 0 \quad (6.13)$$

We again separate the r dependence by letting $\psi = \Psi(k, z, t) J_0(kr)$

and take the Laplace transform of (6.13) to get

$$\frac{\partial}{\partial z} \left[(1 + \gamma - \gamma z)^2 \frac{\partial \bar{\Psi}}{\partial z} \right] - \frac{k^2}{\epsilon_0} \bar{\Psi} = 0 \quad (6.14)$$

We now define the new independent variable $x = 1 + \gamma - \gamma z$, and rewrite (6.14)

in terms of x as

$$\frac{\partial^2 \bar{\Psi}}{\partial x^2} + \frac{2}{x} \frac{\partial \bar{\Psi}}{\partial x} - \frac{1}{x^2} \left(\frac{k^2}{\epsilon_0 \gamma} \right) \bar{\Psi} = 0 \quad (6.15)$$

The boundary conditions (6.7) become

$$\begin{aligned} p \frac{\partial \bar{\Psi}}{\partial x} &= \frac{(1 - e^{-ps})}{p \epsilon_0 \gamma} \quad \text{at } x = 1 \\ p \frac{\partial \bar{\Psi}}{\partial x} + \frac{k^2 \bar{\Psi}}{\sqrt{2} \epsilon_0 \gamma (1 + \gamma^2)^2} &= 0 \quad \text{at } x = 1 + \gamma \end{aligned} \quad (6.16)$$

The solution of (3.15) subject to boundary conditions (3.16) is

$$\bar{\Psi} = \frac{(1 - e^{-pS}) [r_2 x^{r_1} (1+\gamma)^{r_2-r_1} - r_1 x^{r_2}]}{\epsilon_0 \gamma r_1 r_2 A p (p + \alpha)} + \frac{(1 - e^{-pS}) [(1+\gamma)^{r_2-r_1} - r_1 x^{r_2}] a (1+\gamma)}{\epsilon_0 \gamma r_1 r_2 A p^2 (p + \alpha)} \quad (6.17)$$

where

$$r_1, r_2 = \frac{1}{2} \left(-1 \pm \sqrt{1 + 4k_1^2 / \epsilon_0 \gamma^2} \right)$$

$$A = (1+\gamma)^{r_2-r_1} - 1$$

$$a = \frac{k_1^2}{\sqrt{2} \epsilon_0 \gamma (1+\gamma)^2}, \quad \alpha = \frac{a(1+\gamma)}{A r_2} \left[(1+\gamma)^{r_2-r_1} - \frac{r_2}{r_1} \right]$$

Inverting the Laplace transform we obtain

$$\nabla^2 \psi = \left\{ \frac{r_2 x^{r_1} (1+\gamma)^{r_2-r_1} - r_1 x^{r_2}}{\epsilon_0 \gamma r_1 r_2 A \alpha} G(t) + \frac{a(1+\gamma) [(1+\gamma)^{r_2-r_1} x^{r_1} - x^{r_2}]}{\epsilon_0 \gamma r_1 r_2 A \alpha} H(t) \right\} J_0(k_1 r) \quad (6.18)$$

where $G(t)$ and $H(t)$ are the functions defined in (5.9) but γ is

here defined as in (6.12). Again we see that for $t \gg S$ only the baro-

clinic mode remains and

$$\nabla^2 \psi = - \frac{[(1+\gamma)^{r_2-r_1} x^{r_1} - x^{r_2}] k_1^2 S}{\epsilon_0 \gamma r_1 [(1+\gamma)^{r_2-r_1} - r_2/r_1]} J_0(k_1 r)$$

The vertical structures of the steady state baroclinic modes in the constant and variable static stability models are shown in Figure 6.3 for the horizontal scale length $L = 10^8$ cm. In the variable static stability model the vertical shear of the current is enhanced near the surface. Hence, the baroclinicity of the response is increased by allowing ϵ to vary with depth in a realistic manner. The partition of energy between the barotropic and baroclinic modes is, however, not much changed from the constant static stability results shown in Figure 6.1.

The solutions for the constant static stability, two-layer, and variable static stability models (6.9), (6.11) and (6.18) enable us to estimate the spin-down time as a function of horizontal scale. For comparison we choose the two scales $L=100\text{ km}$ and $L=1,000\text{ km}$. The former corresponds to the Gulf Stream eddy scale (not a directly wind driven system) and the latter is the cyclone scale previously considered in this chapter.

In the constant static stability model the spin-down time is

$$\frac{\sqrt{2}\epsilon}{k_1} \tanh \frac{k_1}{\sqrt{\epsilon}} \approx \begin{cases} \sqrt{2} (.98) & \text{for } L=1,000\text{ km., } \epsilon=100 \\ \sqrt{2} (.41) & \text{for } L=100\text{ km., } \epsilon=1 \end{cases}$$

In the two-layer model if we let $H_1=5\text{ km}$ and $H_2=4.5\text{ km}$ then the spin-down

time is

$$\frac{\sqrt{2} (1 + \frac{\epsilon_1 + \epsilon_2}{k_1^2})}{(1 + \frac{\epsilon_1}{k_1^2}) H/H_2} \approx \begin{cases} \sqrt{2} & \text{for } L=1,000\text{ km., } \epsilon_1=10^3 \\ \sqrt{2} (.97) & \text{for } L=100\text{ km., } \epsilon_1=10 \end{cases}$$

whereas in the variable static stability model the time is from (6.17)

$$\frac{\sqrt{2} \epsilon_0 \gamma (1+\gamma) [(1+\gamma)^{r_2-r_1} - 1] r_2}{k_1^2 [(1+\gamma)^{r_2-r_1} - r_2/r_1]} \approx \begin{cases} \sqrt{2} (.99) & \text{for } L=1,000\text{ km., } \epsilon_0=8 \\ \sqrt{2} (.74) & \text{for } L=100\text{ km., } \epsilon_0=.08 \end{cases}$$

In all three cases the spin-down time approaches that of a homogeneous incompressible fluid as the horizontal scale is increased. But for small scales, in which baroclinic effects are important, the two-layer model with the top layer depth taken as approximately the depth of the permanent thermocline fails to exhibit the marked reduction in spin-down time characteristic of the continuously stratified models.

Although the models considered in this chapter are a vast oversimplification of the physical processes occurring in the real oceans, enough of the dynamics has been retained to indicate that bottom friction is an important mechanism in the production and maintenance of the highly baro-

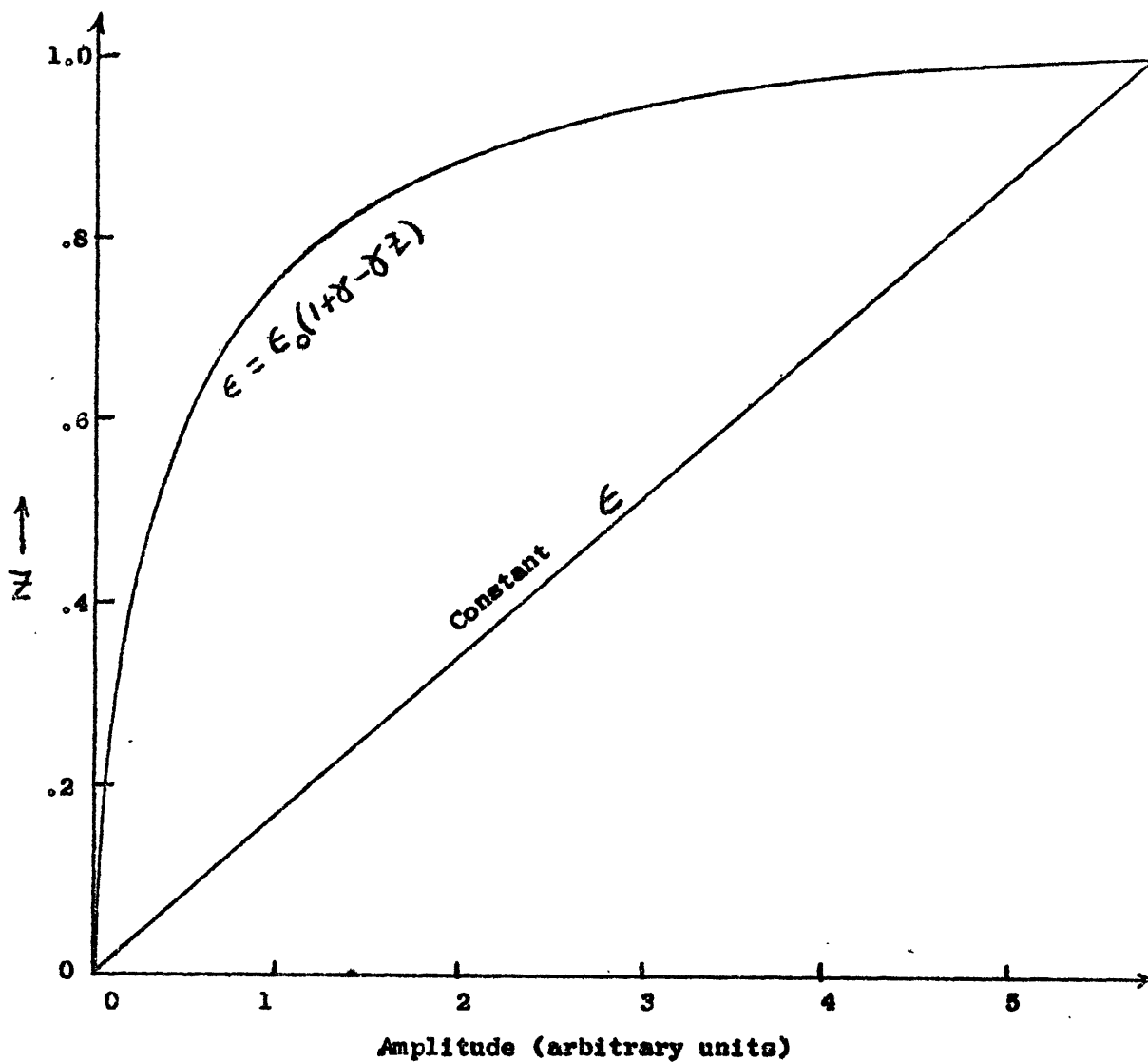


Figure 6.3

Vertical Structure of the Baroclinic Mode for the Constant and Variable Static Stability Models, $L = 10^8$ cm.

clinic current structure in the oceans. If, however, the earth were not in rotation, bottom friction could influence the flow in the interior only through the slow process of viscous diffusion. In that case bottom friction would have a negligible effect in damping the barotropic currents. Once again we see the profound effect which rotation has on the nature of planetary fluid flows.

Chapter 7

The Evolution of a Baroclinic Vortex

In the previous chapter it was shown that a wind driven circulation in a stratified ocean consists of a barotropic component which decays at the Ekman layer spin-down rate, and a baroclinic mode which, in the absence of internal friction, is nondecaying. In the present chapter we consider a slightly different initial value problem. At $t = 0$ we suppose that a circularly symmetric vortex exists, with a given vertical momentum distribution. We then wish to determine the time evolution of the vortex. By analogy to the laboratory spin-up problem we anticipate that the vortex will decay on the spin-up time scale until the vorticity at $z = 0$ becomes zero. The remaining baroclinic mode must then be dissipated on the much longer diffusion time scale.

Eddies which develop in the Gulf Stream and cut off as closed vortices are a possible example of the sort of free vortices to which this theory may apply. Typical scales for a Gulf Stream eddy (see Stommel(1960)) are

$$\begin{aligned} L &\approx 10^7 \text{ cms.} & H &\approx 4 \times 10^5 \text{ cms.} \\ U &\approx 40 \text{ cm sec}^{-1} & \nu_z &\approx 10^2 \text{ cm}^2 \text{ sec}^{-1} \end{aligned} \quad (7.1)$$

The horizontal eddy diffusion is difficult to estimate but is probably in the range $\nu_r \approx 10^4 - 10^6 \text{ cm}^2 \text{ sec}^{-1}$. The above estimates lead to typical values of the nondimensional parameters,

$$E \approx 1, \quad K \approx 10^{-2}, \quad \lambda \approx 10^{-2}, \quad \delta_1^2 \approx 10^2$$

As an initial distribution of vorticity we choose a Gaussian distribution in the horizontal and a hyperbolic sine in the vertical

$$\nabla^2 \psi = e^{-r^2} \sinh \lambda z \quad (7.2)$$

If λ is assigned the value 4, the initial current distribution has an e-folding depth of about 1 km.

For a baroclinic vortex in which $\nabla^2 \psi = 0$ at $z=0$ we must include internal viscous dissipation to get a time dependent solution. The decay will thus be controlled by the eddy diffusion time scales H^2/ν_z and L^2/ν_r , where ν_z is a vertical eddy diffusion coefficient and ν_r is a horizontal eddy diffusion coefficient. We now rescale the equations of motion by defining the time scale as $t^* = \frac{H^2}{\nu_z} t$. For convenience in reducing the number of parameters which explicitly appear in the nondimensional equations we define the velocity scale as

$$U = L \left(\frac{f \nu_z}{H^2} \right)^{1/2}$$

The nondimensional velocity will then be $\sim O(1)$ provided that $\frac{U}{fL} \sim \sqrt{\frac{\nu_z}{f}} / H$

i.e. the Rossby number must be of the same order as the ratio of the Ekman layer depth to the scale height. For the scales given in (7.1)

$$\frac{U}{fL} \approx \sqrt{\frac{\nu_z}{H^2 f}} \approx 10^{-2}$$

If we define the additional nondimensional parameter $\delta_2 = \frac{L}{H} \sqrt{\frac{\nu_z}{\nu_r}}$, which expresses the ratio of vertical to horizontal diffusion, the nondimensional rescaled equations may be written

$$\lambda^2 \frac{\partial v_r}{\partial t} + \lambda \left(v_r \frac{\partial v_r}{\partial r} - \frac{v_\theta^2}{r} + w \frac{\partial v_r}{\partial z} \right) - v_\theta = -\frac{\partial p}{\partial r} + \lambda^2 \left(\frac{\nabla^2}{\delta_2^2} + \frac{\partial^2}{\partial z^2} \right) v_r \quad (7.3)$$

$$\lambda^2 \frac{\partial v_\theta}{\partial t} + \lambda \left(v_r \frac{\partial v_\theta}{\partial r} + \frac{v_r v_\theta}{r} + w \frac{\partial v_\theta}{\partial z} \right) + v_r = \lambda^2 \left(\frac{\nabla^2}{\delta_2^2} + \frac{\partial^2}{\partial z^2} \right) v_\theta \quad (7.4)$$

$$\lambda^2 \frac{\partial w}{\partial t} + \lambda \left(v_r \frac{\partial w}{\partial r} + w \frac{\partial w}{\partial z} \right) = \delta_1^2 \left(T - \frac{\partial p}{\partial z} \right) + \lambda^2 \left(\frac{\nabla^2}{\delta_2^2} + \frac{\partial^2}{\partial z^2} \right) w \quad (7.5)$$

$$\kappa \epsilon \lambda^2 \frac{\partial T}{\partial t} + \kappa \epsilon \lambda \left(v_r \frac{\partial T}{\partial r} + w \frac{\partial T}{\partial z} \right) + \kappa w = -\frac{1}{r} \frac{\partial (r v_r)}{\partial r} - \frac{\partial w}{\partial z} \quad (7.6)$$

$$\lambda^2 \frac{\partial T}{\partial t} + \lambda \left(v_r \frac{\partial T}{\partial r} + w \frac{\partial T}{\partial z} \right) = -\frac{w}{\epsilon} + \frac{\lambda^2}{\sigma_z^2} \left(\nabla^2 + \frac{\partial^2}{\partial z^2} \right) T \quad (7.7)$$

where the ρ -effect has again been neglected.

In a stratified turbulent system such as the ocean the Prandtl number σ_z is generally a function of depth and is greater than one. According to Munk and Anderson (1948) $\sigma_z \approx 10$ in the region above the thermocline. Since the high velocity in Gulf Stream eddies is confined quite near the surface, at least initially, we shall for the present assume that $\frac{1}{\sigma_z} \ll 1$ so that the temperature diffusion terms may be neglected in equation (7.7). This course has the additional advantage of eliminating the need for boundary conditions on the temperature field.

The boundary conditions for the velocity field are

$$V_\theta = V_r = w \quad \text{at } z = 0 \quad (\text{rigid bottom})$$

and

$$\frac{\partial V_\theta}{\partial z} = \frac{\partial V_r}{\partial z} = w = 0 \quad \text{at } z = 1 \quad (\text{free surface})$$

If we again expand the equation (7.2) through (7.9) in a perturbation series in λ we obtain for the interior,

$$V_\theta^I = \frac{\partial P_0}{\partial r} = \frac{\partial \psi}{\partial r} \quad (7.8)$$

$$\frac{\partial V_\theta^I}{\partial t} + V_r^I = \left(\nabla^2 + \frac{\partial^2}{\partial z^2} \right) V_\theta^I \quad (7.9)$$

$$T_0^I = \frac{\partial P_0}{\partial z} = \frac{\partial \psi}{\partial z} \quad (7.10)$$

$$\frac{\partial T_0^I}{\partial t} + \frac{w_2^I}{\epsilon} = 0 \quad (7.11)$$

$$\frac{1}{r} \frac{\partial (r V_r^I)}{\partial r} = -\frac{\partial w_2^I}{\partial z} \quad (7.12)$$

These may be combined into a single equation for the stream function

$$\frac{\partial}{\partial t} \left(\nabla^2 \psi + \epsilon \frac{\partial^2 \psi}{\partial z^2} \right) = \left(\frac{\nabla^2}{\delta_0^2} + \frac{\partial^2}{\partial z^2} \right) \nabla^2 \psi \quad (7.13)$$

The boundary condition at $z=0$ is the usual condition derived from the rigid surface Ekman boundary layer theory (see equation 2.24). In the time scaling of this chapter

$$\epsilon \frac{\partial^2 \psi}{\partial t \partial z} + \frac{\nabla^2 \psi}{\sqrt{2} \lambda} = 0 \quad \text{at } z=0 \quad (7.14)$$

which indicates that $\nabla^2 \psi \sim o(\lambda)$ at $z=0$.

The no stress boundary condition at the free surface cannot be satisfied by the interior geostrophic velocity V_{θ}^I because $\frac{\partial V_{\theta}^I}{\partial z} = \frac{\partial T_{\theta}^I}{\partial r}$ and in general $\frac{\partial T_{\theta}^I}{\partial r} \neq 0$ at $z=1$. Hence, a boundary layer must be present. Defining the stretched coordinate $-\lambda \bar{z} = 1 - z$ and using superscript B to represent boundary layer variables we obtain the boundary condition

$$\frac{\partial V_{\theta}^B}{\partial \bar{z}} + \frac{\partial V_r^B}{\partial \bar{z}} = 0 \quad \text{at } \bar{z}=1, \bar{z}=0 \quad (7.15)$$

$$\frac{\partial V_r^B}{\partial \bar{z}} = 0$$

Therefore, the free surface boundary conditions requires a second order boundary layer. The boundary layer equations are

$$V_{\theta}^B = \frac{\partial P^B}{\partial r} - \frac{\partial^2 V_r^B}{\partial \bar{z}^2} \quad (7.16)$$

$$V_r^B = \frac{\partial^2 V_{\theta}^B}{\partial \bar{z}^2} \quad (7.17)$$

$$\frac{\partial P^B}{\partial \bar{z}} = 0 \quad (7.18)$$

$$\frac{1}{r} \frac{\partial (r V_r^B)}{\partial r} = - \frac{\partial W_{\theta}^B}{\partial \bar{z}} \quad (7.19)$$

The solution of (7.16) - (7.19) is an Ekman spiral

$$V_{1\theta}^B = \left[-\frac{\partial V_{0\theta}^I}{\partial z} \right] e^{z/\sqrt{2}} \sin\left(\frac{z}{\sqrt{2}} + \frac{\pi}{4}\right) \quad (7.20)$$

$$V_{1r}^B = \left[-\frac{\partial V_{0r}^I}{\partial z} \right] e^{z/\sqrt{2}} \cos\left(\frac{z}{\sqrt{2}} + \frac{\pi}{4}\right) \quad (7.21)$$

From (7.21) we obtain after differentiating by $\frac{1}{r} \frac{\partial}{\partial r}(r \quad)$ and integrating across the boundary layer

$$W_2^B(0) = -W_2^I = \left[\frac{\partial \nabla^2 \psi}{\partial z} \right]_{z=0} \quad (7.22)$$

Substituting into equation (7.11) we get the boundary condition

$$\epsilon \frac{\partial^2 \psi}{\partial t \partial z} - \frac{\partial \nabla^2 \psi}{\partial z} = 0 \quad \text{at } z=1 \quad (7.23)$$

Equation (7.12) subject to initial condition (7.2) and the boundary conditions (7.14) and (7.23) suffices to determine the internal diffusion. The solution for arbitrary ϵ and δ_2 is rather complicated, but it is possible to examine certain asymptotic cases to obtain some insight into the physics.

As a first case let $\epsilon \gg 1$ and $\delta_2^2 \gg 1$, corresponding to an eddy of large horizontal extent. Then the equation for ψ reduces to

$$\left(\epsilon \frac{\partial}{\partial t} - \nabla^2 \right) \frac{\partial^2 \psi}{\partial z^2} = 0 \quad (7.24)$$

with boundary conditions

$$\left(\epsilon \frac{\partial}{\partial t} - \nabla^2 \right) \frac{\partial \psi}{\partial z} = 0 \quad z=1$$

$$\epsilon \frac{\partial^2 \psi}{\partial t \partial z} + \frac{\nabla^2 \psi}{\sqrt{2} \lambda} = 0 \quad z=0$$

The solution is simply $\nabla^2 \psi = \frac{1}{\left(1 + \frac{4\tau}{\epsilon}\right)} e^{\frac{-r^2}{(1+4\tau/\epsilon)}} \sinh \lambda z + o(\lambda)$

(7.25)

A similar solution may be obtained in the special case $\epsilon = 1$, $\delta_2^2 = 1$ (which may be realistic for Gulf Stream eddies). Hence,

$$\nabla^2 \psi = \frac{1}{(1+4t)} e^{-\frac{r^2}{(1+4t)}} \sinh \lambda z + o(\lambda) \quad (7.26)$$

In both of these solutions the current spreads horizontally in time with no change in the vertical structure. This seems paradoxical especially in the first case where horizontal eddy diffusion has been ignored. However, any vertical momentum diffusion must be accompanied by changes in the slopes of the isotherms because $\frac{\delta V_\theta}{\delta z} = \frac{\delta T}{\delta r}$. In the absence of heat diffusion the thermal field can be changed only through vertical advection of the mean temperature, $T_r^*(z)$, by a divergent velocity field. This divergence is sufficient to balance the vertical diffusion of vorticity so that there is no change in the vertical distribution.

To test this physical argument we consider the asymptotic case $\epsilon \ll 1$. This case corresponds to very large static stability, and only very small vertical velocities are required for large changes in the temperature field. Thus, we anticipate that the divergent velocity field will not effect the diffusion process appreciably.

In this case equation (7.1?) reduces to

$$\left[\frac{\partial}{\partial t} - \left(\nabla_{\delta_2}^2 + \frac{\partial^2}{\partial z^2} \right) \right] \nabla^2 \psi = 0 \quad (7.27)$$

and the boundary conditions are

$$\frac{\partial \psi}{\partial z} = 0 \quad \text{at } z=1, \quad \nabla^2 \psi = 0 \quad \text{at } z=0$$

It is convenient to redefine the initial condition so that the vertical distribution $\sinh \lambda z$ is expressed in terms of a Fourier series

$$\nabla^2 \psi = e^{-r^2} \sum_{n=1}^{\infty} \frac{2\lambda \cosh \lambda}{\left[\lambda^2 + \left(\frac{n\pi}{2} \right)^2 \right]} \sin \frac{n\pi}{2} z \quad (7.28)$$

The solution of (7.27) may then be written

$$\nabla^2 \psi = \frac{e^{-\frac{y}{\delta_2}}}{(1 + 4t/\delta_2^2)} \sum_{n=1}^{\infty} \frac{2l \cosh l}{l^2 + (\frac{n\pi}{2})^2} \sin \frac{n\pi}{2} z e^{-\left(\frac{n\pi}{2}\right)^2 t}$$

This is just ordinary three dimensional diffusion. If $\delta_2^2 \gg 1$, then the current diffuses very little in the horizontal but diffuses vertically because the higher wave numbers in the Fourier series decrease in amplitude as t increases.

The asymptotic cases considered here indicate that vertical diffusion is suppressed for the quasi-geostrophic scale motions in a stratified fluid, and it is unlikely that an initially baroclinic eddy would become barotropic simply due to vertical momentum diffusion. Inclusion of temperature diffusion terms would probably modify these results. However, the resulting equation is fourth order in z , and very difficult to solve unless rather arbitrary boundary conditions are imposed on the temperature, and it will not be attempted here.

Chapter 2

The Influence of a Variable Coriolis Force

The analytic solutions obtained in the previous chapter are all derived on the assumption of a constant Coriolis force. This is correct for the rotating dish pan. But in applying these results to the oceans it must be kept in mind that the Coriolis parameter $f = 2\Omega_s \sin\phi$ varies with the latitude ϕ . For currents of the scale of Gulf Stream eddies and larger this variation introduces the so called β -effect into the potential vorticity equation. Unfortunately, the inclusion of β makes the mathematical methods employed in our treatment of the spin-up problem unfeasible. We can, however, obtain certain special solutions for harmonic forcing functions which suggest that β acts to increase the baroclinicity of the response of a stratified ocean to wind stresses. The response of a two-layer β -plane ocean to variable wind stresses has been studied by Charney (1955), and Veronis and Stommel (1956). The latter included inertio-gravity waves in their study but neglected bottom friction. Their analysis demonstrates that if the variable wind stress period is greater than one pendulum day the response of the ocean is essentially geostrophic for horizontal scales $\lambda \gtrsim 30$ km. and a negligible amount of energy goes into the inertio-gravity oscillations. Therefore, we can again use the quasi-geostrophic system in our examination of the modifications due to bottom friction.

We will employ the β -plane approximation, in which the equations of motion are referred to a cartesian coordinate system with x positive in the eastward direction, y positive northward and z positive upward along the local vertical. The important dynamic effect of the earth's sphericity referred to above will be retained by letting $\frac{df}{dy} = \beta$ where β is a constant.

The equations of motion for the two-layer model including the β -effect may be written

$$\frac{\partial}{\partial t} \nabla^2 \psi_1 + \epsilon_1 \frac{\partial}{\partial t} (\psi_2 - \psi_1) + \beta \frac{\partial \psi_1}{\partial x} = F(t) \quad (8.1)$$

$$\frac{\partial}{\partial t} \nabla^2 \psi_2 - \epsilon_2 \frac{\partial}{\partial t} (\psi_2 - \psi_1) + \beta \frac{\partial \psi_2}{\partial x} - s_2 \nabla^2 \psi_2 = 0 \quad (8.2)$$

where $\beta = \frac{L}{a\lambda}$, $s_2 = H/H_2$ and $F(t)$ is the wind stress curl.

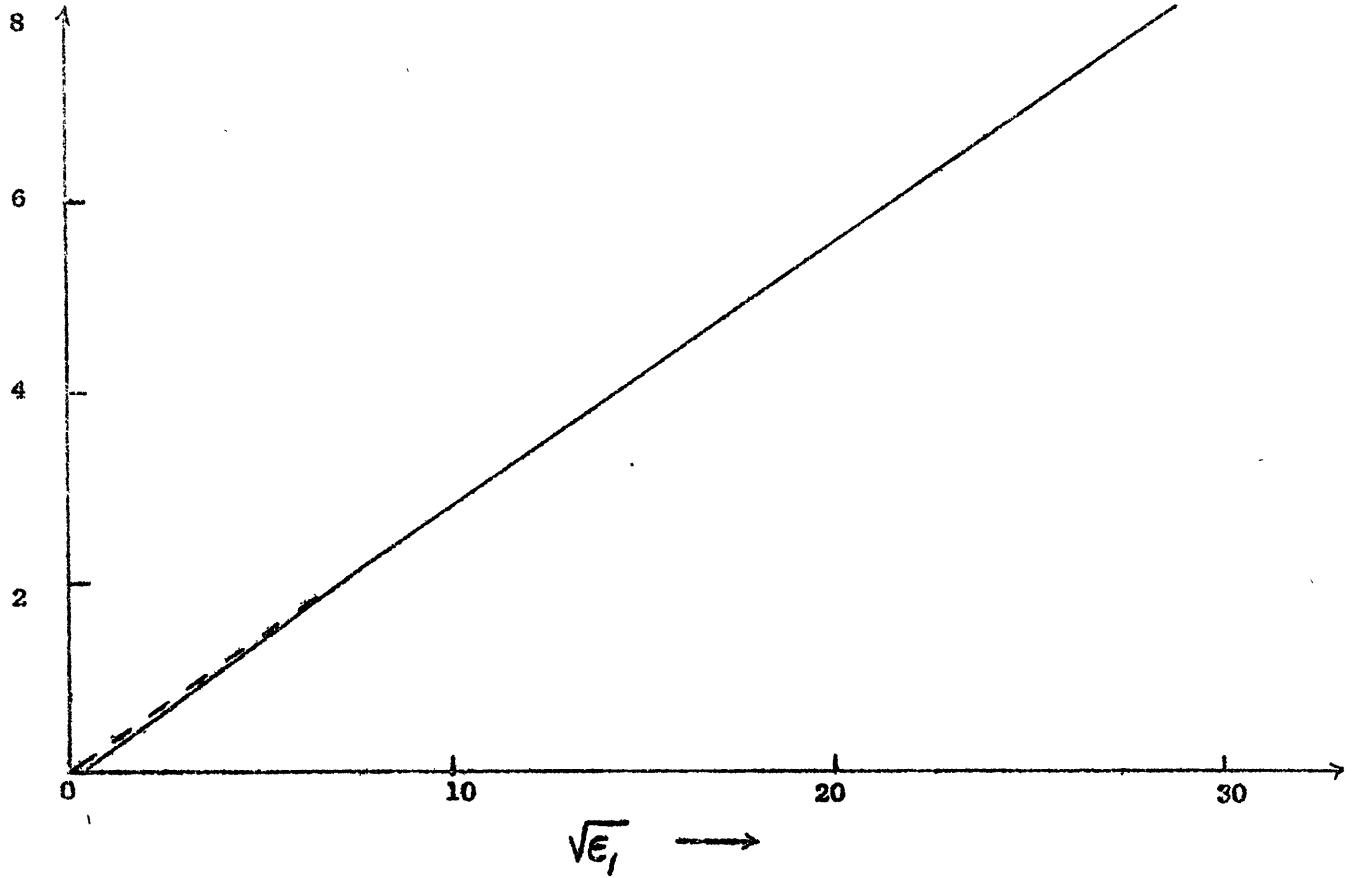
For horizontal scales $L \approx 100$ km all terms in equations (8.1) and (8.2) are important, but for large scale systems $L \approx 1,000$ km the second and third terms on the left dominate and the Ekman friction effect should not be of great importance except at low frequency forcing. The inclusion of the β effect changes the nature of the dynamics in a very significant way, for now the equations (8.1) and (8.2) have free wave solutions for the homogeneous case $F(t) \equiv 0$. As a first step we examine the influence of friction on the frequencies of the free waves. We assume solutions of the form

$$\begin{aligned} \psi_1 &= A \sin ly e^{ik(x+ct)} \\ \psi_2 &= C \sin ly e^{ik(x+ct)} \end{aligned}$$

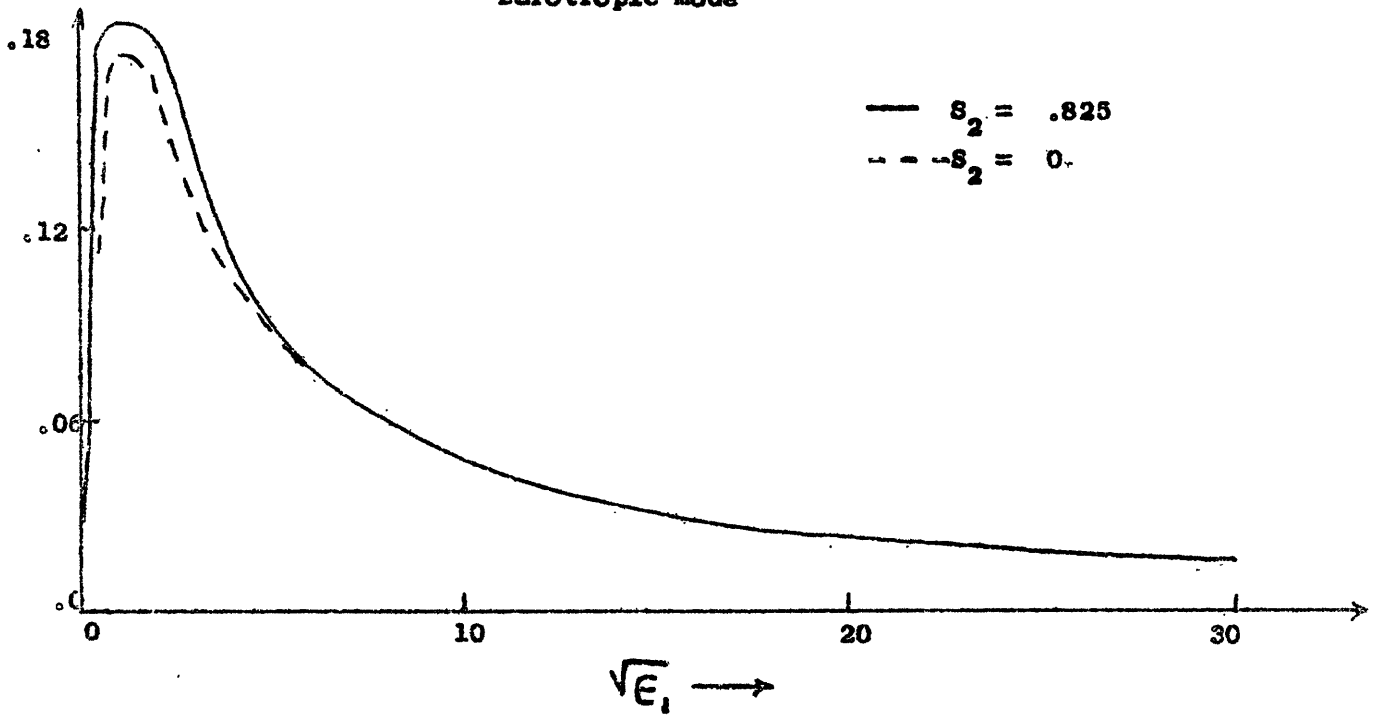
Substituting into (8.1) and (8.2) we obtain as the determinant of the coefficients A and C:

$$\begin{vmatrix} ck(\mu^2 + \epsilon_1) - \beta k & -\epsilon_1 ck \\ -\epsilon_2 ck & ck(\mu^2 + \epsilon_2) - \beta k - i s_2 \mu^2 \end{vmatrix} = 0$$

where $\mu^2 = k^2 + l^2$



Barotropic Mode



Baroclinic Mode

Figure 8.1

Rossby Wave Frequencies For The Two-Layer Model vs.
Horizontal Scale of Motion

Therefore,

$$c_{1,2} = \frac{\beta(2\mu^2 + \epsilon_1 + \epsilon_2) + i s_2 \mu^2 (\mu^2 + \epsilon_1)}{2\mu^2 (\mu^2 + \epsilon_1 + \epsilon_2)} \quad (8.3)$$

$$= \frac{\sqrt{[\beta k (\epsilon_1 + \epsilon_2) + i s_2 \mu^2 (\mu^2 + \epsilon_1)]^2 - 4 i s_2 \mu^4 \beta k \epsilon_2}}{2k\mu^2 (\mu^2 + \epsilon_1 + \epsilon_2)}$$

Now if friction is neglected (8.3) becomes

$$c_1 = \frac{\beta}{\mu^2} \quad , \quad c_2 = \frac{\beta}{\mu^2 + \epsilon_1 + \epsilon_2}$$

c_1 and c_2 are the barotropic and baroclinic Rossby wave speeds respectively.

For large horizontal scales ϵ_1 and $\epsilon_2 \gg 1$, and (8.3) may be written approximately as

$$c_1 = \frac{\beta}{\mu^2} + \frac{i s_2 (\mu^2 + \epsilon_1)}{k (\mu^2 + \epsilon_1 + \epsilon_2)} \quad , \quad c_2 = \frac{\beta}{\mu^2 + \epsilon_1 + \epsilon_2}$$

Thus the barotropic wave is rapidly decaying but the baroclinic wave is non-decaying.

In Figure 8.1 the real frequency of the barotropic and baroclinic waves is plotted as a function of $\sqrt{\epsilon_1}$ for parameters corresponding to the real oceans: $H_1 = .5$ kms. , $H_2 = 3.5$ kms. , $\frac{\Delta\rho}{\rho} = 2 \times 10^{-3}$ and $\epsilon_1 = 7\epsilon_2$. Friction has a negligible effect on the frequencies of the free modes except for small ϵ_1 , in which case it acts to lower the frequency of the barotropic mode and raise the frequency of the baroclinic mode. Therefore, friction acts to increase the baroclinicity of the ocean's response in this model mainly by damping the free barotropic wave, but also by raising the frequency of the baroclinic wave.

We now consider a simple forcing function $F(t) = F \sin \lambda y \sin(kx + \omega t)$ which corresponds to a harmonic series of circular storms traveling across the ocean. In middle latitudes C will generally be negative, corresponding

to eastward moving storms. We assume solutions of (8.1) and (8.2) of the

$$\begin{aligned} \Psi_1 &= A \sin ly \cos k(x+ct) + B \sin ly \sin k(x+ct) \\ \Psi_2 &= C \sin ly \cos k(x+ct) + D \sin ly \sin k(x+ct) \end{aligned} \quad (8.4)$$

Substituting (8.4) into (8.1) and (8.2) we obtain, letting $\nu = ck$ be the frequency:

$$\begin{aligned} A &= \frac{F + C \epsilon_1 \nu}{(\nu \mu^2 + \epsilon_1 \nu - \beta k)} \\ B &= \frac{-\epsilon_1 \epsilon_2 \nu^2 s_2 \mu^2 F}{[(\nu \mu^2 - \beta k)^2 (\nu \mu^2 - \beta k + \epsilon_1 \nu + \epsilon_2 \nu)^2 + s_2^2 \mu^4 (\nu \mu^2 + \epsilon_1 \nu - \beta k)^2]} \\ C &= \frac{D s_2 \mu^2 (\nu \mu^2 - \beta k + \epsilon_1 \nu) + F \epsilon_2 \nu}{(\nu \mu^2 - \beta k) (\nu \mu^2 - \beta k + \epsilon_1 \nu + \epsilon_2 \nu)} \\ D &= \frac{-\epsilon_2 \nu s_2 \mu^2 (\nu \mu^2 + \epsilon_1 \nu - \beta k) F}{[(\nu \mu^2 - \beta k)^2 (\nu \mu^2 - \beta k + \epsilon_1 \nu + \epsilon_2 \nu)^2 + s_2^2 \mu^4 (\nu \mu^2 + \epsilon_1 \nu - \beta k)^2]} \end{aligned}$$

In Figure 8.2 the amplitude A, B, C, and D are plotted against the forcing frequency for the case $\epsilon_1 = 10$, $\epsilon_2 = 1.43$ and $\beta = 1.67$ corresponding to a horizontal scale of $L = 100 \text{ km}$. Solid lines are the solution with bottom friction, the dashed line shows the lower layer component C in the frictionless case. Amplitude of component A is not affected by friction. Figure 8.3 is a similar plot for $L = 1,000 \text{ km}$. In this case the amplitudes of components B and D are negligible.

The main effect of friction is to reduce the amplitude of the coefficient C for low frequency forcing, that is to damp the lower layer velocity. At frequencies greater than unity the spin-up process does not have time to appreciably damp the lower layer velocity and the current is barotropic for $L \approx 10^8 \text{ cm}$. For smaller horizontal scales the motion has a strong baroclinic component even at higher frequencies. This feature was noted by Charney and also Veronis and Stommel in the papers cited above.

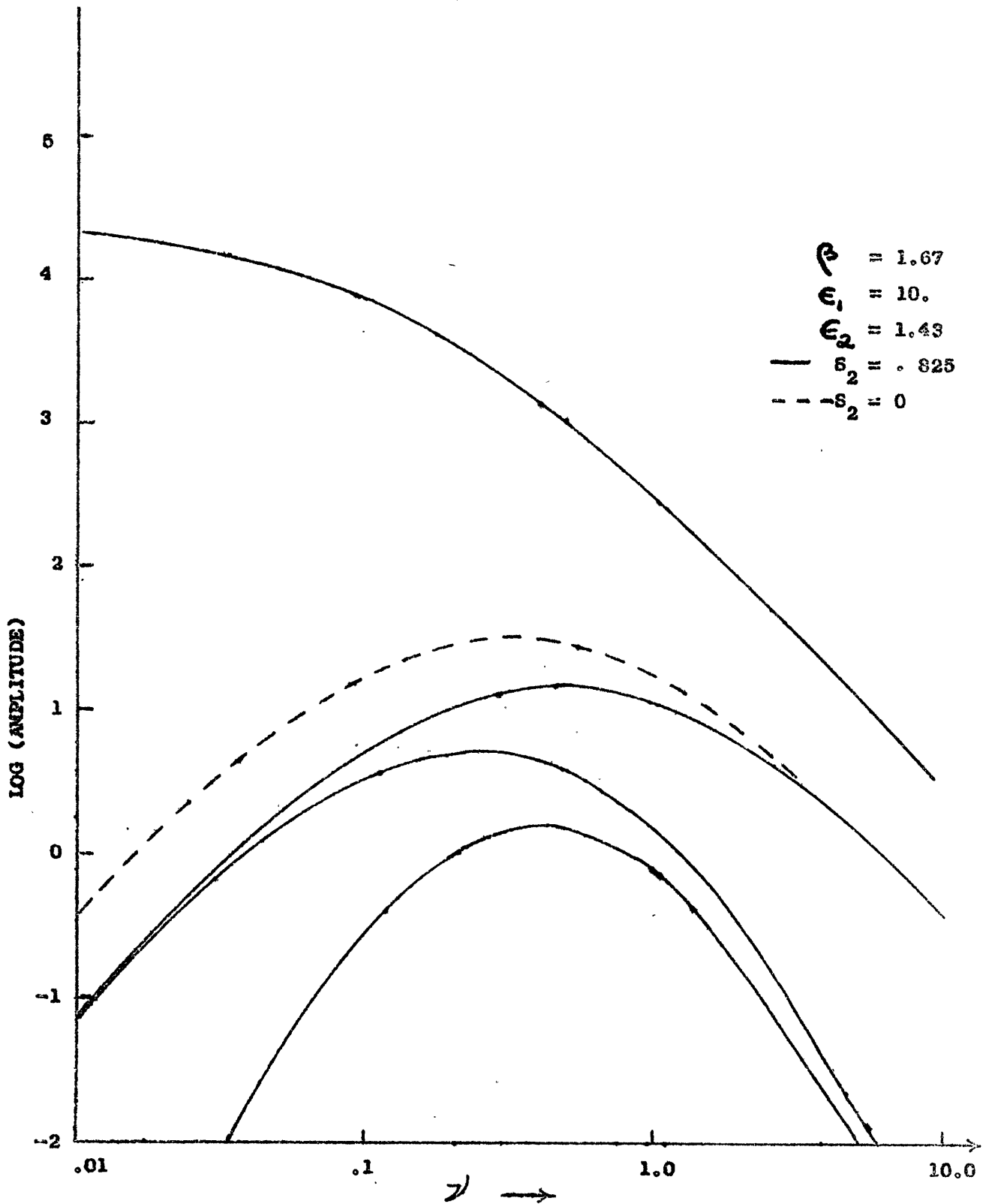


Figure 8.2
Amplitudes of Coefficients in The
Two-Layer Model vs. forcing frequency
for $L = 107$ cm.

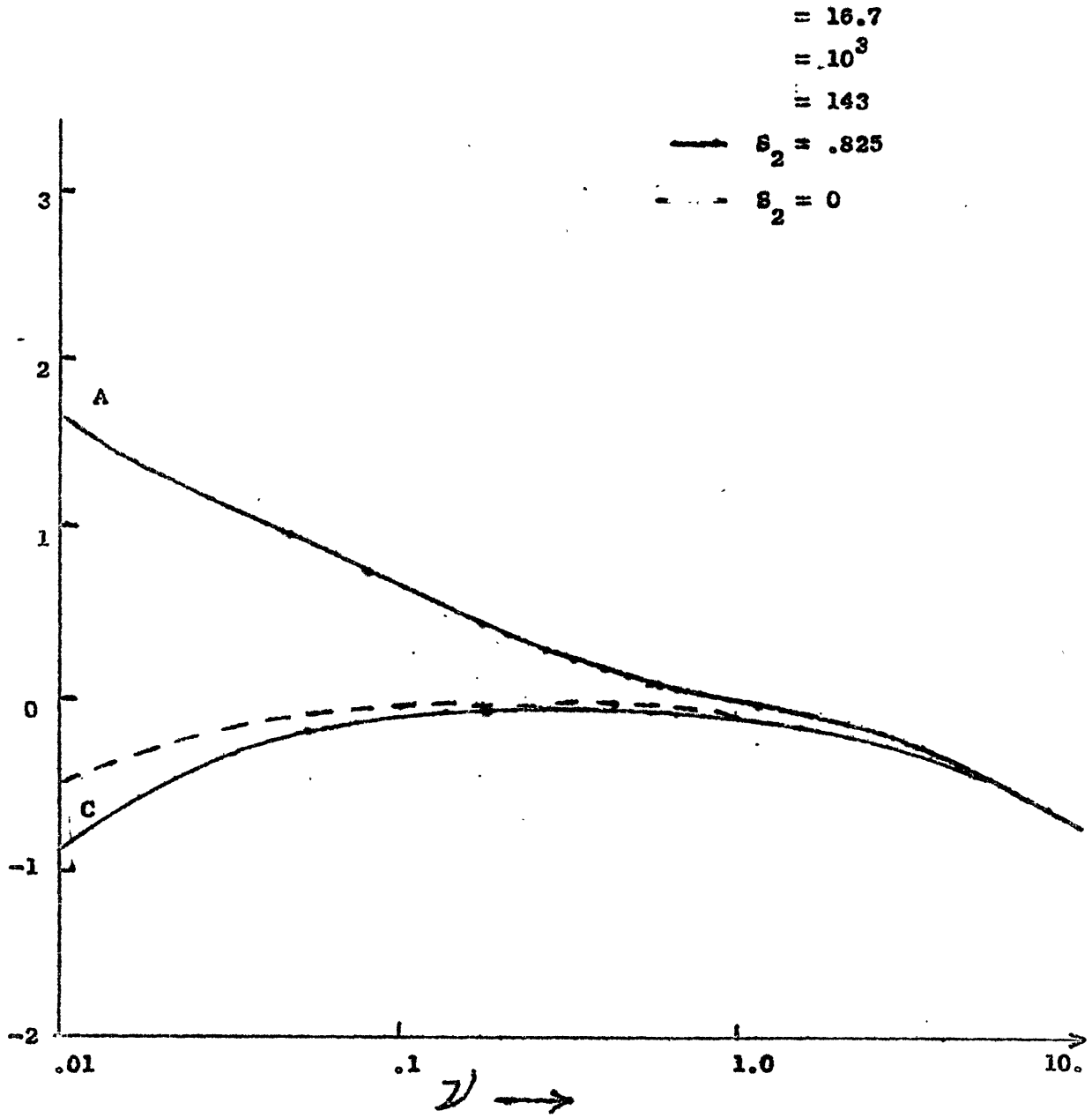


Figure 8.3
Amplitudes of Coefficients in the
Two-Layer Model vs. Forcing Frequency
for $L = 10^8$ cm

A second effect of bottom friction is to introduce a component of motion which is ninety degrees out of phase with the directly driven current. This component is caused by the divergence field associated with Ekman friction and has its maximum amplitude in the lower layer. The amplitude of this component is, however, extremely small even for $L = 10^7$ cm, and at $L = 10^8$ cm, it is utterly negligible.

We next consider the continuous stratification case with the inclusion of β . The potential vorticity equation (6.6) becomes now

$$\frac{\partial}{\partial t} (\nabla^2 \psi + \epsilon \frac{\partial^2 \psi}{\partial z^2}) + \beta \frac{\partial \psi}{\partial x} = 0 \quad (8.5)$$

and the boundary conditions are

$$\frac{\partial^2 \psi}{\partial t \partial z} = - \frac{F(t)}{\epsilon} \quad \text{at } z = 1 \quad (8.6)$$

$$\frac{\partial^2 \psi}{\partial t \partial z} = - \frac{\nabla^2 \psi}{\sqrt{2} \epsilon} \quad \text{at } z = 0$$

We again let the forcing be of the form $F(t) = F \sin \lambda y \sin k(x+ct)$. In this case solutions of (8.5) may be written as

$$\psi = A(z) \sin \lambda y \cos k(x+ct) + B(z) \sin \lambda y \sin k(x+ct) \quad (8.7)$$

where the coefficients $A(z)$ and $B(z)$ must satisfy the relations

$$\frac{d^2 A}{dz^2} - \lambda^2 A = 0, \quad \frac{d^2 B}{dz^2} - \lambda^2 B = 0 \quad (8.8)$$

where $\lambda^2 = \frac{-\beta + c\mu^2}{c\epsilon}$. The boundary conditions are

$$\frac{dB}{dz} = 0, \quad \frac{dA}{dz} = \frac{F}{\nu\epsilon} \quad \text{at } z = 1 \quad (8.9)$$

and

$$\frac{dB}{dz} - \frac{\mu^2 A}{\sqrt{2} \epsilon k c} = 0, \quad \frac{dA}{dz} + \frac{\mu^2 B}{\sqrt{2} \epsilon k c} = 0 \quad \text{at } z = 0$$

Solutions of (8.8) may be written as

$$B = C_1 \sinh \lambda z + C_2 \cosh \lambda z$$

$$A = C_3 \sinh \lambda z + C_4 \cosh \lambda z$$

where

$$C_1 = \frac{\sqrt{2} \mu^2 \sinh \lambda F}{[\lambda^2 \sinh^2 \lambda (2\epsilon^2 \nu^2) + \mu^4 \cosh^2 \lambda]}$$

$$C_2 = \frac{-\sqrt{2} \mu^2 \cosh \lambda F}{[\lambda^2 \sinh^2 \lambda (2\epsilon^2 \nu^2) + \mu^4 \cosh^2 \lambda]}$$

$$C_3 = \frac{\mu^4 \cosh \lambda F}{\nu \epsilon \lambda [\lambda^2 \sinh^2 \lambda (2\epsilon^2 \nu^2) + \mu^4 \cosh^2 \lambda]}$$

$$C_4 = \frac{2\lambda \sinh \lambda \epsilon \nu F}{[\lambda^2 \sinh^2 \lambda (2\epsilon^2 \nu^2) + \mu^4 \cosh^2 \lambda]}$$

The response of the β -plane ocean thus takes the form of external waves; a barotropic wave proportional to $\cosh\left(\frac{\mu^2}{\epsilon} - \frac{\beta k}{\epsilon \nu}\right)^{1/2}$ and a baroclinic component proportional to $\sinh\left(\frac{\mu^2}{\epsilon} - \frac{\beta k}{\epsilon \nu}\right)^{1/2}$.

In the unusual circumstance of a westward moving storm with $\nu < \frac{\beta k}{\mu^2}$

λ becomes imaginary and the response is an internal vertically propagating wave. In this case the wind stress would be expected to communicate energy all the way to the bottom of the ocean. This sort of resonance with the free Rossby waves may conceivably occur at low latitudes, but will not be considered further here. Our main interest is to note the ways in which friction and β act to modify the response of the ocean to the typical mid-latitude westerly flow.

If the friction is neglected the solution (8.7) simplifies to

$$\psi = \frac{F \cosh \lambda z}{\nu \epsilon \lambda \sinh \lambda} \sin \lambda y \cos k(x + cT)$$

Now $\lambda = \left(\frac{\mu^2}{\epsilon} - \frac{\beta k}{\nu \epsilon}\right)^{1/2}$, so if $\beta \equiv 0$ we see that $\lambda \rightarrow 0$ as $\epsilon \rightarrow \infty$.

Therefore, the flow is barotropic for large ϵ regardless of the value of frequency. But the inclusion of β makes λ frequency dependent so that for small enough ν , $\lambda \sim O(1)$ even for large ϵ , and the current is much greater at the surface than at the bottom.

The introduction of bottom friction further enhances the baroclinicity by adding terms proportional to $\sinh \lambda z$ in the solution. The amplitudes at $z=1$ of the components defined in (8.10) are plotted as a function of frequency in Figure 8.4 for the case $L = 10^7$ cms. At low frequencies the highly baroclinic terms proportional to $\sinh \lambda z$ dominate for this horizontal scale.

Increasing the scale L has the effect of shifting the frequency scale to the right so that the baroclinic ($\sinh \lambda z$) terms become of significant amplitude at lower frequency. The results of this chapter indicate that both the β -effect and friction contribute to the baroclinic response of the oceans to low frequency forcing. In the case of friction, the spin-down effect of the Ekman layer acting on the barotropic mode limits the amplitude of that mode, but the baroclinic mode is not damped by Ekman friction. The β amplification of the baroclinic mode is due to a different mechanism. The presence of β allows self-propagating neutral waves in both the barotropic and baroclinic modes. As the forcing period increases it approaches resonance with the long period baroclinic free wave and amplification of the baroclinic mode occurs.

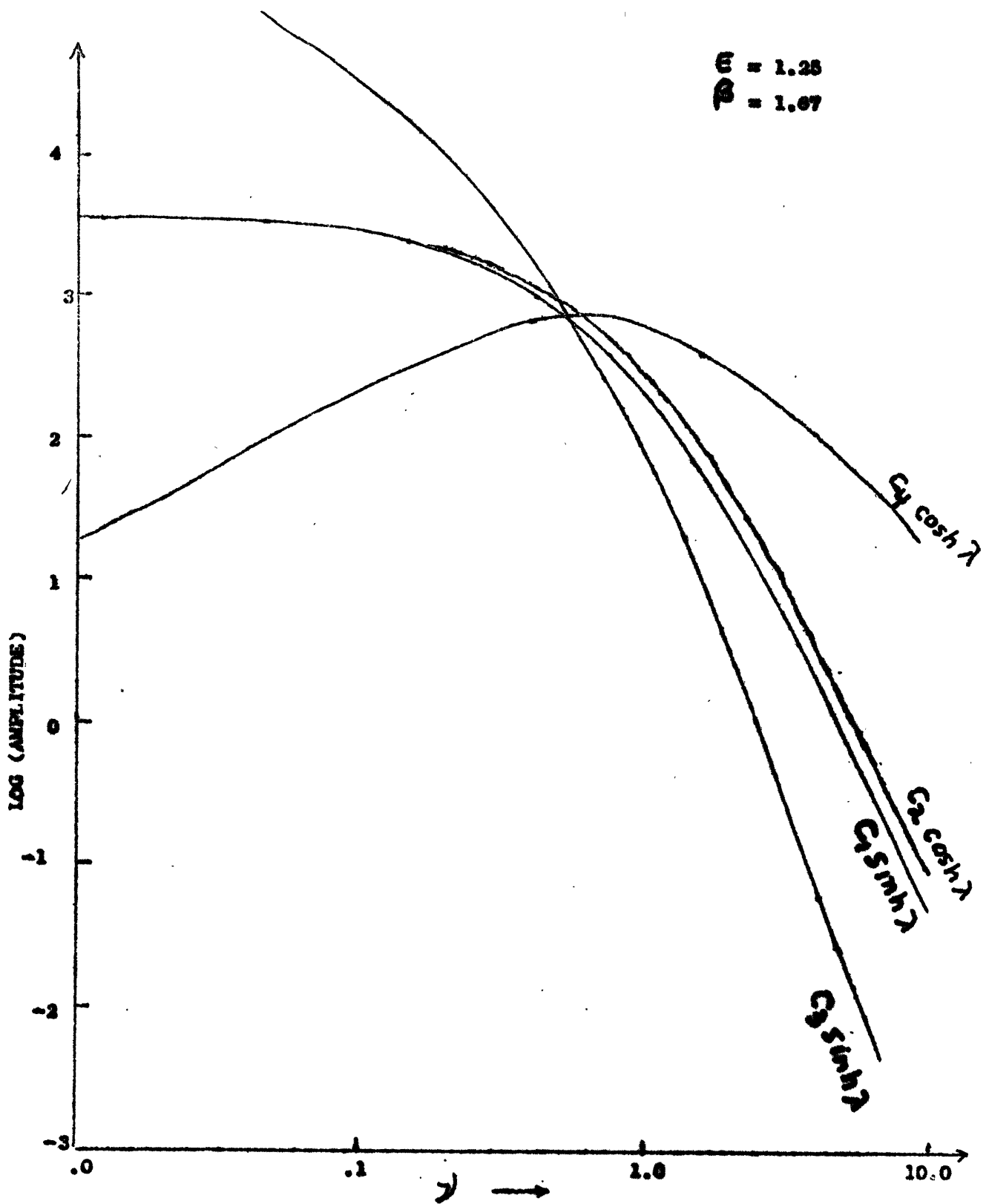


Figure 8.4

Amplitudes of Coefficients in the
Continuously Stratified Model vs.
Forcing Frequency, $L = 10^7$ cm.

Appendix A

Baroclinic Instability

The validity of the solutions previously derived for the spin-up of the two-layer or continuously stratified systems depends on the flow being stable with respect to small perturbations. In the quasi-geostrophic system the vertical shear of the horizontal velocity is coupled to horizontal gradients in the density field by the thermal wind relationship. Hence, vertical shear implies the presence of available potential energy which may be released by motions in which the slope of particle trajectories is less than or equal to the slope of the potential density surfaces. The parameter $\epsilon = \frac{4\Omega^2 l^2}{g\Delta\rho H}$ is a measure of the slope of potential density surfaces. Therefore, we expect the system to become increasingly unstable as ϵ is increased.

Phillips (1954) studied the baroclinic instability of a two-layer system for flow in an infinite channel. His model included the effect but not Ekman friction. Eady (1949) studied a continuously stratified system. He also referred the motion to an infinite channel but neglected both β and friction. Barcilon (1964) extended the Eady model to include Ekman friction at top and bottom rigid boundaries. He found that friction not only stabilized the system but damped the growth rates of disturbances in the unstable regime. If Ekman friction is included in an asymmetric manner, which is the case for our free surface models, the analysis becomes considerably more complex. Since we only wish to determine the approximate value of ϵ at which instability will begin to occur in the experiments we shall merely derive the stability criteria for the inviscid two-layer model.

To investigate stability with respect to zonally asymmetric perturbations we must include Θ dependence in the equations for the geostrophic stream function. The two-layer model equations are then,

$$\left(\frac{\partial}{\partial t} + \frac{\partial \Psi_1}{\partial r} \frac{\partial}{r \partial \Theta} - \frac{1}{r} \frac{\partial \Psi_1}{\partial \Theta} \frac{\partial}{\partial r} \right) \left[\nabla^2 \psi_1 + \frac{1}{r^2} \frac{\partial^2 \psi_1}{\partial \Theta^2} + \epsilon_1 (\psi_2 - \psi_1) \right] = 0 \quad (A.1)$$

$$\left(\frac{\partial}{\partial t} + \frac{\partial \Psi_2}{\partial r} \frac{\partial}{r \partial \Theta} - \frac{1}{r} \frac{\partial \Psi_2}{\partial \Theta} \frac{\partial}{\partial r} \right) \left[\nabla^2 \psi_2 + \frac{1}{r^2} \frac{\partial^2 \psi_2}{\partial \Theta^2} - \epsilon_2 (\psi_2 - \psi_1) \right] = 0 \quad (A.2)$$

The time has here been rescaled as $t = t^*/\omega$. All other scaling is the same as in Chapter 4. We now assume that solutions of (A.1) and (A.2) exist in the form

$$\psi_{1,2} = \bar{\psi}_{1,2} + \phi_{1,2} J_0(kr) e^{i\alpha(\Theta + ct)} \quad (A.3)$$

where $\bar{\psi}_{1,2}$ are the mean stream functions averaged over the Θ coordinate. The mean zonal velocities will be denoted by $\frac{\partial \bar{\psi}_1}{\partial r} = \Omega_1 r$, $\frac{\partial \bar{\psi}_2}{\partial r} = \Omega_2 r$ where the angular velocities of the basic upper and lower layer currents (Ω_1 and Ω_2 respectively) are independent of time. In the spin-up problem Ω_1 and Ω_2 are actually transients but since it turns out that the growth rate of unstable waves is small compared to the spin-up time we may treat Ω_1 and Ω_2 as constants in the stability analysis without fear of serious error.

Substituting (A.3) into (A.1) and (A.2) we obtain, after discarding products of the perturbed variables and subtracting out the mean field, the first order perturbation equations,

$$\begin{aligned} i\alpha(\Omega_1 - c) \left[-\mu^2 \phi_1 + \epsilon_1 (\phi_2 - \phi_1) \right] - i\alpha \epsilon_1 (\Omega_2 - \Omega_1) \phi_1 &= 0 \\ i\alpha(\Omega_2 - c) \left[-\mu^2 \phi_2 - \epsilon_2 (\phi_2 - \phi_1) \right] + i\alpha \epsilon_2 (\Omega_2 - \Omega_1) \phi_2 &= 0 \end{aligned} \quad (A.4)$$

where $\mu^2 = k_1^2 + \frac{\alpha^2}{v^2}$ is the total horizontal wave number for the perturbations. Equations (A.4) form a linear homogeneous pair of equations in ϕ_1 and ϕ_2 . If there are to be nontrivial solutions the determinant of the matrix of coefficients of ϕ_1 and ϕ_2 must equal zero. This requirement leads to a quadratic equation in c . If the imaginary part of c is greater than zero the perturbations grow exponentially and the flow is unstable. c must satisfy the equation,

$$(\mu^2 + \epsilon_1 + \epsilon_2)c^2 - [\mu^2(\Omega_1 + \Omega_2) + 2\epsilon_1\Omega_2 + 2\epsilon_2\Omega_1]c + (\mu^2\Omega_1\Omega_2 + \epsilon_1\Omega_2^2 + \epsilon_2\Omega_1^2) = 0 \quad (A.5)$$

This equation, which is a quadratic of the form $Ac^2 + Bc + D = 0$ will have complex roots if the discriminant $B^2 - 4AD < 0$. For the particular case (A.5) this criterion indicates that $\mu^2 < 2\sqrt{\epsilon_1\epsilon_2}$ for instability. The growth rate of the disturbance αc_i is given by

$$\alpha c_i = \frac{\sqrt{4\epsilon_1\epsilon_2 - \mu^2} |\Omega_1 - \Omega_2| \alpha}{2(\mu^2 + \epsilon_1 + \epsilon_2)} \quad (A.7)$$

where α is the imaginary part of the phase speed. The minimum of μ^2 is $\mu^2 = k_1^2 + \alpha^2 = 6.78$ therefore, $\epsilon_1 \sqrt{\frac{H_1}{H_2}} > 3.39$ for instability.

In the experiments described in Chapter 5 instability was detected for $\epsilon \geq 4$. Barcilon (1934) showed that friction acts to stabilize the flow increasingly for decreasing values of the shear $|\Omega_1 - \Omega_2|$. Therefore, in experimental work we must keep the Rossby number very small when ϵ exceeds the neutral stability value (A.8)

Appendix B

The Side Wall Boundary Layers

In the laboratory apparatus the downward flux of mass into the Ekman boundary layer over the interior of the tank must be balanced by flow out of the Ekman layer along the vertical boundary surface. In a stratified fluid this vertical flow along the side wall will carry dense fluid from lower levels into the lighter fluid above, and may lead to unstable overturning and mixing. As a rough measure of this effect we assume that a particle which penetrates a distance h_{max}^* above its equilibrium density surface can cause mixing over a horizontal distance h_{mix}^* . We must then estimate under what conditions h_{mix}^* will be small enough so that the mixing is confined to a boundary layer along the wall. The maximum value of the vertical velocity W^* obviously occurs in the first few revolutions of the spin-up during which the Ekman layer develops and acts as a centrifugal pump to extract fluid from the interior at the rate

$$W^{*I} = 2\omega \sqrt{\frac{\nu}{4\Omega_0}} = 2\sqrt{2} R_0 \lambda \Omega_0 \quad (B.1)$$

where all symbols are defined in Chapter 3.

Initially the side boundary layer is formed by the forced upturning of the Ekman boundary layer flow and should, therefore, also have a width λ . Hence, by continuity of mass the vertical velocity out of the Ekman layer into the side wall boundary layer of width λ is

$$W^{*B} = \frac{W^{*I} \pi r^2}{2\pi r^2 \lambda} = \sqrt{2} R_0 H \Omega_0 \quad \text{at } z = -1 \quad (B.2)$$

Considering first the two-layer model, we let h^* be the height above the mean H_2 to which the denser fluid of the lower layer penetrates into the

upper layer. The vertical momentum equation in the side boundary layer is approximately

$$\frac{\partial w^*}{\partial t^*} + g \frac{\Delta p}{P} = 0 \quad (B.3)$$

Integrating twice in time we obtain

$$h^* = -g \frac{\Delta p}{P} \frac{t^{*2}}{2} + w_0^{*B} t^*$$

where w_0^{*B} is the initial velocity at $h^* = 0$ ($z^* = H_2$). Thus h_{max}^* occurs at $t^* = w_0^{*B} / g \frac{\Delta p}{P}$ and we have

$$h_{max}^* = \frac{w_0^{*B 2}}{2g \frac{\Delta p}{P}} \quad (B.4)$$

Substituting from (B.2) we find

$$h_{max} = \frac{h_{max}^*}{H_2} = \frac{R_0^2 \delta^2 \epsilon_2}{4} \quad \text{where } \delta = H_2/L \quad (B.5)$$

As an example, typical values are $\epsilon_2 \leq 10$, $\delta = 1/2$, then for $R_0^2 < .1$ $h_{max} \sim 0(10^{-2}) \sim 0(\lambda)$. For larger values of the Rossby number mixing would become important, but the linear theory is not valid for large R_0 anyway.

An analogous discussion applies to the continuous model. In this case the vertical momentum equation in the boundary layer is

$$\frac{d^2 z^*}{dt^{*2}} = \frac{dw^*}{dt^*} = \frac{gK z^*}{H} \quad \text{where } K = \frac{H}{P^*} \frac{d\rho^*}{dz^*} \quad (B.6)$$

with initial conditions

$$z^* = 0 \quad \text{at } t^* = 0$$

$$w^* = w^*(0) \quad \text{at } t^* = 0$$

z^* is taken to be the vertical displacement of a fluid parcel in the side boundary layer.

Thus $z^* = C \sin \sqrt{\frac{gK}{H}} t^*$ (B.7)

where C is a constant determined by the initial conditions

$$C = \frac{R_0 \sqrt{\epsilon} H^2}{L \sqrt{2}}$$

The maximum penetration is nondimensionally

$$z_{max} = \frac{z_{max}^*}{H} = \frac{R_0 \sqrt{\epsilon} \delta}{\sqrt{2}} \quad (B.8)$$

This is the square root of h_{max} in the two-layer case, so although the penetration is greater than in the two-layer model z_{max} is still very small for $R_0 \lesssim 1$ and ϵ not too large. Hence mixing at the side boundaries will not be important for the range of R_0 and ϵ prevailing in our experiments.

In addition to the above considerations we must be sure that the interior solutions which we have derived can be matched to a boundary layer structure which satisfies all boundary conditions at the wall. Greenspan and Howard (1957) considered this problem in detail for the homogeneous incompressible case. They found that the side walls have a double boundary layer structure. There is a main boundary layer of thickness $\lambda^{1/2}$, which is essentially the distance to which viscous effects will penetrate in a time $t \sim O(1)$. This thick boundary layer cannot satisfy the condition at the wall. It turns out that an inner layer of thickness $\lambda^{2/3}$ is required. In the two-layer model (for small R_0) it is obvious that this same structure will hold for the bottom layer because the dynamics at the side walls are the same as in the homogeneous case. In the upper layer, however, there is no Ekman layer effect to force strong vertical motions along the vertical boundary and the single $\lambda^{1/2}$ boundary layer can satisfy all boundary conditions. The above considerations apply to the fresh water - salt water model.

In the case of immiscible fluids the top layer also requires a double side wall boundary layer structure due to the interface Ekman layer.

In the continuous model the problem becomes much more complicated because the upward vertical mass flux at the wall will create density perturbations opposite to those in the interior, so that horizontal density gradients across the boundary layer are an essential feature. The explicit calculation of the boundary layer solutions in the stratified case is very difficult. Here we merely indicate in a heuristic manner that a double boundary layer structure can be matched to the interior provided that the zonal velocity in the interior has vertical shear.

In our discussion of the Ekman boundary layer we assumed that solutions valid throughout the fluid could be written in the form

$$f(z) = f(z)^I + f(\xi)^B$$

where ξ is a stretched coordinate and the boundary layer component f^B becomes exponentially small as $\xi \rightarrow \infty$. In the following discussion it is more convenient to take a somewhat different viewpoint. We let $f^I(r)$ be a solution valid in the interior and f^B be a solution valid in the boundary layer. We then require that $f^B = f^I$ at the interior edge of the boundary layer. Generally this matching may not be possible and an intermediate layer must form which can match to the interior and to the outer boundary layer.

In the present case the boundary conditions to be satisfied at the vertical wall are

$$W = 0, \quad V_r = 0 \quad \text{and} \quad V_\theta = 1$$

To satisfy the first of these conditions we consider a boundary layer of thickness λ . We define the stretched coordinate η as $\lambda\eta = 1-r$. At $z=0$ the vertical mass flux into this boundary layer requires that $w(\eta) \sim o(1)$ as can be seen from equation (B.2). Using superscript B to denote boundary layer variables we obtain from the equations of motion (3.8) - (3.12) of Chapter 3 the following balances correct to $O(R_0)$

$$w^B = \frac{\epsilon}{\sigma\delta^2} \frac{\partial^2 T^B}{\partial \eta^2} \quad (B.9)$$

$$\frac{\partial w^B}{\partial z} = -\frac{\partial v_r^B}{\partial \eta} \quad (B.10)$$

$$\frac{\partial p^B}{\partial \eta} = 0 \quad (B.11)$$

$$\frac{\partial^2 v_\theta^B}{\partial \eta^2} = 0 \quad (B.12)$$

$$T^B - \frac{\partial p^B}{\partial z} = -\frac{1}{\delta^4} \frac{\partial^2 w^B}{\partial \eta^2} \quad (B.13)$$

where w^B , T^B , v_θ^B , and p^B are $O(1)$ and $v_r \sim O(2)$.

Combining (B.9) and (B.13) we obtain

$$\frac{\partial^4 w^B}{\partial \eta^4} + \frac{\nu}{\epsilon} w^B = 0 \quad (B.14)$$

which can satisfy the condition $w=0$ at $\eta=0$. (B.12) indicates that $v_\theta=1$ at $\eta=0$ can be satisfied. Similarly, from (B.10) $v_r=0$ can be also satisfied. All of the balances (B.9) - (B.14) appear to be independent of the time \tilde{t} . This is because the wall effects penetrate a distance λ within the first few revolutions (the same time which it takes the Ekman layer to form). Equation (B.14) has an implicit time dependence because w at $z=0$ is determined by the divergence in the Ekman layer, which is time

dependent. However, the zonal velocity V_θ^B is time independent and hence cannot be matched to the interior zonal flow.

There must also exist, as in the homogeneous case, a layer of order $\lambda^{1/2}$ which can match to the interior. Let $\xi \lambda^{1/2} = 1-r$. The variables are ordered as follows:

$$\begin{aligned} W^{\theta'} &\sim O(\lambda^{3/2}), & T^{\theta'} &\sim O(\lambda^{1/2}), & p^{\theta'} &\sim O(\lambda^{1/2}) \\ V_r^{\theta'} &\sim O(\lambda), & V_\theta &\sim O(1) \end{aligned} \quad (B.15)$$

where the superscript θ' refers to variables in the ξ coordinate. We obtain the following balances:

$$V_\theta^{\theta'} = \frac{\partial p^{\theta'}}{\partial \xi} \quad (B.16)$$

$$T^{\theta'} = \frac{\partial p^{\theta'}}{\partial z} \quad (B.17)$$

$$\frac{\partial V_\theta^{\theta'}}{\partial t} + V_r^{\theta'} = \frac{\partial^2 V_\theta^{\theta'}}{\partial \xi^2} \quad (B.18)$$

$$\frac{\partial V_r^{\theta'}}{\partial \xi} = 0 \quad (B.19)$$

$$\frac{\partial T^{\theta'}}{\partial t} = -\frac{W^{\theta'}}{\epsilon} + \frac{1}{\sigma \delta^2} \frac{\partial^2 T^{\theta'}}{\partial \xi^2} \quad (B.20)$$

The small magnitude of $W^{\theta'}$, $T^{\theta'}$ and $p^{\theta'}$ is reasonable, for in this region these variables must all change sign to match their values near the wall to the internal solution. Differentiating (B.18) with respect to ξ we obtain

$$\frac{\partial^2 V_\theta^{\theta'}}{\partial t \partial \xi} = \frac{\partial^3 V_\theta^{\theta'}}{\partial \xi^3}$$

which is just an ordinary horizontal diffusion equation. Therefore $V_\theta^{\theta'}$ can

obviously be matched to V_{θ}^{β} and V_{θ}^I . From (E.16) and (E.17) we note that V_{θ}^{β} is geostrophic and a function of \bar{z} . Therefore, the interior zonal velocity must also be a function of \bar{z} to achieve matching.

Professor Greenspan has pointed out to me that a stream function of the form $\Psi = a\bar{z}^2 + b\tau^2$ where a and b are functions of time only will satisfy the equations in the case of an infinite plate. For such a stream function $\frac{\partial V_{\theta}^I}{\partial \bar{z}} = 0$ and the spin-up is exactly like the barotropic case. However, for the horizontal boundary at infinity our parameter and our solution reduces to Greenspan and Howard's result for a homogeneous incompressible fluid. For a horizontally finite system this kind of solution cannot exist because it apparently cannot be matched to the side wall boundary layer. Although the above heuristic arguments are not conclusive mathematical proof of this fact, nature has provided the proof in the experimental results reported here.

BIBLIOGRAPHY

- Barcilon, V., Role of the Ekman layers in the stability of the symmetric regime obtained in a rotating annulus. J. Atmospheric Sci. 21, 201-209, 1964.
- Charney, J. G., The generation of ocean currents by wind, J. Marine Res. 14, 477-498, 1955.
- Charney, J. G., and A. Eliassen, A numerical method for predicting the perturbations of the middle latitude westerlies, Tellus 1 (2), 38-54, 1949.
- Charney, J. G., and M. Stern, On the stability of internal baroclinic jets in a rotating atmosphere, J. Atmospheric Sci., 19, 159-172, 1962.
- Defant, A., Physical Oceanography Volume I, p. 118, 1961.
- Eady, E. T., Long waves and cyclone waves, Tellus 1 (2), 27-52, 1949.
- Ekman, V. W., On the influence of the earth's rotation on ocean currents, Arkiv. Matem., Astr., Fysik Stockholm, 2 (11), 1905.
- Greenspan, H. P., and L. N. Howard, On a time dependent motion of a rotating fluid, J. Fluid Mech. 17, 385-404, 1963.
- Hill, M. N., The Sea Volume I, p. 813, p. 821, 1963.
- Munk, W., and E. R. Anderson, Notes on a theory of the thermocline, J. Marine Res. 7, 276-295, 1948.
- Rossby, C. G., On the mutual adjustment of pressure and velocity distribution in certain simple current systems, J. Marine Res. 1, 15-28, 1937, and J. Marine Res. 1 (2), 239-263, 1938.
- Shapiro, R., and F. Ward, The time-space spectrum of the geostrophic meridional kinetic energy, J. Meteor. 17, 621-626, 1950.
- Stommel, H., The Gulf Stream, 202pp., 1960.
- Veronis G., and H. Stommel, The action of variable wind stresses on a stratified ocean, J. Marine Res. 15, 43075, 1956.
- White, R. W., and D. S. Cooley, Kinetic energy spectrum of meridional motion in the mid-troposphere, J. Meteor. 13, 67-69, 1956.